

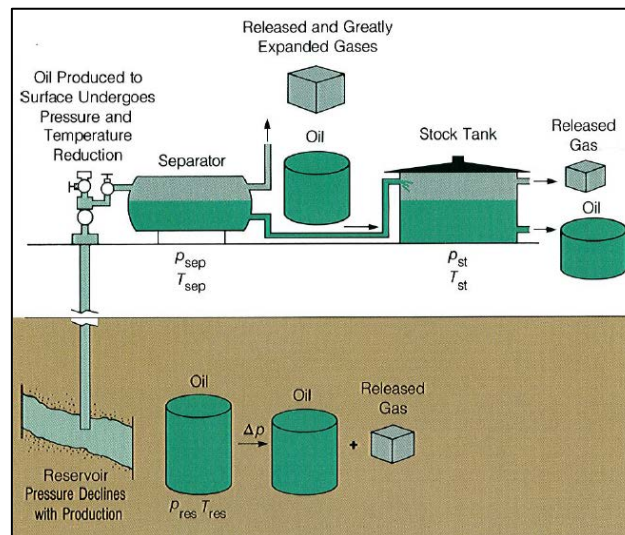
# TECHNICAL UNIVERSITY OF CRETE

## Master of Science in Petroleum Engineering

Department of Mineral Resources Engineering

### Master Thesis

## DEVELOPMENT OF A SIMPLE CORRELATION UTILIZING FIELD DATA AND THE STANDING-KATZ GAS Z-FACTOR METHOD FOR PREDICTING THE OIL FORMATION VOLUME FACTOR AT UNDERSATURATED CONDITIONS



Written By: **Tyrakis M. Nikolaos**

Supervisor:

**Professor, Nikos Varotsis**

**CHANIA, OCTOBER 2016**

# ACKNOWLEDGMENTS

First and foremost, I am deeply indebted to **The Trinitarian God** for establishing me to complete this Petroleum Engineering postgraduate program.

I would like to express my sincere gratitude to my supervisor, Professor Nikos Varotsis, Director of the PVT & Core Analysis Laboratory of Mineral Resources Engineering Department of the Technical University of Crete, for his expert, constant guidance and support during the preparation of the present Master's thesis.

I am also grateful to Professor Nikos Pasadakis and Dr. Vassilis Gaganis for their valuable advises and suggestions throughout the Master's program.

Finally, from the deepest of my heart, I would like to thank once again my close family members for their encouragement, moral and financial support from the beginning until the end of my postgraduate studies. I am really grateful for their caring and understanding.

## DEDICATION

*To the Almighty Trinitarian God.*

*The reason of what I become today.*

*Thanks for Your great support and continuous care.*

*"Without Me ye can do nothing" (John 15:5)*

*Glory be to the Father, and to the Son, and to the Holy Spirit: As it was in the beginning, is now, and ever shall be, world without end.*

*Amen*

# TABLE OF CONTENTS

Cover Page.....	i
Acknowledgments.....	ii
Dedication.....	iii
Table of Contents.....	iv
List of Figures.....	ix
List of Tables.....	xii
Nomenclature.....	xiv
Abstract.....	xvii
<b>CHAPTER 1: Volumetric Behavior of Reservoir Fluids.....</b>	<b>1</b>
1.1 Introduction.....	1
1.2 Definition of Volumetric Factors.....	2
1.2.1 Definition of Oil Isothermal Compressibility Coefficient.....	7
1.3 Reservoir Engineering Use of Volumetric Factors.....	11
1.3.1 Reservoir Engineering Use of Isothermal Compressibility Coefficient.....	16
1.4 Ways of Obtaining Readily Available Reliable Estimates of Volumetric Factors.....	18
<b>CHAPTER 2: Determination of Oil Formation Volume Factor and                 Isothermal Compressibility Coefficient.....</b>	<b>19</b>

<b>2.1</b>	<b>Laboratory Measurements of <math>B_o</math> and <math>c_o</math>.....</b>	<b>20</b>
2.1.1	<b>Determination of Oil Formation Volume Factor.....</b>	<b>20</b>
2.1.1.1	<b>Sampling of Reservoir Fluids.....</b>	<b>20</b>
2.1.1.2	<b>HPHT PVT Cell.....</b>	<b>21</b>
2.1.1.3	<b>Flash Vaporization Experiment.....</b>	<b>23</b>
2.1.1.4	<b>Differential Vaporization (DV) Experiment.....</b>	<b>24</b>
2.1.1.5	<b>Separator Test.....</b>	<b>25</b>
2.1.1.6	<b>Composite Liberation Test.....</b>	<b>27</b>
2.1.1.7	<b>Adjustment of Differential Vaporization and Flash Vaporization Data to Separator Conditions to Give <math>B_o</math> for Use in the Field.....</b>	<b>28</b>
2.1.2	<b>Determination of Isothermal Compressibility Coefficient of Oil.....</b>	<b>32</b>
<b>2.2</b>	<b>Determination <math>B_o</math> of From On-Site PVT Tests.....</b>	<b>35</b>
<b>2.3</b>	<b>Correlations currently used by the oil industry for oil FVF and oil compressibilities prediction.....</b>	<b>37</b>
2.3.1	<b>Correlations for undersaturated oil FVF prediction....</b>	<b>37</b>
2.3.1.1	<b>The Standing's correlation (Californian Crude Oils).....</b>	<b>39</b>
2.3.1.2	<b>The Vasquez-Begg's correlation (Generally Applicable).....</b>	<b>40</b>
2.3.1.3	<b>The Glaso's correlation (North Sea Crude Oils).....</b>	<b>41</b>
2.3.1.4	<b>The Al-Mahroun's correlation (Middle East Crude Oils).....</b>	<b>42</b>
2.3.1.5	<b>The Sulaimon's correlation (Malaysian Crude Oils).....</b>	<b>42</b>
2.3.2	<b>Correlations for oil isothermal compressibility coefficient prediction.....</b>	<b>43</b>

2.3.2.1	The Vasquez-Begg's correlation.....	43
2.3.2.2	The Petrosky-Farshad's correlation.....	44
2.3.2.3	The Ahmed's correlation.....	44
2.4	Prediction of $B_o$ Using Artificial Neural Networks (ANNs) Models.....	45
2.4.1	Advantages of the ANN Approach.....	46
2.4.2	Development of PVT Expert Model.....	46
2.4.3	Case Studies From the Literature.....	48
CHAPTER 3:	The Liquid $Z$ -factor Approach for Predicting $B_o$ at Undersaturated conditions.....	49
3.1	Basic Concepts of Gas Behavior.....	49
3.1.1	Ideal Gas Law.....	49
3.1.2	Specific Gravity of Gas.....	50
3.1.3	Behavior of Real Gases.....	51
3.2	Development of the Liquid $Z$ -factor Based Model.....	52
3.2.1	Determination of Bubble-point Oil Formation Volume Factor.....	52
3.2.1.1	Computation of bubble-point oil density based on the Standing-Katz $Z$ -factor chart.....	55
3.2.2	Determination of undersaturated oil formation volume factor.....	66
3.3	Flow Chart of the Liquid $Z$ -Factor Based $B_o$ prediction Method.....	68
CHAPTER 4:	Evaluation Procedure – Comparison of Correlations.....	70

4.1	Error Analysis – Definitions.....	70
4.1.1	Statistical Error Analysis.....	70
4.1.2	Evaluation Using Crossplots.....	72
4.2	Results of the Error Analysis.....	72
4.2.1	Error analysis for the prediction of the undersaturated $c_o$ .....	74
	4	
4.2.1.1	Vasquez and Begg’s Correlation.....	74
4.2.1.2	Petrosky and Farshad’s Correlation.....	75
4.2.1.3	Ahmed’s Correlation.....	76
4.2.1.4	Mattar’s Correlation.....	76
4.2.1.5	Undersaturated $c_o$ prediction using densities (Equation 3.45).....	77
4.2.2	Error analysis for the prediction of the $B_o$ at bubble-point and at undersaturated conditions.....	78
4.2.2.1	Standing’s Correlation.....	78
4.2.2.2	Vasquez and Begg’s Correlation.....	82
4.2.2.3	Glaso’s Correlation.....	85
4.2.2.4	Al-Mahrour’s Correlation.....	88
4.2.2.5	Sulaimon’s Correlation.....	92
4.2.2.6	Liquid $Z$ -Factor Based $B_o$ Prediction Method.....	95
4.2.3	Effect of the wellstream molecular weight on the accuracy of the $B_{ob}$ and of the undersaturated $B_o$ .....	99
4.3	Comparison of Correlations.....	100

4.3.1	Comparison of correlations for the $B_o$ prediction at bubble-point.....	100
4.3.2	Comparison of correlations for the $c_o$ prediction 500 psi above $p_b$ .....	103
4.3.3	Comparison of correlations for the $B_o$ prediction 500 psi above $p_b$ .....	103
CHAPTER 5: Conclusions.....		105
Appendix A	Experimental data of samples used for testing the performance of the correlations.....	107
Appendix B	Comparison between estimated and experimental values.....	125
References.....		150

# LIST OF FIGURES

<b>Figure 1.1</b>	Schematic of a petroleum reservoir	1
<b>Figure 1.2</b>	Production of reservoir hydrocarbons (a) above bubble point pressure, (b) below bubble point pressure	2
<b>Figure 1.3</b>	Oil formation volume factor versus pressure diagram	3
<b>Figure 1.4</b>	Gas formation volume factor versus pressure diagram	4
<b>Figure 1.5</b>	$B_t$ and $B_o$ versus pressure diagram	5
<b>Figure 1.6</b>	Gas-solubility versus pressure diagram	6
<b>Figure 1.7</b>	Volume change as pressure is reduced below the bubble point at constant reservoir temperature	9
<b>Figure 1.8</b>	Typical shape of the coefficient of isothermal compressibility of oil as a function of pressure at constant reservoir temperature	10
<b>Figure 1.9</b>	Volume changes in the reservoir associated with a finite pressure drop $\Delta p$ ; (a) volumes at initial pressure, (b) at the reduced pressure	12
<b>Figure 1.10</b>	Pressure versus Volume/Compressibility relationship	16
<b>Figure 2.1</b>	Schematic of the HPHT PVT cell and associated equipment	22
<b>Figure 2.2</b>	Illustration of flash vaporization experiment	23
<b>Figure 2.3</b>	Illustration of differential vaporization experiment	24
<b>Figure 2.4</b>	Laboratory separator test	26
<b>Figure 2.5</b>	Typical oil FVF curves from differential vaporization study and separator test	29
<b>Figure 2.6</b>	Adjustment of oil FVF to separator conditions	32
<b>Figure 2.7</b>	FPE portable chromatographs with the PC	36
<b>Figure 2.8</b>	Schematic showing the flow-path followed during an FPE test	37
<b>Figure 2.9</b>	Schematic of an Artificial Neural Network with one hidden layer	45
<b>Figure 2.10</b>	Comparison of the predicted $B_o$ curve from PVT Expert to the PVT Lab one	47
<b>Figure 3.1</b>	Typical Z-factor versus pressure diagram	52
<b>Figure 3.2</b>	Standing and Katz gas Z-factor chart	57
<b>Figure 3.3</b>	Z-factor EOS methods predictions error (All isotherms – $1.05 < T_r < 3.0$ )	62
<b>Figure 3.4</b>	Z-factor EOS methods predictions standard deviation (All isotherms – $1.05 < T_r < 3.0$ )	63
<b>Figure 3.5</b>	DAK method Z-factor prediction error for <i>n</i> -decane	63
<b>Figure 3.6</b>	Oil pseudo-critical property relationships from regression analysis	64
<b>Figure 3.7</b>	Watson characterization factor relationship with crude oil <i>API</i> gravity	65
<b>Figure 4.1</b>	Crossplot for undersaturated $c_o$ (Vasquez and Begg's Correlation)	75

<b>Figure 4.2</b>	Crossplot for undersaturated $c_o$ (Petrosky - Farshad's Correlation)	75
<b>Figure 4.3</b>	Crossplot for undersaturated $c_o$ (Ahmed's Correlation)	76
<b>Figure 4.4</b>	Crossplot for undersaturated $c_o$ (Using Mattar's correlation)	76
<b>Figure 4.5</b>	Crossplot for undersaturated $c_o$ [using densities (Equation 3.45)]	77
<b>Figure 4.6</b>	Crossplot for $B_{ob}$ using Standing's Correlation – TUC database	79
<b>Figure 4.7</b>	Crossplot for $B_{ob}$ using Standing's Correlation - North Sea oil samples	80
<b>Figure 4.8</b>	Crossplot for $B_{ob}$ using Standing's Correlation - Middle East oil samples	80
<b>Figure 4.9</b>	Crossplot for $B_{ob}$ using Standing's Correlation - Malaysian oil samples	80
<b>Figure 4.10</b>	Crossplot for undersaturated $B_o$ at 500psi above $p_b$ - Standing's Correlation	81
<b>Figure 4.11</b>	Crossplot for $B_{ob}$ using Vasquez-Begg's Correlation – TUC database	83
<b>Figure 4.12</b>	Crossplot for $B_{ob}$ using Vasquez-Begg's Correlation – North Sea oil samples	83
<b>Figure 4.13</b>	Crossplot for $B_{ob}$ using Vasquez-Begg's Correlation, Middle East oil samples	83
<b>Figure 4.14</b>	Crossplot for $B_{ob}$ using Vasquez-Begg's Correlation, Malaysian oil samples	84
<b>Figure 4.15</b>	Crossplot for undersaturated $B_o$ at 500psi above $p_b$ - Vasquez and Begg's Correlation	85
<b>Figure 4.16</b>	Crossplot for $B_{ob}$ using Glaso's Correlation – TUC database	86
<b>Figure 4.17</b>	Crossplot for $B_{ob}$ using Glaso's Correlation – North Sea oil samples	86
<b>Figure 4.18</b>	Crossplot for $B_{ob}$ using Glaso's Correlation – Middle East oil samples	87
<b>Figure 4.19</b>	Crossplot for $B_{ob}$ using Glaso's Correlation – Malaysian oil samples	87
<b>Figure 4.20</b>	Crossplot for undersaturated $B_o$ at 500psi above $p_b$ - Glaso's Correlation	88
<b>Figure 4.21</b>	Crossplot for $B_{ob}$ using Al-Mahroun's Correlation – TUC database	89
<b>Figure 4.22</b>	Crossplot for $B_{ob}$ using Al-Mahroun's Correlation – North Sea oil samples	90
<b>Figure 4.23</b>	Crossplot for $B_{ob}$ using Al-Mahroun's Correlation – Middle East oil samples	90
<b>Figure 4.24</b>	Crossplot for $B_{ob}$ using Al-Mahroun's Correlation - Malaysian oil samples	90

<b>Figure 4.25</b>	Crossplot for undersaturated $B_o$ at 500psi above $p_b$ – Al-Mahroun's Correlation	91
<b>Figure 4.26</b>	Crossplot for $B_{ob}$ using Sulaimon's Correlation – TUC database	92
<b>Figure 4.27</b>	Crossplot for $B_{ob}$ using Sulaimon's Correlation – North Sea oil samples	93
<b>Figure 4.28</b>	Crossplot for $B_{ob}$ using Sulaimon's Correlation – Middle East oil samples	93
<b>Figure 4.29</b>	Crossplot for $B_{ob}$ using Sulaimon's Correlation - Malaysian oil samples	93
<b>Figure 4.30</b>	Crossplot for undersaturated $B_o$ at 500psi above $p_b$ – Sulaimon's Correlation	94
<b>Figure 4.31</b>	Crossplot for the $\rho_{ob}$	95
<b>Figure 4.32</b>	Crossplot for $B_{ob}$ using the liquid Z-factor based Correlation – TUC database	96
<b>Figure 4.33</b>	Crossplot for $B_{ob}$ using the liquid Z-factor based Correlation – North Sea oil samples	97
<b>Figure 4.34</b>	Crossplot for $B_{ob}$ using the liquid Z-factor based Correlation – Middle East oil samples	97
<b>Figure 4.35</b>	Crossplot for $B_{ob}$ using the liquid Z-factor based Correlation - Malaysian oil samples	97
<b>Figure 4.36</b>	Crossplot for undersaturated $B_o$ at 500psi above $p_b$ – Liquid Z-factor Based Correlation	97

## LIST OF TABLES

<b>Table 2.1</b>	Separator Test Data	26
<b>Table 2.2</b>	Differential and Flash Test data	31
<b>Table 2.3</b>	Adjustment of the oil FVF curve to separator conditions	31
<b>Table 2.4</b>	Flash liberation data	34
<b>Table 2.5</b>	$C_1$ , $C_2$ and $C_3$ coefficients for Vasquez and Begg's correlation	41
<b>Table 2.6</b>	Statistical comparison of Sulaimon's with other commonly used correlations	43
<b>Table 4.1</b>	Statistical error analysis for the prediction of undersaturated $c_o$ using Vasquez and Begg's correlation	74
<b>Table 4.2</b>	Statistical error analysis for the prediction of undersaturated $c_o$ using Petrosky and Farshad's correlation	75
<b>Table 4.3</b>	Statistical error analysis for the prediction of undersaturated $c_o$ using Ahmed's correlation	76
<b>Table 4.4</b>	Statistical error analysis for the prediction of undersaturated $c_o$ using Mattar's correlation	76
<b>Table 4.5</b>	Statistical error analysis for the prediction of undersaturated $c_o$ using densities (Equation 3.45)	77
<b>Table 4.6</b>	Accuracy of Standing's Correlation for the determination of $B_{ob}$	79
<b>Table 4.7</b>	Accuracy of undersaturated $B_o$ using Standing's Correlation for the estimation of the $B_{ob}$ and Petrosky-Farshad's method for the $c_o$ calculation	81
<b>Table 4.8</b>	Accuracy of Vasquez-Begg's Correlation for the determination of $B_{ob}$	82
<b>Table 4.9</b>	Accuracy of undersaturated $B_o$ using Vasquez-Begg's Correlation for the estimation of the $B_{ob}$ and Petrosky-Farshad's method for the $c_o$ calculation	84
<b>Table 4.10</b>	Accuracy of Glaso's Correlation for the determination of $B_{ob}$	85
<b>Table 4.11</b>	Accuracy of undersaturated $B_o$ using Glaso's Correlation for the estimation of the $B_{ob}$ and Petrosky-Farshad's method for the $c_o$ calculation	88
<b>Table 4.12</b>	Accuracy of Al-Mahroun's Correlation for the determination of $B_{ob}$	89
<b>Table 4.13</b>	Accuracy of undersaturated $B_o$ using Al-Mahroun's Correlation for the estimation of the $B_{ob}$ and Petrosky-Farshad's method for the $c_o$ calculation	91
<b>Table 4.14</b>	Accuracy of Sulaimon's Correlation for the determination of $B_{ob}$	92

<b>Table 4.15</b>	Accuracy of undersaturated $B_o$ using Sulaimon's Correlation for the estimation of the $B_{ob}$ and Petrosky-Farshad's method for the $c_o$ calculation	94
<b>Table 4.16</b>	Accuracy of the $\rho_{ob}$	95
<b>Table 4.17</b>	Accuracy of Liquid Z-factor based Correlation for the determination of $B_{ob}$	96
<b>Table 4.18</b>	Accuracy of undersaturated $B_o$ using the liquid Z-factor based Correlation for the estimation of the $B_{ob}$ and Petrosky-Farshad's method for the $c_o$ calculation	98
<b>Table 4.19</b>	Effect of $MW_o$ on the accuracy of the $B_{ob}$	99
<b>Table 4.20</b>	Effect of $MW_o$ on the accuracy of the undersaturated $B_o$	100
<b>Table 4.21</b>	Comparison of the presented correlations for the $B_{ob}$ prediction against the TUC database	101
<b>Table 4.22</b>	Comparison of the presented correlations for the $B_{ob}$ prediction against the North Sea oil samples	101
<b>Table 4.23</b>	Comparison of the presented correlations for the $B_{ob}$ prediction against the Middle East oil Samples	102
<b>Table 4.24</b>	Comparison of the presented correlations for the $B_{ob}$ prediction against the Malaysian oil Samples	102
<b>Table 4.25</b>	Comparison of the presented correlations for the $c_o$ prediction, 500 psi above $p_b$	103
<b>Table 4.26</b>	Comparison of the presented correlations for the $B_o$ prediction, 500 psi above $p_b$	103

## NOMENCLATURE

<b>A</b>	Correlating parameter, Equation 2.18
<b>API</b>	American Petroleum Institute (API) gravity, $^{\circ}API$
<b><math>B_g</math></b>	Formation Volume Factor (FVF) of gas, ft <sup>3</sup> free gas/scf gas [res m <sup>3</sup> / std m <sup>3</sup> ]
<b><math>B_o</math></b>	Formation Volume Factor (FVF) of oil, res bbl / STB [res m <sup>3</sup> / std m <sup>3</sup> ]
<b><math>B_{ob}</math></b>	Formation Volume Factor (FVF) of oil at the bubble-point pressure, res bbl / STB [res m <sup>3</sup> / std m <sup>3</sup> ]
<b><math>B_{ob}^*</math></b>	Correlating parameter defined by Equation 2.19
<b><math>B_{oi}</math></b>	Formation Volume Factor (FVF) of oil at initial reservoir pressure, res bbl / STB [res m <sup>3</sup> / std m <sup>3</sup> ]
<b><math>B_{oDb}</math></b>	Formation Volume Factor at bubble-point from differential vaporization test
<b><math>B_{oDi}</math></b>	Formation Volume Factor (FVF) of oil at <i>i</i> th stage in the differential vaporization test
<b><math>B_{oDn}</math></b>	Formation Volume Factor (FVF) of oil - the subscript n corresponds to the number of stages in the differential vaporization test
<b><math>B_{oSb}</math></b>	Formation Volume Factor at bubble-point from separator test
<b><math>B_t</math></b>	Total Formation Volume Factor (FVF), res bbl / STB [res m <sup>3</sup> / std m <sup>3</sup> ]
<b><math>B_w</math></b>	Formation Volume Factor (FVF) of Water, res bbl / STB [res m <sup>3</sup> / std m <sup>3</sup> ]
<b><math>C_1, C_2, C_3</math></b>	Coefficients for the Vasquez-Beggs correlation
<b><math>c_o</math></b>	Isothermal compressibility coefficient of oil, 1/psi
<b><math>c_f</math></b>	Pore compressibility, 1/psi
<b><math>c_r</math></b>	Reduced isothermal compressibility coefficient
<b><math>c_w</math></b>	Water compressibility, 1/psi
<b><math>E_a</math></b>	Average Absolute Percent Relative Error (AAPRE)
<b><math>E_i</math></b>	Relative deviation between estimated and experimental value
<b><math>E_{max}</math></b>	Maximum Absolute Percent Relative Error
<b><math>E_{min}</math></b>	Minimum Absolute Percent Relative Error
<b><math>E_r</math></b>	Average Percent Relative Error (APRE)
<b>F</b>	Correlating parameter defined by Equation 2.21
<b><math>K_w</math></b>	Watson characterization factor
<b><math>m</math></b>	Mass of gas phase, lb [kg]
<b><math>m_g</math></b>	Mass of solution gas, lb [kg]
<b><math>m_o</math></b>	Mass of stock-tank oil, lb [kg]
<b><math>m_t</math></b>	Total mass of hydrocarbon system, lb [kg]
<b>M</b>	Ratio of initial hydrocarbon volume of the gas-cap to the initial hydrocarbon volume of the oil
<b><math>MW_a</math></b>	Apparent molecular weight, lb/mol [kg/mol]
<b><math>MW_{air}</math></b>	Apparent molecular weight of dry air, equal to 28.96 lb/mol
<b><math>MW_o</math></b>	Wellstream oil molecular weight, lb/mol [kg/mol]

$MW_o$	Stock-tank oil molecular weight, lb/mol [kg/mol]
$n$	Number of gas moles
$n_d$	Number of experimental data points
$N$	Initial oil in place in stock tank barrels (STB)
$N_p$	Cumulative oil production in stock tank barrels (STB)
$p_i$	Initial reservoir pressure, psi [kPa]
$p_b$	Reservoir pressure at the bubble-point, psi [kPa]
$p_{ci}$	Critical pressure of $i$ th component in the gas mixture
$p_{pc}$	Pseudo-critical pressure
$p_{pr}$	Pseudo-reduced pressure
$p_{res}$	Reservoir pressure, psi [kPa]
$p_{sep}$	Separator pressure, psi [kPa]
$r^2$	Correlation coefficient
$R$	Universal gas constant which has the value of 10.7316 psia ft <sup>3</sup> mole <sup>-1</sup> °R <sup>-1</sup> (or 8.3145 Pa m <sup>3</sup> mol <sup>-1</sup> K <sup>-1</sup> )
$R_p$	Cumulative gas to oil ratio both measured at standard conditions, scf/STB [std m <sup>3</sup> / stock-tank m <sup>3</sup> ]
$R_s$	Solution gas to oil ratio, scf/STB [std m <sup>3</sup> / stock-tank m <sup>3</sup> ]
$R_{sb}$	Solution gas to oil ratio at bubble-point pressure, scf/STB [std m <sup>3</sup> / stock-tank m <sup>3</sup> ]
$R_{sep}$	Solution gas to oil ratio measured at the separator, scf/bbl [std m <sup>3</sup> / m <sup>3</sup> ]
$R_{si}$	Solution gas to oil ratio at initial reservoir pressure, scf/STB [std m <sup>3</sup> / stock-tank m <sup>3</sup> ]
$S_{wc}$	Connate water saturation
$SD$	Standard Deviation (SD)
$t$	Reciprocal of pseudo-reduced temperature, i.e. $T_{pc}/T_{res}$
$T_{ci}$	Critical temperature of $i$ th component in the gas mixture, °R [K]
$T_{pc}$	Pseudo-critical temperature
$T_{pr}$	Pseudo-reduced temperature
$T_{res}$	Reservoir temperature, °R [K]
$T_{sep}$	Separator temperature, °R [K]
$V$	Net bulk volume of reservoir, STB [std m <sup>3</sup> ]
$V_b$	Reservoir fluid volume at bubble-point pressure, STB [std m <sup>3</sup> ]
$V_f$	Total pore volume
$(V_g)_{rc}$	Volume of the gas at reservoir conditions, res ft <sup>3</sup> [m <sup>3</sup> ]
$(V_g)_{sc}$	Volume of the gas at standard conditions, scf [std m <sup>3</sup> ]
$V_m$	Molar volume, defined by 379.4 ft <sup>3</sup> at standard conditions
$(V_o)_{rc}$	Volume of the oil at reservoir conditions, res bbl [m <sup>3</sup> ]
$(V_o)_{sc}$	Volume of the oil at standard conditions, STB [std m <sup>3</sup> ]
$V_t$	Total reservoir fluid volume of the HPHT PVT cell, res bbl [m <sup>3</sup> ]
$(V_t / V_b)_F$	Relative volume - total volume divided by volume at the bubble point for a flash vaporization

$V_w$	Connate water volume
$W_e$	Cumulative water influx from the aquifer into the reservoir, STB [std m <sup>3</sup> ]
$W_p$	Cumulative amount of aquifer water produced, STB [std m <sup>3</sup> ]
$x_{est}$	Estimated value
$x_{exp}$	Experimental value
$x_o$	Mole fraction of oil in the wellstream
$y_i$	Mole fraction of $i$ th component in the gas mixture
$Z$	Gas compressibility factor (or gas deviation factor or super-compressibility factor or Z-factor)
$Z_c$	Critical compressibility factor
$Z_L$	Liquid phase compressibility factor
$\alpha_1, \alpha_2, \alpha_3$	Parameters equals to 24,841.0822 , 14.07428745 and -0.00018473 respectively
$\gamma_o$	Specific gravity of stock-tank oil (air = 1)
$\gamma_g$	Specific gravity of gas phase (water = 1)
$\gamma_{gs}$	Specific gravity of gas, defined by the Equation 2.15
$\rho_{air}$	Density of dry air, lb/ft <sup>3</sup> [kg/m <sup>3</sup> ]
$\rho_g$	Density of gas phase, lb/ft <sup>3</sup> [kg/m <sup>3</sup> ]
$\rho_o$	Density of crude oil, lb/ft <sup>3</sup> [kg/m <sup>3</sup> ]
$\rho_{ob}$	Density of crude oil at the bubble-point pressure, lb/ft <sup>3</sup> [kg/m <sup>3</sup> ]
$\rho_r$	Reduced density, defined as the ratio of the gas density at a specified pressure and temperature to that of the gas at its critical pressure and temperature
$\rho_w$	Density of water phase, lb/ft <sup>3</sup> [kg/m <sup>3</sup> ]
$\phi$	Porosity

# ABSTRACT

The Oil Formation Volume Factor,  $B_o$ , is used in almost all the Reservoir and Production Engineering calculations for converting subsurface fluid volumes to surface ones. The knowledge of its value is a prerequisite for evaluating reliably initial hydrocarbon volumes in place, predicting hydrocarbon recovery and future reservoir performance and identifying the drive mechanism.

The values of the Oil Formation Volume Factor are measured during the PVT study and they become usually available several months after the well has been tested. In the meanwhile, crucial reservoir engineering decisions have to be made by the Operator, including the estimation of the reserves and the future production plans for which values of  $B_o$  are provided by widely used correlations which only require data that are measured in the field during the Well Test (solution  $GOR$ ,  $API$ ,  $S_g$ ,  $T_{res}$ ). Given that these correlations are equations fitted against experimental data of oils from certain origin and composition, their accuracy is doubtful.

The present master thesis deals with the development of a simple correlation, called liquid  $Z$ -factor based method, using fundamental relationships, for the determination of the  $B_o$  at undersaturated conditions. The correlation expresses the  $B_o$  as a function of data that are measured in the field during the Well Test and the reservoir density at reservoir pressure. The DAK representation of the Standing-Katz  $Z$ -factor chart was used for the computation of the crude oil density, and an Excel spreadsheet was developed to incorporate all the above calculations.

A literature review was conducted to qualify 5 correlations currently used by the oil industry. These correlations were also included in the Excel spreadsheet.

The field data of reservoir oils from all over the world was used for testing the performance of the developed correlation against the performance of the other well-known correlations.

The results are very encouraging, since, the proposed method proved not only comparable but even more accurate and applicable in a wider range of  $B_o$  than the other presented correlations.

# C H A P T E R 1

## Volumetric Behavior of Reservoir Fluids

### 1.1. Introduction

**Petroleum** (from Latin: *petra*: "rock" + *oleum*: "oil") is a naturally occurring, yellow to black liquid, consisting predominantly of hydrocarbons (organic compound consisting entirely of hydrogen and carbon) and containing sulfur, nitrogen, oxygen, and helium as minor constituents. It is found beneath the Earth's surface in geological formations, so called **reservoirs**, which are characterized by adequate porosity and permeability. Reservoir rocks are commonly sandstones or limestones. Except from petroleum (an equivalent term is crude oil) in the reservoir may co-exist natural gas and aqueous solutions with dissolved salt. Natural gas is a mixture of hydrocarbon and non-hydrocarbon gases. The hydrocarbon gases consist of methane, ethane, propane, butane, pentane, and small amounts of hexane and heavier. The non-hydrocarbon gases include carbon dioxide, hydrogen sulfide, and nitrogen. Density of gas is lower than oil and water density, thus it always lies at the top of the reservoir forming a gas-cap. Density of water is higher than oil's density therefore it lies below the oil phase. Typical distribution of reservoir fluids into a reservoir is illustrated in the next Figure.

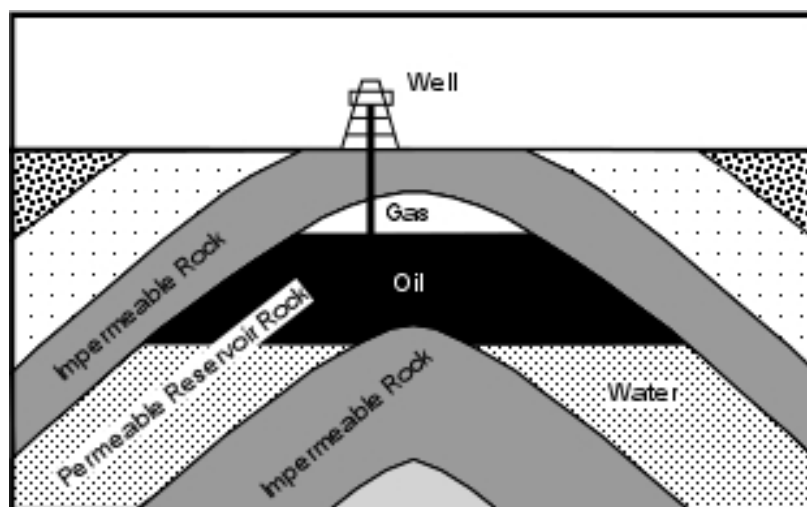
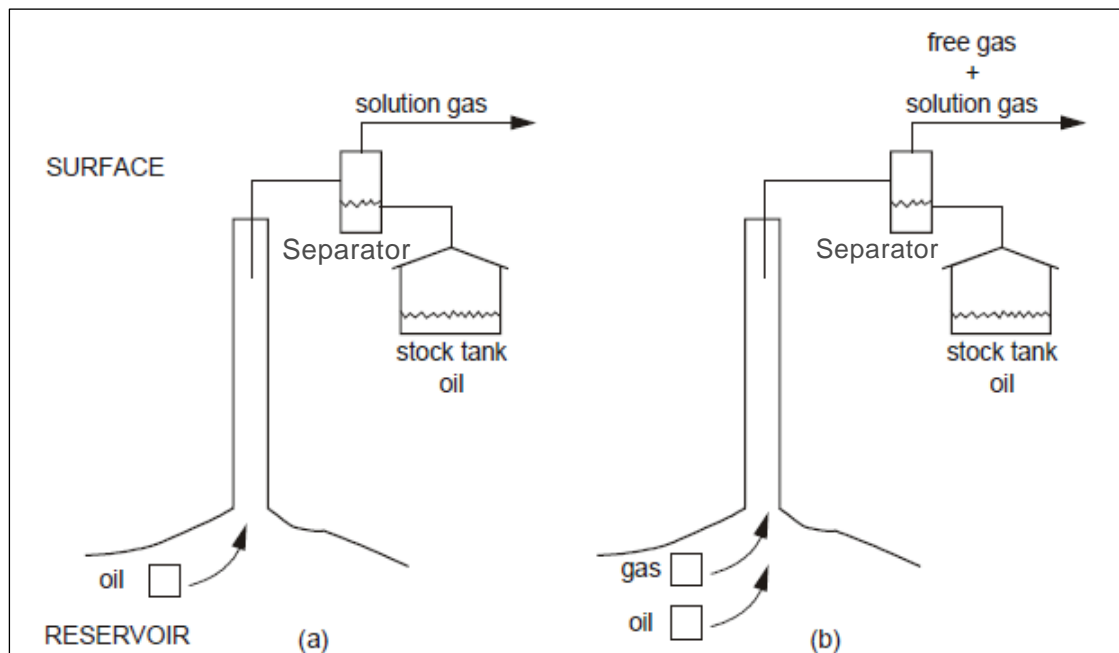


Figure 1.1 Schematic of a petroleum reservoir<sup>[1]</sup>

## 1.2. Definition of Volumetric Factors

The majority of petroleum reservoirs are found within the depth range of 1,600 – 13,000 ft, therefore, reservoir fluids encounter extremely high pressure and temperature conditions. During production, the pressure and temperature of the reservoir fluid are being reduced as it rises to the surface through a production well, until it reaches the stock tank. Figure 1.2 represents a typical scenario of an oil and gas reservoir exploitation which includes the presence of a separator. The separator is used to separate oil, gas and water from the total fluid stream produced by the production well. The initial pressure of the reservoir affects the phase behavior of reservoir fluids, fact that signifies two cases:



**Figure 1.2** Production of reservoir hydrocarbons (a) above bubble point pressure, (b) below bubble point pressure<sup>[2]</sup>

- If the pressure of a reservoir is above a certain value, called *bubble point pressure*, only one phase exists in the reservoir – the liquid oil. The oil in this case is said to be **undersaturated**. The word *undersaturated* is used in this sense to indicate that the oil could dissolve more gas if present. When this undersaturated oil is produced to the surface, gas will be separated from the oil as shown in Figure 1.2(a), **the volume of which depends on the conditions at which the surface separation is set (i.e. pressure and temperature of separator) and on the number of separators.**

- If the reservoir is below bubble point pressure, as depicted in Figure 1.2(b), the situation is more complicated. Now there are two hydrocarbon phases in the reservoir; saturated oil and liberated solution gas. During production to the surface, solution gas will be evolved from the oil phase and the total surface gas production will have two components; the gas which was free in the reservoir and the gas that is liberated from the oil during production.

This volumetric behavior of reservoir fluids during production leads to the requirement of expressing quantitatively the relationship between down-hole and surface hydrocarbon volumes. Control in relating surface volumes of production to underground withdrawal is gained by defining the following three **Volumetric factors (or PVT Parameters)**:

- **$B_o$** : **The oil formation volume factor at reservoir temperature and at a given pressure**, is the volume occupied in the reservoir, at the prevailing pressure and temperature, by one stock tank barrel of oil plus its gas that can dissolve in it at the above conditions. In an equation form, the relationship is expressed as (units – res bbl (oil + dissolved gas)/STB oil):

$$B_o = \frac{(V_o)_{rc}}{(V_o)_{sc}} \quad (1.1)$$

As illustrated in Figure 1.3, when the pressure is reduced below the initial reservoir pressure  $p_i$ , the oil volume increases due to oil expansion. This behavior results in an increase in the oil formation volume factor value which continues until the bubble-point pressure is reached. At  $p_b$ , the oil reaches its maximum expansion and consequently attains a maximum value of  $B_{ob}$  for the oil formation volume factor. As the pressure is reduced below  $p_b$ , the volume of the oil and the  $B_o$  decreases as solution gas is liberated. If the pressure is reduced to atmospheric pressure and the temperature to 60 °F, the value of  $B_o$  should be equal to one.

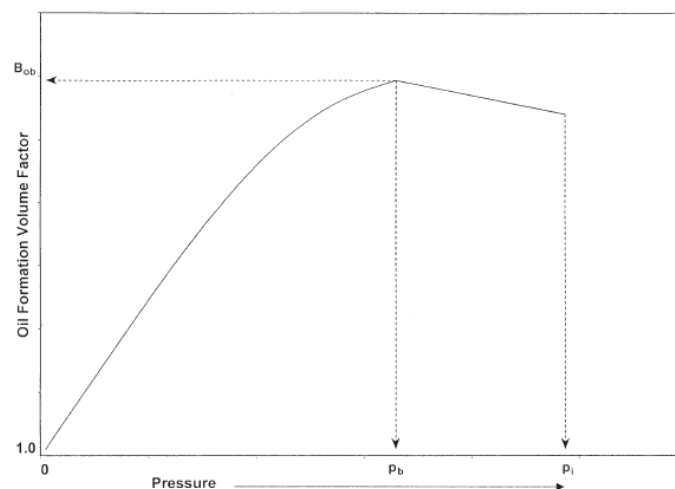


**Figure 1.3** Oil formation volume factor versus pressure diagram<sup>[3]</sup>

- **$B_g$** : **The gas formation volume factor at reservoir temperature and at a given pressure**, is the volume in barrels that one standard cubic foot (or  $m^3$ ) of gas will occupy as free gas in the reservoir at the prevailing reservoir pressure and temperature. It can be expressed mathematically as (units –  $ft^3$  free gas/scf gas):

$$B_g = \frac{(V_g)_{rc}}{(V_g)_{sc}} \quad (1.2)$$

A typical plot of gas formation volume factor versus reservoir pressure at constant temperature is given in Figure 1.4.

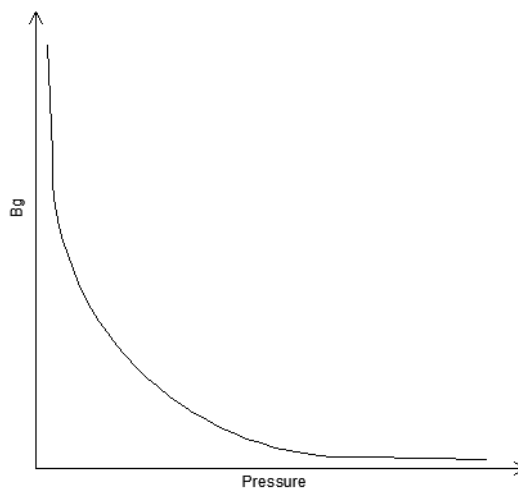


**Figure 1.4** Gas formation volume factor versus pressure diagram

- **$B_t$** : **The total formation volume factor at reservoir temperature and at a given pressure**, is defined as the ratio of the total volume of the hydrocarbon mixture (i.e., oil and free gas, if present), at the prevailing pressure and temperature per unit volume of the stock-tank oil. Mathematically,  $B_t$  is defined as (units – res bbl /STB):

$$B_t = B_o + B_g(R_{si} - R_s) \quad (1.3)$$

Where:

- $(V_o)_{sc}$ : Volume of the oil at standard conditions, STB
- $(V_g)_{sc}$ : Volume of the gas at standard conditions, scf
- $(V_o)_{rc}$ : Volume of the oil at reservoir conditions, res bbl (reservoir barrels)
- $(V_g)_{rc}$ : Volume of the gas at reservoir conditions,  $ft^3$
- $R_s$ : Solution gas to oil ratio defined by Equation 1.4
- $R_{si}$ : Solution gas to oil ratio at initial pressure

A typical plot of  $B_t$  as a function of pressure for an undersaturated crude oil is shown in Figure 1.5. The oil formation volume factor curve is also included in the illustration. As pointed out above,  $B_o$  and  $B_t$  are identical at pressures above or equal to the bubble-point pressure because only one phase, the oil phase, exists at these pressures. It should also be noted that at pressures below the bubble-point pressure, the difference in the values of the two oil properties represents the volume of the evolved solution (free) gas as measured at system conditions per stock-tank barrel of oil.

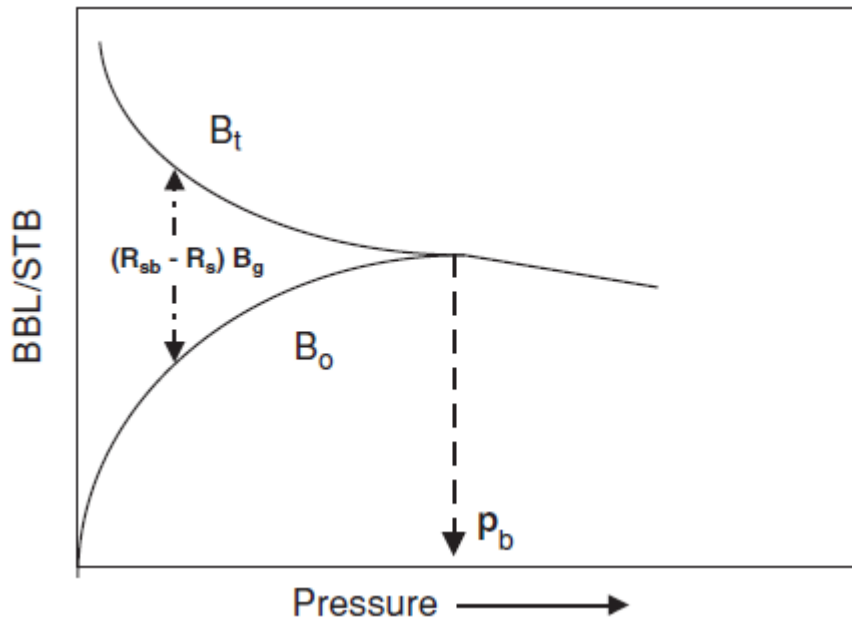
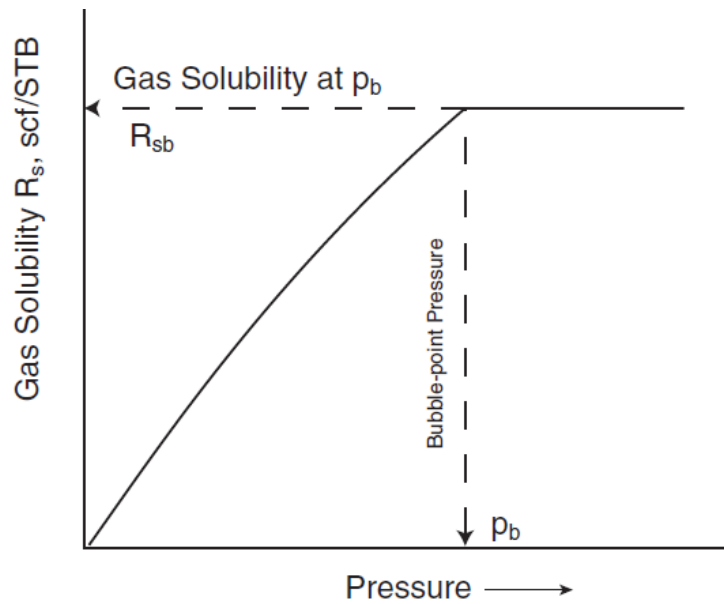


Figure 1.5  $B_t$  and  $B_o$  versus pressure diagram<sup>[4]</sup>

- **$R_s$ : The solution (or dissolved) gas to oil ratio at reservoir temperature and a given pressure**, is the number of standard cubic feet (or  $m^3$ ) of gas which will dissolve in one stock tank barrel of oil when both are taken down to the reservoir at the prevailing reservoir pressure and temperature. It expresses the volatility of an oil. Mathematically,  $R_s$  is defined by the following relationship (units – scf. gas/STB oil):

$$R_s = \frac{(V_g)_{sc}}{(V_o)_{sc}} \quad (1.4)$$

A typical gas solubility curve, as a function of reservoir pressure is shown in Figure 1.6. As the pressure is reduced from the initial reservoir pressure  $p_i$  down to the bubble-point pressure  $p_b$ , no gas evolves from the oil and consequently the gas solubility remains constant at its maximum value of  $R_{sb}$ . Below the bubble-point pressure, the solution gas is liberated and the value of  $R_s$  decreases with pressure.



**Figure 1.6** Gas-solubility versus pressure diagram<sup>[5]</sup>

Both the standard cubic foot (scf) and the stock tank barrel (STB) referred to in the above definitions are defined at standard conditions, which in this text are taken as 60°F and one atmosphere (14.7 psia).

Typical initial values of  $B_o$  and  $R_s$  for medium volatility oils are 1.25 res bbl/STB and 500 scf/STB, respectively. In case of high volatility oils those values are much higher. Staffjord field for example in North Sea has  $B_o=2.7$  res bbl/STB and  $R_{si}=3000$  scf/STB. Obviously, the best possible case, from the point of view of reserves, is the value of  $B_o$  to be as close as possible to unity because in this case the volume of hydrocarbon withdrawal from the reservoir is approximately equal to the produced volume at the surface. Such example is at field in Eastern Turkey with  $B_o=1.05$  res bbl/STB and  $R_{si}=20$  scf/STB.

Figures 1.3 to 1.6 show that  $R_s$ ,  $B_o$ ,  $B_g$  and  $B_t$  are functions of pressure, assuming that the reservoir temperature remains constant during depletion. However, these parameters also depend on:

- The rate of liberation of gas in solution from the oil phase
- The kind of process that takes place in the reservoir and/or in the well
- The pressure, temperature and number of surface separators

The reason why the PVT parameters are also dependent on the three above factors will be explained in the Chapter 2.

### 1.2.1. Definition of oil Isothermal Compressibility Coefficient

Oil production can be said to take place in three phases: the **primary recovery** phase, the **secondary** oil recovery and the **tertiary or enhanced** oil recovery (abbreviated EOR). The recovery of oil by any of the natural drive mechanisms without the use of additional processes to supplement the natural energy of the reservoir is called primary recovery.

During the secondary recovery phase, water or gas or both are injected into the reservoir through an injection well. Secondary recovery may be performed by heat injection using steam or a burning front (in-situ combustion).

Enhanced oil recovery is carried out through physicochemical methods such as surfactant or alkaline flooding which are injected with water into the reservoir. Other techniques include *electromagnetic heating* (the electrical energy supplied from the surface is transmitted to the reservoir either by cables or through metal structures), *microbial injection* (microbes function either by partially digesting long hydrocarbon molecules, or by emitting carbon dioxide) and *miscible displacement* (as injected gas is used CO<sub>2</sub> or liquefied petroleum gas which improves oil displacement by reducing the interfacial tension between oil and water).

In the reservoir's primary recovery phase, several sources of energy may contribute to fluid production. There are five main possible driving mechanisms that provide the natural energy necessary for oil recovery:

- Rock and liquid expansion drive
- Dissolved gas drive
- Gas-cap drive
- Water drive (aquifer)
- Gravity drainage drive

In most cases, a combination of mechanisms is acting which is referred as a combination drive.

It is obvious that the main mechanisms of primary recovery (Rock and liquid expansion drive, Dissolved gas drive, Gas-cap drive) rely on the expansion of reservoir rock and of reservoir fluids and can best be understood by considering the definition of **isothermal compressibility coefficient**,  $c$ . It is defined as the fractional change of fluid volume per unit change in pressure at constant reservoir temperature. Mathematically,  $c$ , is defined by the following relationship:

$$c = -\frac{1}{V} \left( \frac{\partial V}{\partial p} \right)_T \quad (1.5)$$

The unit of isothermal compressibility is the reciprocal of pressure, **psi<sup>-1</sup>**. The negative sign is required in the above equation because compressibility is defined as a positive number, whereas the differential  $\partial V/\partial p$  is always negative, since fluids expand when their confining pressure is decreased. The partial derivative is used rather than the ordinary derivative because only the independent variable, pressure, is permitted to vary. The subscript  $T$  indicates that the temperature is held constant.

The term **isothermal** in the above definition is used because calculation of primary recovery relies on the realistic assumption that the reservoir temperature stays constant during depletion. Thus, hydrocarbon recovery during this phase is considered to be an isothermal process. This is so because as fluids are produced any change in temperature due to production is compensated for by heat from the cap or base rocks, which are considered to be heat sources of infinite capacity.

When using the compressibility definition, to describe reservoir depletion, it is more illustrative to express it in the form

$$\frac{\Delta V}{\Delta t} = q = cV \frac{\Delta p}{\Delta t} \quad (1.6)$$

where,  $\Delta V$  is an expansion,  $\Delta p$  a pressure drop both of which are positive and  $q$  is the volumetric flow rate at the time interval  $\Delta t$  during which pressure has dropped by  $\Delta p$ . **This is the very basic equation underlying all forms of primary recovery mechanism.**

The above definition of isothermal compressibility coefficient is valid for natural gases and for crude oils above bubble point.

In case of crude oils, **at pressures below bubble point pressure** an additional term must be added to the definition of isothermal compressibility coefficient to account for the volume of gas which evolves. As Figure 1.7 shows, the volume of the reservoir liquid shrinks as pressure is reduced below bubble point.

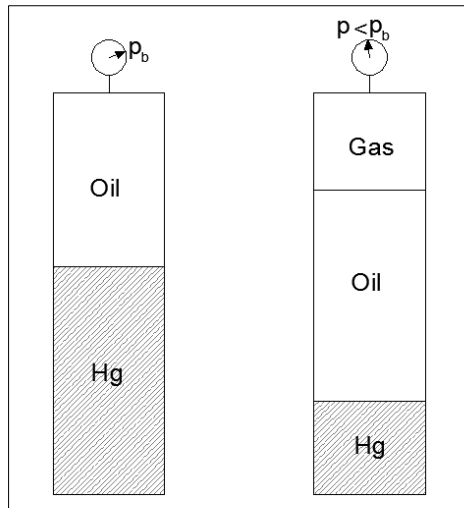


**Figure 1.7** Volume change as pressure is reduced below the bubble point at constant reservoir temperature

Direct substitution of formation volume factor of oil into the Equation 1.5 results in:

$$c_o = -\frac{1}{B_o} \left( \frac{\partial B_o}{\partial p} \right)_T \quad (1.7)$$

the change in liquid volume may be expressed by

$$\left( \frac{\partial B_o}{\partial p} \right)_T$$

the change in volume of free gas is

$$-\left( \frac{\partial R_s}{\partial p} \right)_T$$

Thus, at reservoir pressures below the bubble point, the total change in volume is the sum of the change in liquid volume and the change in free gas volume.

$$\left[ \left( \frac{\partial B_o}{\partial p} \right)_T - B_g \left( \frac{\partial R_s}{\partial p} \right)_T \right]$$

where  $B_g$  is inserted to convert the volume of evolved gas to reservoir conditions. Consequently, the fractional change in volume as pressure changes is:

$$c_o = -\frac{1}{B_o} \left[ \left( \frac{\partial B_o}{\partial p} \right)_T - B_g \left( \frac{\partial R_s}{\partial p} \right)_T \right] \quad (1.8)$$

This is consistent with Equation 1.7 since the derivative of  $R_s$  with respect to pressure is zero at pressures above the bubble point. The complete graph of compressibility as a function of reservoir pressure is given in Figure 1.8. There is a discontinuity at the bubble point. The evolution of the first bubble of gas causes a large shift in the value of compressibility. Equation 1.5 applies at pressures above the bubble point and Equation 1.8 applies at pressures below the bubble point.

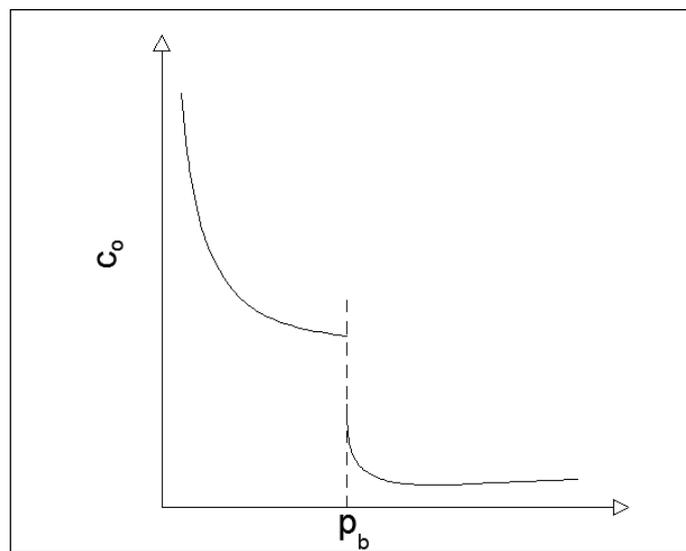


**Figure 1.8** Typical shape of the coefficient of isothermal compressibility of oil as a function of pressure at constant reservoir temperature

### ***1.3. Reservoir Engineering use of Volumetric Factors***

The formation volume factors and the solution gas-oil ratios are used, among others in material balance equations (MBE). The material balance equation has long been recognized as one of the basic tools of reservoir engineers for interpreting and predicting reservoir performance. It can be used to:

- Estimate initial hydrocarbon volumes in place
- Predict future reservoir performance
- Predict ultimate hydrocarbon recovery
- Identify drive mechanism

The general form of the material balance equation was first presented by Schilthuis<sup>[6]</sup> in 1941. The equation is derived as a volume balance which equates the cumulative observed production, expressed as an underground withdrawal, to the expansion of the fluids in the reservoir resulting from a finite pressure drop. The MBE is the only method that employs the dynamic response of the reservoir to production and allows the identification of the natural drives contributing to hydrocarbon production. The situation is depicted in Figure 1.9 in which (a) represents the total reservoir fluid volume at the initial pressure,  $p_i$ , in a reservoir which has a gas-cap. The total fluid volume in this diagram is the hydrocarbon pore volume of the reservoir (HCPV). Figure 1.9 (b) illustrates the effect of reducing the pressure by an amount  $\Delta p$  and allowing the reservoir fluid volumes to expand in the reservoir. The original HCPV is still drawn in this diagram as the solid line. Volume A corresponds to the increment due to the expansion of the oil plus the originally dissolved gas in it, while volume increase B is due to the expansion of the initial gas in the gas-cap. The third volume increment C is the decrease in HCPV due to the combined effects of the expansion of the connate water and reduction in reservoir pore volume.

If the total observed surface production of oil and gas is expressed in terms of underground withdrawal, evaluated at the lower pressure  $p$ , (which means effectively, taking all the surface production back down to the reservoir at this lower pressure) then it should fit into the volume  $A + B + C$  which is the total volume change of the original HCPV. Thus the volume balance can be evaluated in reservoir barrels as:

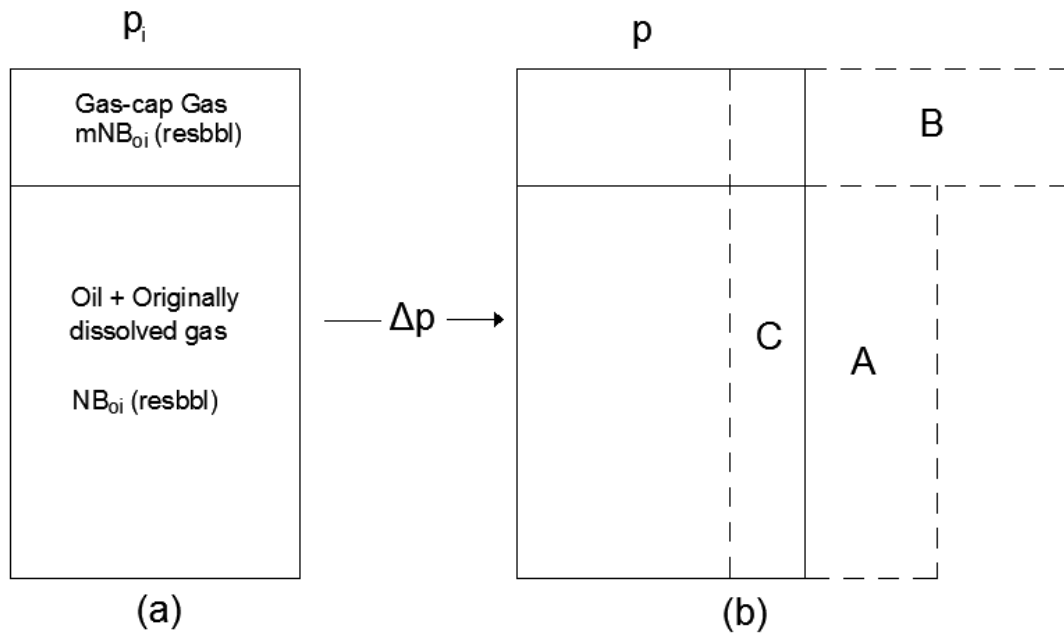


**Figure 1.9** Volume changes in the reservoir associated with a finite pressure drop  $\Delta p$ ; (a) volumes at initial pressure, (b) at the reduced pressure<sup>[7]</sup>

Underground withdrawal (rb) = Expansion of oil + originally dissolved gas (rb)  
 + Expansion of gascap gas (rb)  
 + Reduction in HCPV due to connate water expansion and decrease in the pore volume (rb)

Before evaluating the various components in the above equation it is first necessary to define the following parameters.

$N_p$ : Is the cumulative oil production in stock tank barrels, STB

$R_p$ : Is the cumulative gas to oil ratio both measured at standard conditions

$M$ : Is the ratio of initial hydrocarbon volume of the gas-cap to the initial hydrocarbon volume of the oil

$N$ : is the initial oil in place in stock tank barrels (STB) and is defined by the following expression:

$$N = \frac{V \phi (1 - S_{wc})}{B_{oi}}$$

Where:

$V$ : Net bulk volume of reservoir

$\phi$ : Porosity

$S_{wc}$ : Connate water saturation

$B_{oi}$ : FVF of oil at initial reservoir pressure

Then the expansion terms in the material balance equation can be evaluated as follows.

### a) Expansion of oil plus originally dissolved gas

There are two components in this term:

- Liquid expansion

The  $N$  STB will occupy a reservoir volume of  $NB_{oi}$  resbbl, at the initial pressure, while at the lower pressure  $p$ , the reservoir volume occupied by the  $N$  STB will be  $NB_o$ , where  $B_o$  is the oil formation volume factor at the lower pressure. The difference gives the liquid expansion as:

$$N(B_o - B_{oi}) \text{ (res bbl)}$$

- Liberated gas expansion

Since the initial oil is in equilibrium with a gas-cap, the oil must be at saturation or bubble point pressure. Reducing the pressure below  $p_i$  will result in the liberation of solution gas. The total amount of solution gas in the oil is  $NR_{si}$  scf. The amount still dissolved in the  $N$  STB of oil at the reduced pressure is  $NR_s$  scf. Therefore, the gas volume liberated during the pressure drop  $\Delta p$ , expressed in reservoir barrels at the lower pressure, is:

$$N(R_{si} - R_s)B_g \text{ (resbbl)}$$

### b) Expansion of the gas-cap gas

The total volume of gas-cap gas is  $mNB_{oi}$  resbbl, which in scf may be expressed as:

$$G = \frac{mNB_{oi}}{B_{gi}} \text{ (scf)}$$

This amount of gas, at the reduced pressure  $p$ , will occupy a reservoir volume:

$$mNB_{oi} \frac{B_g}{B_{gi}} \text{ (resbbl)}$$

Therefore, the expansion of the gas-cap, is:

$$mNB_{oi} \left( \frac{B_g}{B_{gi}} - 1 \right) \text{ (resbbl)}$$

**c) Change in the HCPV due to the connate water expansion and pore volume reduction**

The total volume change due to these combined effects can be mathematically expressed as:

$$d(HCPV) = -dV_w + dV_f$$

or, as a reduction in the hydrocarbon pore volume, as:

$$d(HCPV) = -(c_w V_w + c_f V_f) \Delta p$$

Where:

$V_w$ : Is the connate water volume equal to  $V_f \times S_{wc} = (HCPV) S_{wc} / (1 - S_{wc})$

$V_f$ : Is the total pore volume equal to  $HCPV / (1 - S_{wc})$

$c_w$ : Water compressibility

$c_f$ : Pore compressibility

Since the total HCPV including the gas-cap, is:

$$(1 + m)NB_{oi}$$

then, the HCPV reduction can be expressed as:

$$-d(HCPV) = ((1 + m)NB_{oi} \left( \frac{c_w S_{wc} + c_f}{1 - S_{wc}} \right) \Delta p$$

This reduction in the volume which can be occupied by the hydrocarbons at the lower pressure,  $p$ , must correspond to an equivalent amount of fluid production expelled from the reservoir, and hence should be added to the fluid expansion terms.

**d) Underground withdrawal**

The observed surface production during the pressure drop  $\Delta p$  is  $N_p$  STB of oil and  $N_p R_p$  scf of gas. When these volumes are taken down to the reservoir at the reduced pressure  $p$ , the volume of oil plus dissolved gas will be  $N_p B_o$  res bbl. All that is known about the total gas production is that, at the lower pressure,  $N_p R_s$  scf will be dissolved in the  $N_p$  STB of oil. The remaining produced gas,  $N_p (R_p - R_s)$  scf is therefore, the total amount of liberated and gas-cap gas produced

during the pressure drop  $\Delta p$  and will occupy a volume  $N(R_p - R_s)B_g$  resbbl at the lower pressure. The total underground withdrawal term is therefore:

$$N_p(B_o + (R_p - R_s)B_g) \text{ (resbbl)}$$

Therefore, equating this withdrawal to the sum of the volume changes in the reservoir, gives the general expression for the material balance, as:

$$\begin{aligned} N_p(B_o + (R_p - R_s)B_g) = \\ = NB_{oi} \left[ \frac{(B_o - B_{oi}) + (R_{si} - R_s)B_g}{B_{oi}} + m \left( \frac{B_g}{B_{gi}} - 1 \right) + (1 + m) \left( \frac{c_w S_{wc} + c_f}{1 - S_{wc}} \right) \Delta p \right] \\ + (W_e - W_p)B_w \end{aligned}$$

in which the final term  $(W_e - W_p)B_w$  is the net water influx into the reservoir. This has been added to the right hand side of the expression since any such influx must expel an equivalent amount of production from the reservoir thus increasing the left hand side of the equation by the same amount. In this influx term:

$W_e$ : Is the cumulative water influx from the aquifer into the reservoir, STB

$W_p$ : Is the cumulative amount of aquifer water produced, STB

$B_w$ : Is the water formation volume factor, res bbl / STB

$B_o$ : Is generally close to unity since the solubility of gas in water is rather small and this condition will be assumed throughout this text.

Nevertheless, material balance equation contains some limitations which should be taken into account:

- It is a zero dimensional tank model, meaning that it is evaluated at a point in the reservoir
- It considers average values of fluid properties for the entire reservoir
- Cannot be used to calculate fluid or pressure distributions
- Cannot be used to locate well locations
- Cannot be used to calculate the effect of well locations and production on hydrocarbon recovery

### 1.3.1. Reservoir Engineering use of Isothermal Compressibility Coefficient

The value of the isothermal compressibility coefficient is essentially the controlling factor in identifying the type of reservoir fluid. Reservoir fluids are generally classified into three groups:

- **Incompressible fluids** – These are fluids whose volume does not change considerably with pressure i.e. the values of the coefficient of isothermal compressibility for these fluids can be considered as being rather constant. Incompressible fluid does not exist in the real world; however, this behavior may be assumed for black oils to simplify the derivation and the final form of flow equations.
- **Slightly Compressible fluids** – These “slightly” compressible fluids exhibit small changes in volume, or density, with changes in pressure i.e. there is a slight change in the value of the coefficient of isothermal compressibility with changes in pressure. Crude oil and formation water fit into this category.
- **Compressible fluids** – These fluids experience a large change in volume as a function of a change in pressure i.e. the coefficient of isothermal compressibility changes drastically with a change in pressure. All gases are considered as compressible fluids

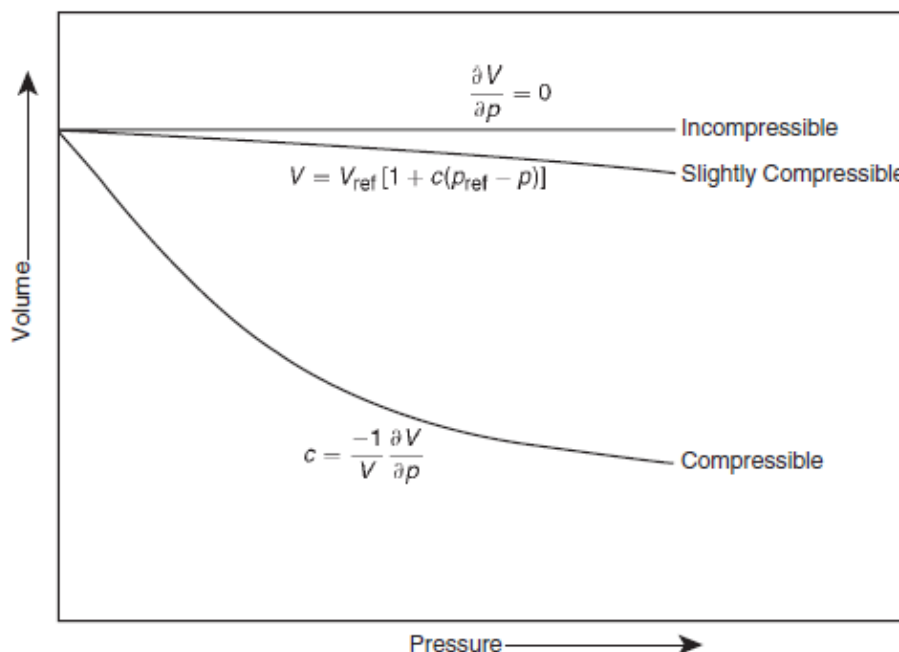


Figure 1.10 Pressure versus Volume/Compressibility relationship<sup>[8]</sup>

The isothermal compressibility is used also for the extension of reservoir fluid properties such as oil formation volume factor, specific volume and oil density at pressures higher than their bubble point pressure. This application is used for crude oil production simulation. Indicatively, computation of  $B_o$  for pressures above bubble point pressure is presented below.

Equation 1.7 can be integrated if  $c_o$  is assumed to remain constant as pressure changes.

$$c_o \int_{p_b}^p dp = - \int_{B_{ob}}^{B_o} \frac{1}{B_o} \partial B_o$$

results in

$$c_o(p - p_b) = -\ln\left(\frac{B_o}{B_{ob}}\right)$$

applying the exponential function in the above equation, we get

$$EXP[-c_o(p - p_b)] = EXP[\ln(B_o/B_{ob})]$$

Eventually, we end up with the following expression which calculates the oil formation volume factor for pressures above bubble point pressure given the value of that pressure.

$$B_o = B_{ob}EXP[-c_o(p - p_b)] \quad (1.9)$$

Moreover, the isothermal compressibility coefficient is required in solving other reservoir engineering problems, including:

- Transient fluid flow problems
- Determination of the physical properties of the undersaturated crude oil.
- Extension of fluid properties from values at the bubble point pressure to higher pressures of interest
- Design of high-pressure surface equipments

## ***1.4. Ways of obtaining readily available reliable estimates of Volumetric Factors***

Accurate estimation of  $R_s$ ,  $B_o$ ,  $B_g$ ,  $B_t$  and  $c_o$  is carried out by laboratory experiments performed on samples of the reservoir oil, known as PVT Study. Once PVT report becomes available, a tuned Equation of State (EOS) model of the fluid is developed and all these volumetric factors are then calculated using this model. A thorough PVT analysis takes about three weeks to be conducted and in the case of remote field locations, expedition and transportation problems can sometimes delay the results for months, or even 1 year. It also requires a lot of money to be spent. In the meantime, crucial reservoir engineering decisions have to be made. The oil industry is in need for getting reliable values of the volumetric factors early enough and before the EOS model is developed and tuned.

To avoid long PVT report delivery times particularly for remote locations on-site PVT tests have been developed which are often performed with portable miniature equipment to provide in situ measurements of fluid properties and compositional analysis that both can be used to tune an EOS. The EOS can then be used right away to predict approximately the phase behavior and PVT properties of the reservoir fluids.

An alternative and much more frequently used method to obtain PVT data on-site is by employing empirical correlations that relate easily obtained production data acquired during the well test, such as oil gravity, reservoir temperature and gas-oil ratio (GOR) to parameters such as the oil formation volume factor and the bubble-point pressure. All these methods will be analyzed in detail in Chapter 2.

## *C H A P T E R 2*

# **Determination of Oil Formation Volume Factor and Isothermal Compressibility Coefficient**

This chapter deals with the methods of obtaining the formation volume factor of oil,  $B_o$ , and isothermal compressibility coefficient of oil,  $c_o$ , for crude oil systems under undersaturated conditions. Determination of these PVT properties is done using the following methods:

- **Laboratory measurements** (or PVT Studies) performed on bottom-hole or recombined surface oil samples
- **On-site PVT Tests**
- **Empirical Correlations** within appropriate range of application
- **Artificial Neural Networks (ANN) models**
- **Equations of State (EOS)** with appropriate calibrations

Each one of these first four methods will be examined in details in the following lines, while the last one will be analyzed separately in the next chapter.

## 2.1. Laboratory measurements of $B_o$ and $c_o$

### 2.1.1. Determination of Oil Formation Volume Factor

Firstly, the PVT studies that are performed will be analyzed and then the appropriate conversion of the results of these studies into fluid properties of petroleum engineering interest (i.e.  $B_o$  and  $c_o$ ), where necessary will be presented.

A PVT study is performed on crude oil samples collected from the bottom of the wellbore or from the surface and constitutes the most accurate and reliable way for reservoir fluid's physical properties determination. Standard PVT fluid studies are designed to simulate the phase behavior that prevails during the simultaneous fluid flow of oil and gas from the reservoir to the surface. The production path of reservoir fluids from the reservoir to surface is also simulated in the laboratory at reservoir temperature. During this process, the bubble-point pressure,  $p_b$ , is measured. Likewise, the oil volumes and the amount of gas released are measured and used to determine oil FVF as function of pressure. The main procedures performed on reservoir fluid samples include:

- Decompression of the fluid sample to determine the bubble point pressure and the coefficient of isothermal compressibility of the oil,  $c_o$ .
- Differential expansion of the fluid sample to determine the PVT parameters  $B_o$ ,  $R_s$  and  $B_g$ .
- Flash expansion of fluid samples through various separator trains to enable the adjustment of laboratory derived PVT data to match field separator conditions.

#### 2.1.1.1. Sampling of Reservoir Fluids

For a PVT study to be accurate, **representative samples** of the reservoir fluid for the laboratory work are required. The following discussion considers the available procedures for obtaining a sample from a well. Particular emphasis is placed on the limitations of methods which may cause the sample to be non-representative of the reservoir fluid.

The field situation usually determines the method of sampling employed. The observed properties of the field sample and the sampling conditions should be recorded prior to the shipment of the sample to the laboratory for testing. Obtaining several samples provides accurate estimation of reservoir fluid

properties and confirms the accuracy of the sampling technique. In case that the field operating conditions will change, new PVT analyses should be performed to take into account of this factor.

### *Bottom-Hole Samples*

Many types of bottom-hole samplers have been devised and described in the literature<sup>[1],[2],[3],[4],[5]</sup>. The mechanical design of the devices introduces some error into the sampling operation; however, these errors are probably of less importance than those resulting from other difficulties that might be encountered.

It is often questionable whether the fluids in the tubing at the point where a bottom-hole sample is taken are representative of the reservoir hydrocarbons. This is particularly true if there has been considerable drawdown of the well prior to sampling, if several zones containing fluids of dissimilar properties are produced together, if the gas and liquid are not homogeneously mixed in the proportions in which they existed in the formation, and if both gas cap and oil zones of a reservoir are open simultaneously to the well bore.

### *Recombined Samples*

According to this method, both the produced liquid and gas are sampled, usually from the high pressure separator while the production rate is carefully controlled. These two samples are then combined at the same proportion as the two phases are produced from the well.

There are also some possible inaccuracies in using recombined samples and they must be corrected for, if the results obtained from the recombination are to be representative. There is necessity for accurate gauging and steady-state well conditions during sampling. If the well is producing both gas from a gas cap and gas released from solution there is no expectation of taking representative sample.

## **2.1.1.2. HPHT PVT Cell**

A widely used apparatus for performing a reservoir fluid study is the HPHT (High Pressure High Temperature) PVT cell (also called DB Robinson Jefri PVT cell) developed by schlumberger company. A schematic diagram of the apparatus is presented in Figure 2.1. The cell is used to test both surface and bottom-hole samples and the recombination of the former is done in the cell. The PVT cell is placed in an air-bath which controls the PVT cell temperature to within  $\pm 0.1$  °C. The sample is placed in a glass cylinder, secured between two full-length sight glass windows, inside a stainless steel frame. This design allows

for unimpaired visibility of the entire contents of the cell. Moreover, the exposure of the sample to metal components has been eliminated. Equilibration of the fluid under investigation is achieved by means of a magnetically coupled impeller mixer, called magnetic stirrer, mounted on the bottom end cap. The volume of the cell and hence the pressure of the sample is controlled by a variable volume computer-controlled positive displacement pump which is allowed for the injection or the removal of the transparent displacing fluid (hydraulic oil). The hydraulic oil is connected to the outer steel shell to maintain a balanced (minimal) differential pressure on the glass cylinder.

The maximum capacity of the PVT cell is 8.3 in<sup>3</sup> (135.6 cm<sup>3</sup>), the maximum operating temperature is 400 °F (200 °C) and the maximum operating pressure is 15,000 psi (103 MPa).

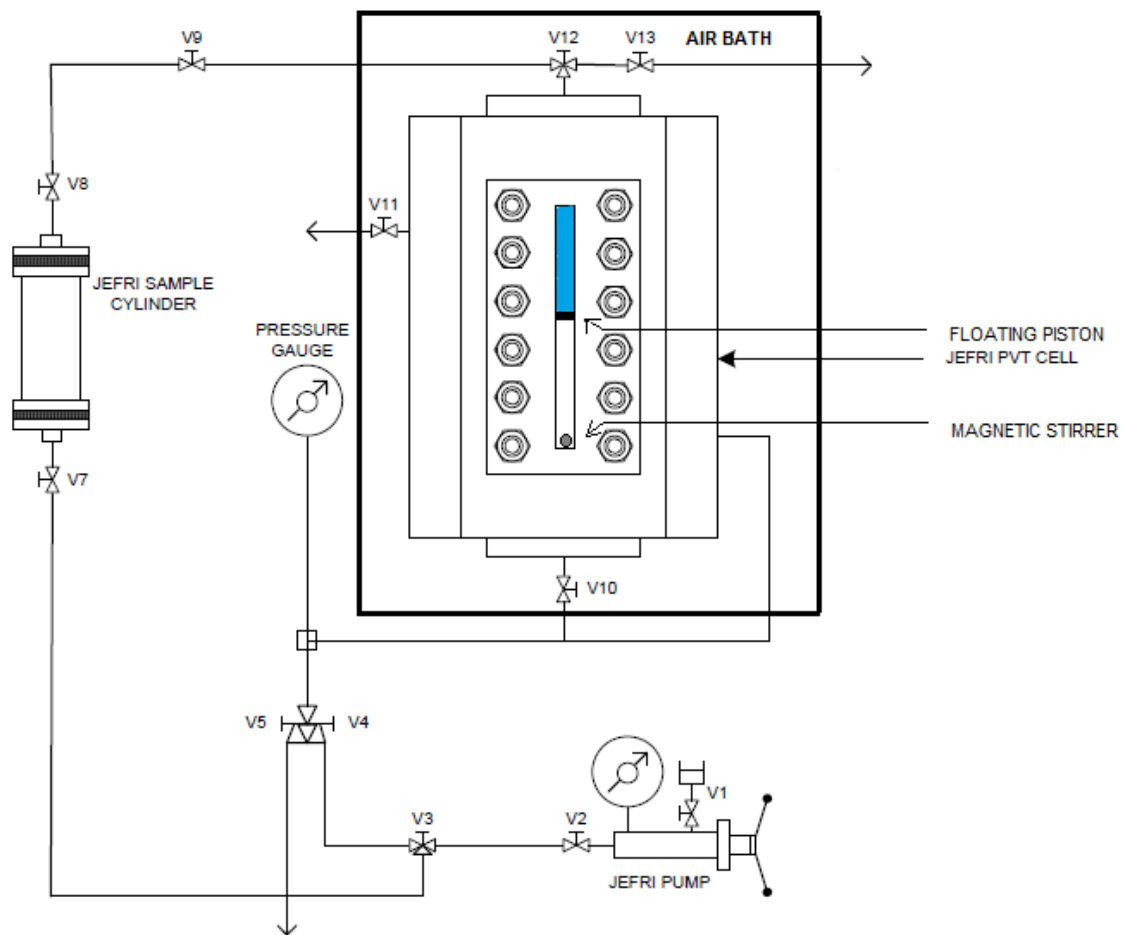


**Figure 2.1** Schematic of the HPHT PVT cell and associated equipment<sup>[6]</sup>

### 2.1.1.3. Flash Vaporization Experiment

The flash vaporization study is presented schematically in Figure 2.2. In this experiment (also called *flash liberation*, *flash expansion*, *constant composition expansion* and *constant mass study*) the pressure in the PVT cell is adjusted equal to or greater than initial reservoir pressure and the temperature is set at reservoir temperature. The pressure is subsequently reduced in stages by increasing the volume of the liquid and at each step the pressure and the total volume,  $V_t$ , of the cell contents are recorded. The cell is agitated regularly to ensure that the contents are at equilibrium. As soon as the bubble point pressure is reached, gas is liberated from the oil and the overall compressibility of the system increases significantly.

Thereafter, small changes in pressure will result in large changes in the total fluid volume contained in the PVT cell. In this manner, the flash expansion experiment can be used to "feel" the bubble point. All values of total volume,  $V_t$ , are divided by the volume at the bubble point pressure and the data are reported as **relative volume**. The symbol  $(V_t/V_b)_F$  is used which means total volume divided by volume at the bubble point for a flash vaporization.

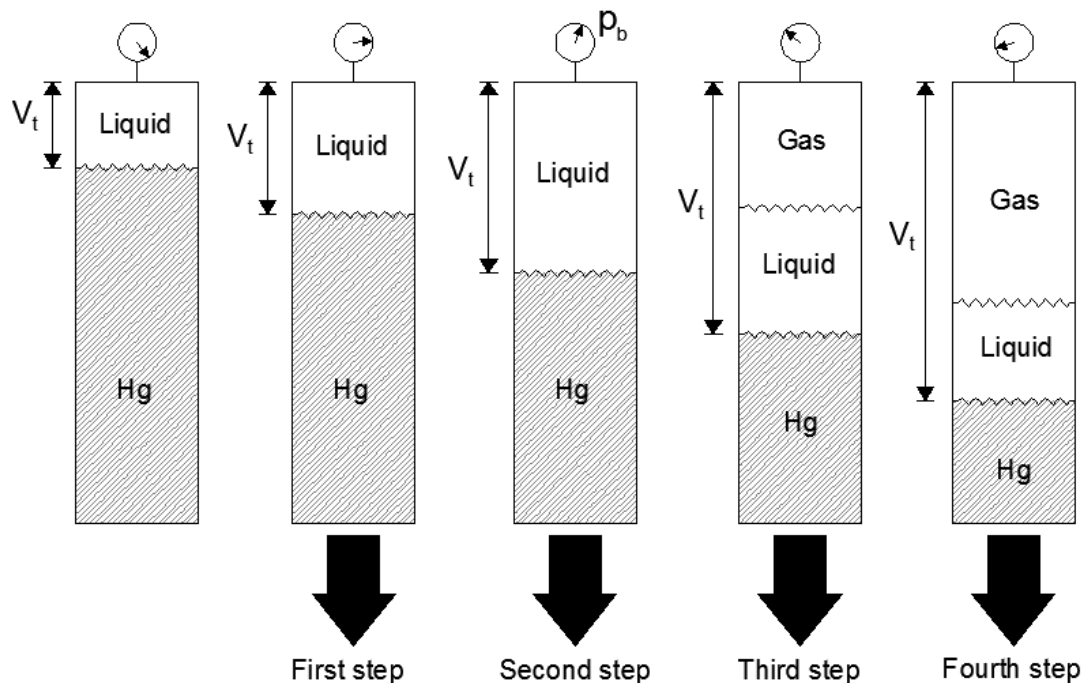


Figure 2.2 Illustration of flash vaporization experiment<sup>[7]</sup>

### 2.1.1.4. Differential Vaporization (DV) Experiment

Figure 2.3 illustrates the *differential vaporization* (also called *differential liberation*) study. The experiment starts at bubble point pressure (since above this pressure the flash and differential experiments are identical) and temperature is set at reservoir temperature. Pressure is reduced by increasing cell volume and the cell is agitated to ensure equilibrium between gas and liquid. In contrast to the flash expansion, after each stage of the differential liberation, the total amount of gas liberated during the latest pressure drop is removed from the PVT cell at constant pressure and as a result, the new overall composition of the reservoir fluid becomes heavier. The gas is collected and its specific gravity and volume are measured both at cell and at standard conditions. The volume of the liquid remaining in the cell,  $V_o$ , is measured as well. The process is repeated in steps until atmospheric pressure is reached. Then, temperature is reduced to 60 °F and the volume of the remaining liquid is measured. This is called **residual oil**,  $V_{sc}$ . Each one of the values of volume of cell liquid,  $V_o$ , is divided by the volume of the residual oil. The result is called **oil formation volume factor** and is given the symbol  $B_{oD}$ . The subscript  $D$  refers to the fact that this parameter was determined by the differential vaporization test. Mathematically,  $B_o$  is expressed as:

$$B_{oD} = \frac{V_o}{V_{sc}} \quad (2.1)$$

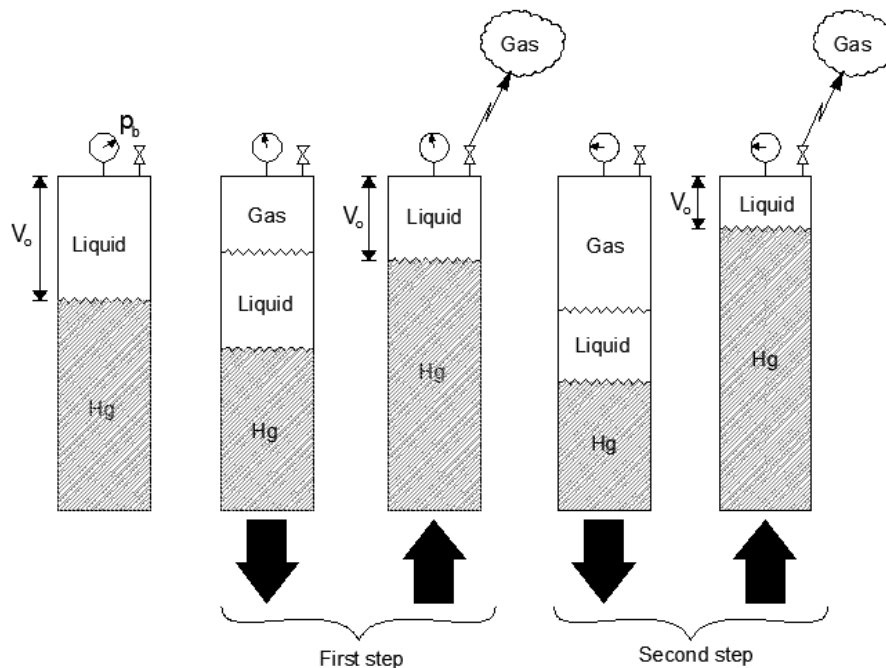


Figure 2.3 Illustration of differential vaporization experiment<sup>[8]</sup>

### 2.1.1.5. Separator Test

The two objectives of conducting a separator test is to provide the essential laboratory information necessary for determining the optimum surface separation conditions, which in turn will maximize the stock-tank oil production and for being able to generate those  $B_o$  and  $R_s$  values versus pressure that correspond to the actual production path and will be used for reservoir and production engineering calculations. The test involves placing an oil sample at its bubble point pressure and reservoir temperature in a PVT cell, Figure 2.1. The volume of the sample is measured as  $V_b$ . The oil sample is then displaced and flashed through a laboratory multistage separator system—commonly one to three stages, Figure 2.4. The pressure and temperature of these stages are set to represent the desired or actual surface separation facilities. Pressure in the cell is held constant at the bubble point by reducing cell volume as the liquid is expelled. The gas liberated from each stage is removed and its specific gravity and volume at standard conditions are measured. The volume of the remaining oil in the last stage (representing the stock-tank condition) is measured at standard conditions and recorded as  $(V_o)_{sc}$ . These experimental measured data can then be used to determine the *oil formation volume factor at the bubble point pressure* as follows:

$$B_{osb} = \frac{V_b}{(V_o)_{sc}} \quad (2.2)$$

The subscript  $S$  indicates that is a result of a separator test, and the subscript  $b$  indicates bubble point conditions in the reservoir.

The above laboratory procedure is repeated at a series of different separator pressures and different separator temperatures. It is usually recommended that four of these tests be used to determine the **optimum separator pressure**, which is usually considered the separator pressure that results in minimum oil formation volume factor. At this pressure, the API gravity will be a maximum and the total evolved gas, i.e., the volume of the separator gas and the stock-tank gas will be at a minimum.

The above procedure can be understood by considering Table 2.1 which was reported by Moses (1986)<sup>[9]</sup> and represents a typical example of a set of separator tests for a two-stage separation.

**Table 2.1**  
Separator Test Data

Separator Pressure, (psig)	Temperature (°F)	$B_{oSb}$
50 to 0	75	1.481
100 to 0	75	1.474
200 to 0	75	1.483
300 to 0	75	1.495

By examining the laboratory results it is obvious that the oil formation volume factor varies from 1.474 bbl/STB to 1.495 bbl/STB. The optimum separator pressure is around 100 psia, considered to be the separator pressure that results in the minimum value of oil formation volume factor.

The conclusion reached, from the foregoing description of the effects of surface separation, is **that the volume of equilibrium oil collected in the stock tank is dependent on the production path**. This in turn means that the oil formation volume factor which is measured in terms of volume "per stock tank barrel" must also be dependent on the selected separation train and cannot be assigned an absolute value.

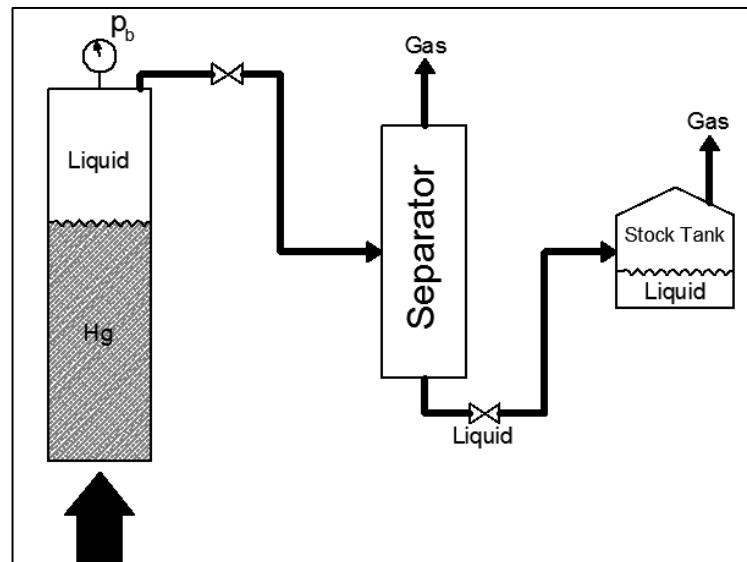


**Figure 2.4** Laboratory separator test

Generally, petroleum engineers consider that the gas liberation process in the reservoir can be represented by the differential vaporization process. The above assumption it sounds reasonable because the gas phase is more mobile than the oil phase and leaves the oil in which it was originally contained behind

as both are flowing to the wellbore. The fluid produced from the reservoir to the surface is considered to have undergone a flash process.

The currently used PVT measurements based on these assumptions for estimating the value of  $B_o$  for pressures above and below bubble-point pressure are presented next.

### 2.1.1.6. Composite Liberation Test

Another type of test, called a **composite liberation test**, has been suggested by Dodson, Goodwill, and Mayer (1953)<sup>[10]</sup> and represents a combination of differential and flash liberation processes. The laboratory test, commonly called the *Dodson test*, provides the most accurate way of obtaining the value of oil formation volume factor as it illustrates exactly the volumetric behavior of reservoir fluid during production from the reservoir to the stock-tank. The experimental procedure is summarized in the following steps.

**Step 1** A large representative fluid sample is placed into the main test cell at a pressure high enough to insure single phase behavior. The temperature of the cell then is raised to reservoir temperature.

**Step 2** The pressure is reduced in steps, and the change in the oil volume is recorded. The process is repeated until the first bubble of gas is evolved.

**Step 3** A carefully measured small volume of single phase oil from the main test cell is removed at constant pressure to another, smaller auxiliary test cell. The temperature of this cell is held to that existing in the first separator at the well head; the sample of oil in the auxiliary cell is flashed to the pressure of the first surface separator after noting the original volume of oil. The gas liberated from this first auxiliary cell flash is removed from the cell and its volume and specific gravity measured. The remaining volume of oil in the auxiliary cell is recorded. This oil is then flashed to the pressure of the next separator while the cell is held at the temperature of this separator. This flashing process is repeated as many times as there are surface separators, including a final flash to simulate the liberation to stock tank conditions. The oil formation volume factor,  $B_o$ , is then calculated from the measured volumes:

$$B_o = \frac{(V_o)_{p,T}}{(V_o)_{st}} \quad (2.3)$$

where

$(V_o)_{p,T}$ : Volume of oil removed from the test cell at constant pressure  $p$

$(V_o)_{st}$ : Volume of stock-tank oil

**Step 4** The volume of the oil remaining in the main cell is allowed to expand through a pressure decrement while being held at reservoir temperature. The gas evolved in this pressure decrement is removed as in the differential liberation.

**Step 5** Following the gas removal, step 3 is repeated and  $B_o$  is calculated.

**Step 6** Steps 3 through 5 are repeated at several progressively lower reservoir pressures to secure a complete PVT relationship.

This type of analysis, while more accurately representing the PVT behavior of complex hydrocarbon mixtures up to the tank oil, is more difficult and costly to perform than the other conventional tests. It also requires the availability of large samples of the reservoir fluid, therefore, composite liberation test usually is not included in a routine fluid property analysis.

An alternative to overcome the drawbacks that imposes the Dodson method for the accurate prediction of  $B_o$  value is the use of computational techniques which combine the differential and flash vaporization data with the data of separator tests.

#### **2.1.1.7. Adjustment of Differential Vaporization and Flash Vaporization Data to Separator Conditions to Give $B_o$ for Use in the Field**

In the DV study the separation of gas at surface conditions is not taken into account, as the experiment is performed at reservoir temperature. Additionally, the conditions at which the vaporization of the oil is conducted in the DV test, are more intensive than the conditions prevailing during production.

For those reasons the  $B_o$  value resulting from a DV study corresponds to higher values than the  $B_o$  value resulting from the actual separator test as Figure 2.5 shows.

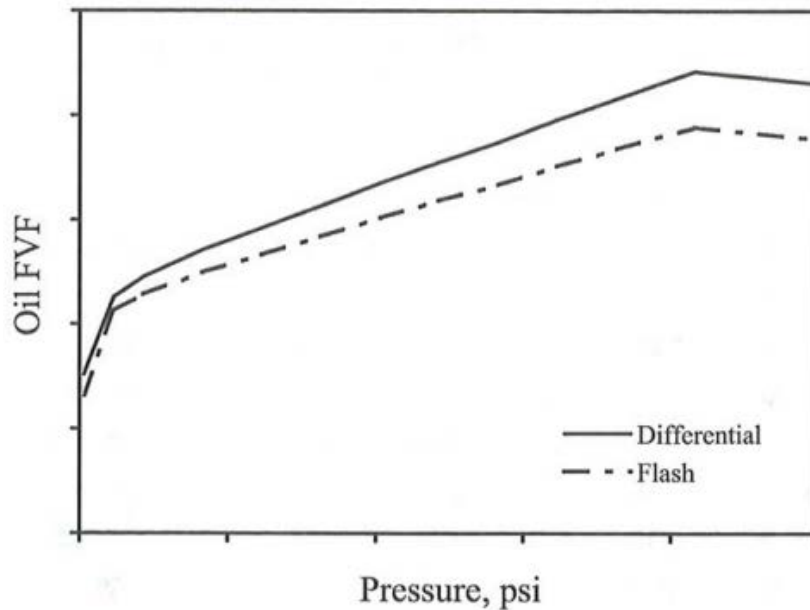


**Figure 2.5** Typical oil FVF curves from differential vaporization study and separator test<sup>[11]</sup>

- **Prediction of  $B_o$  for pressures above bubble-point pressure**

At pressures *above bubble-point pressure* oil formation volume factor can be calculated from a combination of constant mass (flash vaporization) data and separator test data. McCain W.D, in 1990<sup>[12]</sup> proposed the following expression:

$$B_o = \left( \frac{V_t}{V_b} \right)_F B_{oSb} \quad (2.4)$$

- **Prediction of  $B_o$  for pressures below bubble-point pressure**

Amyx et al (1960), Dake, P.L. (1978), Ahmed, T. (1989) and McCain W.D. (1990)

At pressures *below the bubble-point pressure* oil formation volume factor is calculated from a combination of differential vaporization and separator test data. The most widely used method which has been proposed by Amyx et al (1960)<sup>[13]</sup>, Dake, P.L. (1978)<sup>[14]</sup>, Ahmed, T. (1989)<sup>[15]</sup> and McCain W.D. (1990)<sup>[12]</sup> is expressed by the following equation:

$$B_o = B_{oD} \frac{B_{oSb}}{B_{oDb}} \quad (2.5a)$$

or equivalently:

$$B_o = \left( \frac{V_o}{V_b} \right)_D B_{oSb} \quad (2.5b)$$

The main drawback of this method is that for low pressures the  $B_o$  may lead to a value of less than 1, which does not conform to the physical behavior. Because of this problem, the range of application of the calculation procedure is limited to pressures above 500 psi<sup>[11]</sup>.

#### Al-Mahroun (2003)<sup>[11]</sup>

The oil formation volume factor for pressures below bubble-point pressure, as proposed by Al-Mahroun (2003), is adjusted proportionally and is evaluated from the following equation:

$$B_{oi} = B_{oSb} + \frac{B_{oDb} - B_{oDi}}{B_{oDb} - B_{oDn}} (B_{oDn} - B_{oSb}) \quad (2.6)$$

The subscript  $i$  refers to the  $i$ th differential stage, while the subscript  $n$  corresponds to the number of stages in the differential vaporization test.

#### **Example**

As an example for the calculation of oil FVF for pressures below the bubble-point pressure with the two methods presented previously, the results of a differential liberation and a separator test are listed in Table 2.2<sup>[11]</sup>

**Table 2.2**  
Differential and Flash Test data

No	p (psi)	B <sub>oD</sub>
1	p <sub>b</sub> = 2,079	1.342
2	1,815	1.316
3	1,615	1.296
4	1,415	1.274
5	1,215	1.255
6	1,015	1.235
7	815	1.213
8	615	1.192
9	415	1.171
10	215	1.145
11	115	1.126
12	15	1.053
Flash	2,079	B <sub>oSb</sub> = 1.289

Table 2.3 presents the adjustment of oil FVF to the separator conditions according to the Amyx (1960) and Dake's (1978) and to the Al-Mahroun's (2003) method. Columns 1 and 2 in Table 2.3 are from Table 2.2, while, Column 3 is calculated from Equation 2.5a and Column 4 is determined from Equation 2.6.

**Table 2.3**  
Adjustment of the oil FVF curve to separator conditions

Pressure (psi)	Differential Data Curve	Amyx & Dakes	Al-Mahroun's (2003) Method
2,079	1.342	1.2890	1.2890
1,815	1.316	1.2640	1.2678
1,615	1.296	1.2448	1.2514
1,415	1.274	1.2237	1.2335
1,215	1.255	1.2054	1.2180
1,015	1.235	1.1862	1.2016
815	1.213	1.1651	1.1837
615	1.192	1.1449	1.1665
415	1.171	1.1248	1.1494
215	1.145	1.0998	1.1281
115	1.126	1.0815	1.1126
15	1.053	1.0114	1.0530

Figure 2.6 compares the three curves: differential data, the Amyx and Dake's method (Equation 2.5) and the Al-mahroun's method (Equation 2.6). The figure shows that at the bubble-point pressure, both this method and the Amyx and Dake's method are giving the same value of oil FVF, and it is equal to the bubble-point value obtained from the flash liberation. At atmospheric pressure,

the oil FVF values obtained from both the differential liberation and this method are the same. This is because the last differential step is similar to a flash liberation. The data between the two endpoints are corrected proportionally, according to Equation 2.6. The Amyx and Dake's method gives values for oil FVF lower than the values obtained from the differential liberation at atmospheric pressure, which cannot be explained rationally.

As shown in Figure 2.6 the limitation imposed by the Amyx's et al. (1960) and Dake's (1978) method for the estimation of  $B_o$  for low pressures has been eliminated in this study, as even for atmospheric pressure the value of  $B_o$  is more than unity.

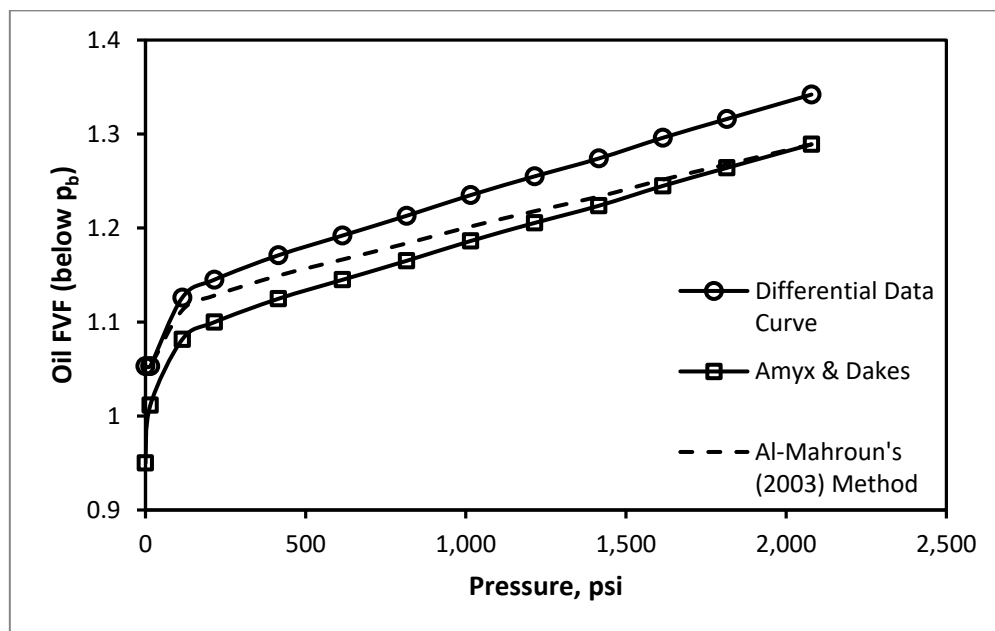


Figure 2.6 Adjustment of oil FVF to separator conditions<sup>[11]</sup>

## 2.1.2. Determination of Isothermal Compressibility Coefficient of Oil

- **Determination of  $c_o$  for pressures above bubble-point pressure**

The exact definition of isothermal oil compressibility coefficient,  $c_o$ , above the bubble-point pressure was presented by Equation 1.5 in Chapter 1 which expresses the fractional change of fluid volume per unit change in pressure (at constant reservoir temperature) in terms of derivatives.

Some applications require an average value of  $c_o$ . This value is determined by calculating the changes in the relative volume (from a flash liberation test) at

the indicated pressure interval and evaluating the relative volume at the lower pressure, or:

$$c_o = -\frac{1}{(V_t/V_b)_F} \frac{\Delta(V_t/V_b)_F}{\Delta p} \quad (2.7a)$$

or equivalently:

$$c_o = -\frac{1}{(V_t/V_b)_{F_2}} \frac{(V_t/V_b)_{F_1} - (V_t/V_b)_{F_2}}{p_1 - p_2} \quad (2.7b)$$

The subscripts 1 and 2 represent the corresponding values at the higher and lower pressure range, respectively.

Equation 2.7a is an expression of Equation 1.5 in terms of *differences*. Equation 2.7b is useful in approximating the  $c_o$  for single phase fluids undergoing small pressure changes. This assumption is not valid when the  $c_o$  varies during small pressure changes. It is further limited over large pressure changes by confusion over whether the denominator of Equation 2.7b should be  $(V_t/V_b)_{F_1}$  or  $(V_t/V_b)_{F_2}$ , or some value in between.

### **Example**

The following example illustrates the calculation of the average oil isothermal compressibility in the pressure range of 2,500 to 2,000 psi using the measured relative volume data presented in Table 2.4 from a flash liberation test<sup>[16]</sup>.

Apply Equation 2.7b to give:

$$c_o = -\frac{1}{0.9987} \frac{0.9890 - 0.9987}{2,500 - 2,000} = 19.43 \times 10^{-6} \text{ psi}^{-1}$$

**Table 2.4**  
Flash liberation data

Pressure, psig	Relative Volume
6500	0.9371
6000	0.9422
5500	0.9475
5000	0.9532
4500	0.9592
4000	0.9657
3500	0.9728
3000	0.9805
2500	0.9890
2400	0.9909
2300	0.9927
2200	0.9947
2100	0.9966
2000	0.9987
1936	1.0000

- **Determination of  $c_o$  for pressures below bubble-point pressure**

At pressures *below bubble-point pressure*, Equation 2.8 applies.

$$c_o = -\frac{1}{B_o} \left[ \left( \frac{\partial B_o}{\partial p} \right)_T - B_g \left( \frac{\partial R_s}{\partial p} \right)_T \right] \quad (2.8)$$

The derivative of  $B_o$  with respect to  $p$  is the slope of a plot of  $B_o$  against  $p$ . The slope is measured at the pressure of interest. The derivative of  $R_s$  with respect to  $p$  is obtained by plotting  $R_s$  against  $p$ . Equation 2.8 can be converted to:

$$c_o = -\frac{1}{B_o} \left( \frac{\partial R_s}{\partial p} \right)_T \left[ B_g - \left( \frac{\partial B_o}{\partial R_s} \right)_T \right]$$

The derivative of  $B_o$  with respect to  $R_s$  is relatively easy to determine since the slope of a plot of  $B_o$  against  $R_s$  is virtually constant for most crude oils. The above equations become:

$$c_o = -\frac{1}{B_{oD}} \left[ \left( \frac{\partial B_{oD}}{\partial p} \right)_T - B_g \left( \frac{\partial R_{sD}}{\partial p} \right)_T \right]$$

and

$$c_o = -\frac{1}{B_{oD}} \left( \frac{\partial R_{sD}}{\partial p} \right)_T \left[ B_g - \left( \frac{\partial B_{oD}}{\partial R_{sD}} \right)_T \right]$$

The current practice used to obtain as accurate as possible estimates of  $B_o$  value is tune an EOS based model against laboratory measurements, on representative reservoir fluid samples, to simulate the Dodson test. However, the laboratory measurements require long PVT report delivery times (months or even one year) and big volume of sample, that usually is not available. Those limitations have led to the development of alternative ways that give on-site and early enough satisfactorily estimates of  $B_o$  value. Such a method is presented below.

## ***2.2. Determination of $B_o$ from on-site PVT Tests***

A Schlumberger service called *Fluid Properties Estimation (FPE)* system, developed by Nikos Varotsis, and Paul Guieze<sup>[17]</sup>, provides simple measurements of key physical properties, specially selected to characterize the reservoir fluid, which are performed on site with easily operated, portable equipment. These measurements are used as calibration points to tune an EOS-based simulator that subsequently predicts the phase behavior of the fluids at reservoir, well, and surface conditions.

The FPE method is not intended to replace the PVT laboratory study performed on representative samples. Its purpose is to make fairly accurate estimates of physical property data as close as possible to their true values readily available and to offer fluid analysis data from samples that rarely pass the PVT laboratory's doorstep under typical circumstances.

The method currently is used only for testing oil reservoirs and, in particular, for bottom-hole samples (BHS's) representative of the reservoir fluid taken with either the repeat formation tester (DST/RFT) or a production sampler. The bubble-point pressure,  $p_b$ , of the sample at ambient temperature is determined conventionally by plotting recorded pressure versus sample volume.

The FPE service requires the flash of about 50 cm<sup>3</sup> of BHS to atmospheric pressure and ambient temperature inside a specially designed separator.

Density and mass measurements of the recovered stock tank liquid (STL) and volumetric measurements of the gas with calibrated syringes provide accurate calculation of the GOR of the direct flash.

For compositional analysis, the FPE system consists of two portable gas chromatographs GC's that are housed in a rack mounted inside an antivibration container. Figure 2.7 shows the two analyzers with the portable PC that controls the chromatographic runs, acquires and processes the signal, and performs the PVT simulation.

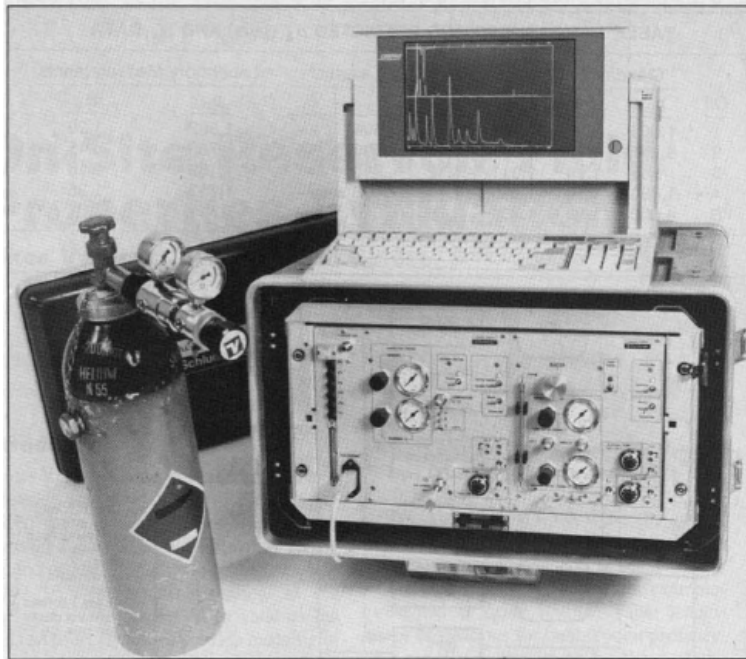


**Figure 2.7** FPE portable chromatographs with the PC

Other measurements performed on the samples include specific gravity, viscosity, and refractive index.

Then, the measurements obtained are introduced to an equation of state (EOS) – based thermodynamic model.

The final report includes the reservoir fluid's composition, bubble-point at bottom-hole conditions, and properties at saturation conditions, as well as predictions of how such important properties as separator GOR, tank GOR, densities, viscosities, FVF's, and compressibilities will vary as the reservoir pressure declines during production. The time required to complete the FPE service and to issue the final report is 2 hours. Figure 2.8 shows the flow path followed during an FPE test.

The FPE can also be used with surface samples but the bubble-point pressure, which is a very important calibration point for the regression analysis, will not be measurable. A bubble-point estimate must be made using correlations but the accuracy of FPE predictions will depend heavily on this estimate.

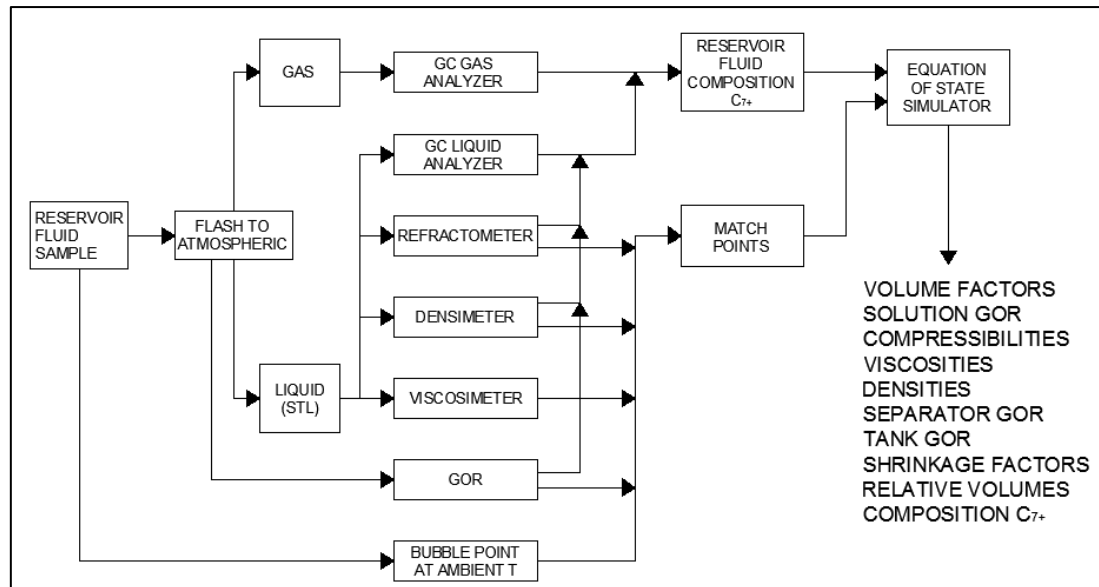


**Figure 2.8** Schematic showing the flow-path followed during an FPE test

In order to check the accuracy of the FPE results, wherever a full PVT report was available, 12 comparative studies were performed on reservoir oil samples with bubble-point range 109 to 4,780 psi and separator oil FVF range 1.03 to 3.20 taken either with the RFT or with a production sampler. The results of the FPE showed the estimated physical properties and compositional analyses of the fluids to be very close (less than 5% deviation) to values measured in the laboratory with the exception of the oil viscosity, where higher deviations occasionally had been encountered.

## ***2.3. Correlations currently used by the oil industry for oil FVF and oil compressibilities prediction***

### **2.3.1. Correlations for undersaturated oil FVF prediction**

An alternative to detour the limitations (discussed in the previous section) that imposes the acquiring of lab measurements required to tune an EOS model for the determination of  $B_o$  value is the use of empirical correlations. The accuracy that the empirical correlations provide (as it will be shown in Chapter 4) for the estimation of  $B_o$  value is fairly satisfactorily.

There are many empirical correlations for predicting PVT properties, most of them were developed using linear or non-linear multiple regression or graphical techniques. Although in several cases, fairly large databases have been employed in the development of these correlations, their inherent simplicity leads to a low degree of accuracy due to the small number of independent variables taken into account, the number of which rarely exceeds four. Moreover, geological conditions are considered important for the development of a correlation, because the chemical composition of crude oil differs from region to region. For this reason, it is difficult to obtain the same accurate results through empirical correlations for different oil samples having different physical and chemical characteristics. Engineers should modify these correlations for their application by recalculating the correlation constants for the region of interest.

The history of reservoir fluid properties correlation equations in the petroleum industry started more than five decades ago. Several reliable empirical correlations for calculating oil viscosity, oil formation volume factor, oil bubble point pressure, solution gas-oil ratio, gas formation volume factor and isothermal compressibility have been proposed over the years. Since the 1940's engineers have realized the importance of developing empirical correlation for oil bubble point pressure and oil formation volume factor. Studies carried out in this field resulted in the development of new correlations. Several studies of this kind were published by Katz (1942)<sup>[18]</sup>, Standing (May, 1947)<sup>[19]</sup> and Lasater (May, 1958)<sup>[20]</sup>. For several years, these correlations were the only source available for estimating bubble point pressure and oil formation volume factor when experimental data were unavailable. In the last thirty years there has been an increasing interest in developing new correlations for crude oils obtained from the various regions in the world. Glaso (May, 1980)<sup>[21]</sup>, Vazquez and Beggs (1980)<sup>[22]</sup>, Al-Marhoun (March, 1988)<sup>[23]</sup>, Elmabrouk (December, 2010)<sup>[24]</sup>, and Sulaimon et al (August, 2014)<sup>[25]</sup> carried out some of the recent studies.

The majority of published correlations provide the  $B_o$  at bubble-point pressure,  $B_{ob}$ , as functions of data measured during Well Test or estimated from other correlations. Such data include; solution GOR at bubble-point pressure,  $R_{sb}$ , gas specific gravity,  $\gamma_g$ , separator GOR, separator pressure,  $p_{sep}$ , stock-tank oil gravity,  $\gamma_o$ , and reservoir temperature,  $T_{res}$ .

The  $B_o$  at pressures above the bubble-point pressure is less than  $B_o$  at bubble-point pressure because of the contraction of the oil as reservoir pressure is increased. This compression is the only factor which affects  $B_o$  at pressures above the bubble-point with respect to the  $B_o$  at  $p_b$  as oils at both pressures will provide the same volume of stock tank oil.

The normal procedure for estimating  $B_o$  at pressures above the bubble-point is first to estimate the oil factor at bubble-point pressure and reservoir temperature using one of the methods presented below. Then, adjust the  $B_o$  to higher pressures through the use of the coefficient of isothermal compressibility,  $c_o$ , which can be obtained from correlations discussed in section 2.3.2. The equation used for this adjustment follows directly from the definition of the compressibility coefficient at pressures above the bubble-point.

$$B_o = B_{ob}EXP[-c_o(p - p_b)] \quad (2.9)$$

The derivation of the above equation has been presented in detail in Chapter 1. **It should be pointed out that all of the correlations that will be presented below are used only for pressures equal to or below the bubble-point pressure.**

### 2.3.1.1. The Standing's correlation (Californian Crude Oils)

Standing (1947) presented a graphical correlation for estimating the oil formation volume factor with the solution GOR, gas gravity, oil gravity, and reservoir temperature as the correlating parameters. This graphical correlation originated from examining a total of 105 experimental data points on 22 different California hydrocarbon systems. An average error of 1.2% was reported for the correlation.

Standing (1981) showed that the oil formation volume factor can be expressed more conveniently in a mathematical form by the following equation:

$$B_{ob} = 0.9759 + 0.000120 \left[ R_{sb} \left( \frac{\gamma_g}{\gamma_o} \right)^{0.5} + 1.25(T_{res} - 460) \right]^{1.2} \quad (2.10)$$

where

- $B_{ob}$ : Oil formation volume factor at bubble-point pressure
- $T_{res}$ : Reservoir temperature, °R
- $\gamma_g$ : Specific gravity of gas
- $R_{sb}$ : Solution GOR at bubble-point pressure
- $\gamma_o$ : Specific gravity of stock-tank oil, defined by the following expression:

$$\gamma_o = \frac{\rho_o}{\rho_w} \quad (2.11)$$

where

- $\rho_o$ : Density of the crude oil, lb/ft<sup>3</sup>
- $\rho_w$ : Density of the water, lb/ft<sup>3</sup>

In the above equation both densities are measured at standard conditions (i.e. 60 °F and atmospheric pressure), thus  $\gamma_o$  is dimensionless. The density of the water at standard conditions is approximately 62.4 lb/ft<sup>3</sup>, or:

$$\gamma_o = \frac{\rho_o}{62.4} \quad (2.12)$$

Bubble-point solution GOR,  $R_{sb}$ , can be obtained as the sum of the stock-tank vent GOR ( $R_{st}$ ) (seldom field measurement) and of the measured separator GOR ( $R_{sep}$ ). This is valid only if the  $R_{sep}$  and  $R_{st}$  are measured while the reservoir pressure is above the bubble-point pressure (sometimes, the sum of the two producing GOR is called flash bubble-point solution GOR ( $R_{sfb}$ ) or total GOR).

### 2.3.1.2. The Vasquez-Begg's correlation (Generally Applicable)

Vasques and Beggs, in 1980 used laboratory measurements resulted from the study of more than 600 crude oil systems to develop empirical correlations for several oil parameters including the solution gas-oil ratio and the oil formation volume factor (both at bubble-point). Their database included approximately 6,000 measured values over wide ranges of reservoir condition (pressure and temperature) and oil and gas gravities. Vasquez and Beggs found the following equation to be the best form to reproduce the measured data:

$$B_{ob} = 1.0 + C_1 R_{sb} + (T_{res} - 520) \left( \frac{API}{\gamma_{gs}} \right) [C_2 + C_3 R_{sb}] \quad (2.14)$$

where

$\gamma_{gs}$ : Gas specific gravity as defined by the following expression:

$$\gamma_{gs} = \gamma_g \left[ 1 + 5.912 \times 10^{-5} (API) (T_{sep} - 460) \log \left( \frac{p_{sep}}{114.7} \right) \right] \quad (2.15)$$

where

$p_{sep}$ : Separator pressure, psia

$T_{sep}$ : Separator Temperature, °R

$^{\circ}API$ : American Petroleum Institute gravity or °API gravity. It is related to the oil specific gravity, by the equation:

$$API = \frac{141.5}{\gamma_o} - 131.5 \quad (2.16)$$

$API$  gravity is a measure of how heavy or light a reservoir fluid is. The  $API$  gravities of crude oil usually range from 47°  $API$  for the lighter crude oils to 10°  $API$  for the heavier asphaltic crude oils.

Values for the coefficients  $C_1$ ,  $C_2$ , and  $C_3$  are given in Table 2.5:

**Table 2.5**  
 $C_1$ ,  $C_2$  and  $C_3$  coefficients for Vasquez and Begg's correlation

Coefficient	API ≤ 30	API > 30
$C_1$	$4.677 \times 10^{-4}$	$4.670 \times 10^{-4}$
$C_2$	$1.751 \times 10^{-5}$	$1.100 \times 10^{-5}$
$C_3$	$-1.811 \times 10^{-8}$	$1.337 \times 10^{-9}$

Vasquez and Begg's reported an average error of 4.7% for the proposed correlation.

### 2.3.1.3. The Glaso's correlation (North Sea Crude Oils)

Glaso (1980) proposed Equation 2.17 for calculating the oil formation volume factor for North Sea oils. The author claims that the correlation should be valid for all types of oil and gas mixtures after correcting for non-hydrocarbons in the surface gases and for the paraffinicity of the oil.

$$B_{ob} = 1.0 + 10^A \quad (2.17)$$

where

$$A = -6.58511 + 2.91329 \log B_{ob}^* - 0.27683(\log B_{ob}^*)^2 \quad (2.18)$$

$B_{ob}^*$  is a *correlating number* and is defined by the following equation:

$$B_{ob}^* = R_{sb} \left( \frac{Y_g}{Y_o} \right)^{0.526} + 0.968(T_{res} - 460) \quad (2.19)$$

The above correlations were originated from studying PVT data on 45 oil samples. The average error of the correlation was reported at -0.43% with a standard deviation of 2.18%.

Sutton and Farshad (1984) concluded that Glaso's correlation offers the best accuracy when compared with the Standing and Vasquez-Beggs correlations. In general, Glaso's correlation under-predicts formation volume

factor. Standing's expression tends to overpredict oil formation volume factors greater than 1.2 bbl/STB. The Vasquez-Beggs correlation typically over-predicts the oil formation volume factor.

### 2.3.1.4. The Al-Mahrour's correlation (Middle East Crude Oils)

Al-Marhoun (1988) developed a correlation for determining the oil formation volume factor as a function of solution GOR, stock-tank oil gravity, gas gravity, and temperature. The empirical equation was developed by use of the nonlinear multiple regression analysis on 160 experimental data points. The experimental data were obtained from 69 Middle Eastern oil reserves. The author proposed the following expression:

$$B_{ob} = 0.497069 + 0.862963 \times 10^{-3} T_{res} + 0.182594 \times 10^{-2} F + 0.318099 \times 10^{-5} F^2 \quad (2.20)$$

with the correlating parameter F as defined by the following equation:

$$F = R_{sb}^{0.742390} \gamma_g^{0.323294} \gamma_o^{-1.202040} \quad (2.21)$$

### 2.3.1.5. The Sulaimon's correlation (Malaysian Crude Oils)

Sulaimon (2014) developed a correlation for estimating  $B_{ob}$ , using a Group Method of Data Handling (GMDH) technique. GMDH is a family of inductive algorithms which executes computer-based mathematical modeling of multi-parametric data sets. In developing the correlation, 93 PVT data sets from Malaysian crude oil analyses were used. The data sets consist of solution gas oil ratio,  $R_s$ , oil FVF,  $B_o$ , crude oil viscosity,  $\mu_o$ , oil gravity,  $\gamma_o$ , and reservoir temperature,  $T_{res}$ . The database arrangement was made such that  $B_o$  was set as the output while the remaining properties were set as the input parameters. Bubble-point oil formation volume factor is given by the following equation:

$$B_{ob} = 1.081996 - (0.008056\gamma_o) + (0.294013\gamma_g) + (0.000099R_{sb}) - (0.004029\gamma_g\gamma_o) + (9.112963 \times 10^{-6}R_{sb}\gamma_o) + (0.000207R_{sb}\gamma_g) + (0.000134\gamma_o^2) - (0.111668\gamma_g^2) - (5.242391 \times 10^{-8}R_{sb}) \quad (2.23)$$

A total of another 39 PVT data sets from Malaysia, the Niger Delta and the Middle East were used to test the performance of the GMDH correlation. Al-Mahroun's, Standing's Glaso's and Petrosky's (Gulf of Mexico Crude oils) correlations were also used to estimate the oil FVF for the 39 PVT data. Statistical accuracy of the developed correlation was assessed using average absolute relative error (AARE, %), maximum absolute relative error (Max. ARE, %) and minimum relative error (Min. ARE, %). Table 2.6. shows the statistical comparison of Sulaimon's correlation with the correlations mentioned previously. The GMDH correlation gave the most accurate estimation of  $B_{ob}$ .

**Table 2.6**  
Statistical comparison of Sulaimon's with other commonly used correlations

	Sulaimon	Petrosky	Standing	Glaso	Al-Mahroun
AARE, %	0.976	3.435	14.654	22.767	26.342
Max. ARE, %	3.989	7.764	33.893	36.249	33.975
Min. ARE, %	0.001	0.567	0.477	0.188	15.988

### 2.3.2. Correlations for oil isothermal compressibility coefficient prediction

There are several correlations that were developed to estimate the oil compressibility at pressures *above* the bubble-point pressure, i.e., for undersaturated crude oil systems. Three of these correlations are presented below:

- The Vasquez-Beggs correlation (1980)<sup>[22]</sup>
- The Petrosky-Farshad correlation (1993)<sup>[26]</sup>
- The Ahmed's correlation (1985)<sup>[27]</sup>

#### 2.3.2.1. The Vasquez-Begg's correlation

From a total of 4,036 experimental data points used in a linear regression model, Vasquez and Beggs (1980) correlated the isothermal oil compressibility coefficients with  $R_s$ ,  $T_{res}$ ,  $^{\circ}API$ ,  $\gamma_g$ , and  $p_{res}$ . They proposed the following expression:

$$c_o = \frac{-1433 + 5R_{sb} + 17.2(T_{res} - 460) - 1180\gamma_{gs} + 12.61^\circ\text{API}}{10^5 p_{res}} \quad (2.24)$$

where

$T_{res}$ : Reservoir temperature, °R

$p_{res}$ : Reservoir pressure (above the bubble-point), psia

$R_{sb}$ : Gas solubility at the bubble-point pressure, scf/STB

$\gamma_{gs}$ : Corrected gas specific gravity as defined by Equation 2.15

### 2.3.2.2. The Petrosky-Farshad's correlation

Petrosky and Farshad (1993) proposed a relationship for determining the oil compressibility for undersaturated hydrocarbon systems. The equation has the following form:

$$c_o = 1.705 \times 10^{-7} R_{sb}^{0.69357} \gamma_g^{0.1885} \text{API}^{0.3272} (T_{res} - 460)^{0.6729} p_{res}^{-0.5906} \quad (2.25)$$

### 2.3.2.3. The Ahmed's correlation

Ahmed (1985) based on 245 experimental data points developed a mathematical expression for estimating  $c_o$  for pressures *above bubble-point pressure* by using a non-linear regression model. The proposed correlation uses the bubble-point gas solubility  $R_{sb}$  and reservoir pressure,  $p_{res}$ , as the only correlating parameters. Other correlating parameter such as  $\gamma_o$ ,  $\gamma_g$ , and  $T_{res}$  are implemented in the equation through the gas solubility  $R_{sb}$ . The correlation is expressed as:

$$c_o = \frac{1}{\alpha_1 + \alpha_2 R_{sb}} \text{EXP}(\alpha_3 p_{res}) \quad (2.26)$$

where

$$\alpha_1 = 24,841.0822$$

$$\alpha_2 = 14.07428745$$

$$\alpha_3 = -0.00018473$$

The proposed relationship produced an average absolute error of 3.9% when tested against experimental data used in developing the above equation.

## ***2.4. Prediction of $B_o$ using Artificial Neural Networks (ANNs) Models***

The ANN techniques can be applied in several petroleum engineering types of problems such as reservoir characterization, well test interpretation, reservoir simulation and PVT fluid properties estimation. In the following lines emphasis it will be given in those ANNs models which have been employed for the prediction of oil formation volume factor. An ANN can be defined as a multi-dimensional function including large number of parameters which relates input and output data. The ANNs models use as input data key measurements that can be performed rapidly either in the lab or at the well site. Such input data include; reservoir temperature, API gravity, GOR and gas specific gravity.

Neural systems are typically organized in layers. Layers are made up of a number of interconnected nodes (artificial neurons), which contain activation functions. Patterns are presented to the network via the input layer, which communicates to one or more hidden layers where the actual processing is done through a system of fully or partially weighted connections (Figure 2.9). The hidden layers then linked to the output layer. Neural network contains some sort of learning rule that modifies the weights of the connections according to the input patterns.

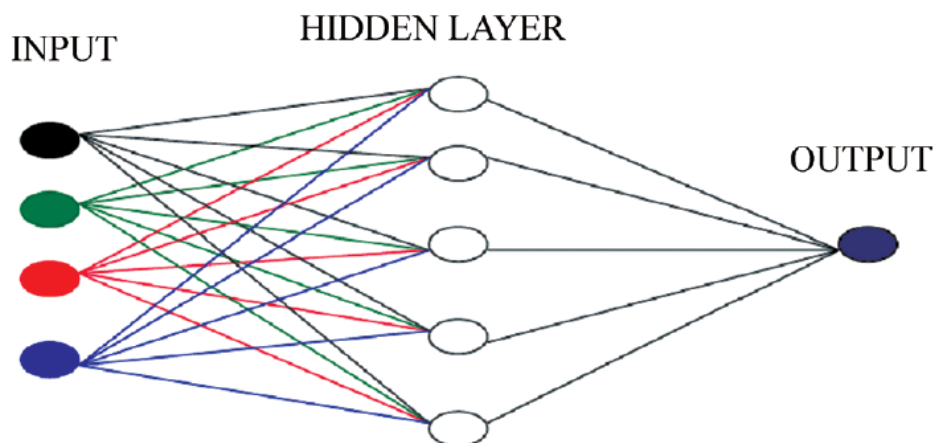


**Figure 2.9** Schematic of an Artificial Neural Network with one hidden layer<sup>[28]</sup>

### **2.4.1 Advantages of the ANN approach<sup>[28]</sup>**

Several advantages can be attributed to ANNs rendering them suitable to petroleum engineering applications as mentioned previously. Firstly, an ANN learns the behavior of a database population by self-tuning its parameters in such a way that the trained ANN matches the employed data accurately. Secondly, if the data used are sufficiently descriptive, the ANN provides a rapid and confident prediction as soon as a new case, which has not been “seen” by the model during the training phase, is applied.

Possibly, the most important aspect of ANNs is their ability to discover patterns in data which are so obscure as to be imperceptible to normal observation and standard statistical methods. This is particularly the case for data exhibiting significantly unpredictable nonlinearities. Traditional correlations are based on simple models which often have to be stretched by adding terms and constants in order for them to become flexible enough to fit experimental data, whereas neural networks are marvelously self-adaptable. Using a sufficiently large database for training, ANNs allow property values to be accurately predicted over a very wide range of input data.

An ANN model can accept substantially more information as input to the model, thereby, improving significantly the accuracy of the predictions and reducing the ambiguity of the requested relationship. Moreover, ANNs are fast-responding systems. Once the model has been “educated” predictions about unknown fluids are obtained with direct and rapid calculations without the need for tuning or iterative computations.

Furthermore, an outstanding attribute of the ANNs is their capability of becoming increasingly “expert” by retraining them using larger databases. Continuous enrichment of the ANN “knowledge” eventually leads to a predictive model exhibiting accuracy comparable to the PVT data itself.

The next paragraphs present an ANN model developed by Varotsis N. et al<sup>[29]</sup>, called PVT Expert, which predicts the PVT behavior of reservoir fluids

### **2.4.2. Development of PVT Expert model**

The PVT Expert model predicts the physical and PVT properties of both reservoir oils and gas condensates over the entire range of operating conditions.

The input data set for the oil ANN models consists of reservoir fluid composition, saturation pressure, reservoir temperature, fluid density at the bubble point, viscosity of the dead oil, flash molar ratio and flash liquid and gas densities. The input for the gas condensate ANNs consists of reservoir fluid composition, dew point, reservoir temperature,  $Z$  factor at the dew point, field GOR and separator and tank liquid densities.

The PVT database of over 650 fluids originating from different parts of the world, was randomly split into a training (80%), a testing (10%) and a validation (10%) subset. The last two data subsets were used for the evaluation of the ANN performance.

In Figure 2.10 the performance of the  $B_o$  prediction for pressures above and below bubble-point is illustrated.

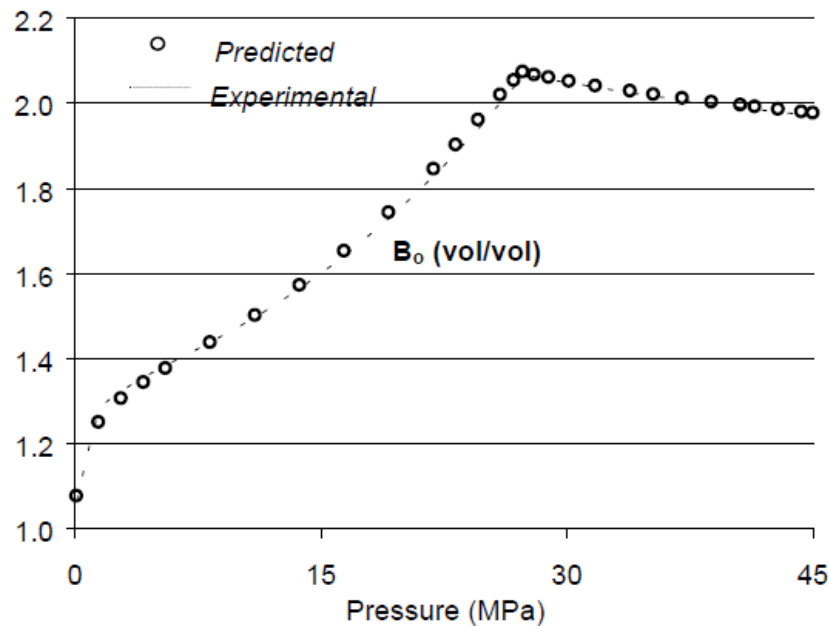


**Figure 2.10** Comparison of the predicted  $B_o$  curve from PVT Expert to the PVT Lab one

PVT Expert gave average prediction relative errors for both reservoir oils and gas condensate fluids between 0.5-2.5%. This level of error is considered better than that provided by tuned Equation of State (EOS) models

In conclusion, several important applications are envisaged for the developed method. Rapid and accurate PVT studies can be generated at the well-site within hours enhancing thus the quality of onsite fluid properties evaluation services such as the FPE and widely extending fluid analysis to reservoir fluid samples recovered by Formation Testers. These readily available quality values of the physical properties can improve the well test and reservoir/production engineering calculations upon which several important decisions are based on and test the data quality of fluid analysis laboratories.

### 2.4.3. Case Studies from the literature

Several studies which have been selected from the literature concerning the determination of bubble point  $B_o$  using ANNs models are presented in the next three paragraphs.

- Artificial neural network technique was developed by Osman, Abdel-Wahhab and Al-Mahrour (March, 2001)<sup>[30]</sup> in order to estimate  $B_{ob}$ . Their model was developed using 803 published data gathered from Malaysia, Middle East, Gulf of Mexico, and Colombia. They designed a three layer network; the input layer has four neurons covering the input data of gas-oil ratio, API gravity, relative gas density, and reservoir temperature; one hidden layer with five neurons and a single neuron for the formation volume factor in the output layer. This model showed a higher accuracy than the empirical correlations with an absolute average percent error of 1.789 %, a standard deviation of 2.2053 % and correlation coefficient of 0.988.
- A work of Shokir et al (2004)<sup>[31]</sup> based on neural network using Matlab 7.5 to predict bubble point oil formation volume factor with the aid of two separated networks. The data used was a set of 160 measured data points collected from the Middle East region; 140 points were used for training, and 20 for testing. The network performed better than empirical correlation with average relative error percent of 0.030704 and correlation coefficient of 0.9981.
- In 2013, publication was made on an artificial neural network models to predict oil formation volume factor for different API gravity ranges<sup>[32]</sup>. The new model was developed using combination of 448 published data from the Middle East, Malaysia, Africa, North Sea, Mediterranean basin, Gulf of Persian fields and 1389 data set collected from the Niger Delta Region of Nigeria. The model was developed for four different API gravity classes: heavy oils for  $API \leq 21$ , medium oils for  $21 < API \leq 26$ , blend oils for  $26 < API \leq 35$  and light oils for  $API > 35$ . This model performed better than conventional empirical correlation developed to predict the same fluid property.

## *C H A P T E R 3*

# **The Liquid Z-Factor Approach for predicting $B_o$ at undersaturated conditions**

### ***3.1. Basic concepts of Gas Behavior***

A technique for estimating oil formation volume factor at undersaturated conditions using field data and the Standing-Katz Z-factor chart is presented below. Prior to the development of the method some fundamental concepts are essential to be discussed.

#### **3.1.1. Ideal Gas Law**

The kinetic theory of gases postulates that the gas is composed of a very large number of particles called molecules. For an ideal gas, the volume of these molecules is insignificant compared with the total volume occupied by the gas. It is assumed that these molecules have no attractive or repulsive forces between them and that all collisions of molecules are perfectly elastic.

Based on the above kinetic theory of gases, a mathematical equation called Equation of State (EOS) can be derived to express the relationship existing between pressure, volume and temperature for a given quantity of an ideal gas. This relationship is called Ideal Gas Law and is expressed mathematically by the following equation:

$$pV = nRT \quad (3.1)$$

where

$p$ : Absolute pressure, psia (or Pa)

$V$ : Volume, ft<sup>3</sup> (or m<sup>3</sup>)

$T$ : Absolute temperature, °R (or K)

$n$ : Number of moles of gas, mol

$R$ : Universal gas constant which, for the above units, has the value 10.7316 psia ft<sup>3</sup> mole<sup>-1</sup> °R<sup>-1</sup> (or 8.3145 Pa m<sup>3</sup> mol<sup>-1</sup> K<sup>-1</sup>)

The number of gas moles of a pure substance is defined by the following equation:

$$n = \frac{m}{MW} = \frac{V}{V_m} \quad (3.2)$$

where

- $m$ : Mass of gas, lb ( g)
- $MW$ : Molecular weight, lb/mol (or g/mol)
- $V_m$ : Molar volume, scf/mol (or  $\text{sm}^3/\text{mol}$ )

It is worthily to be mentioned that for gas mixtures the  $MW$  is replaced by  $MW_a$  which is the apparent molecular weight.

$V_m$  is defined as the volume that occupies 1 mole of any ideal gas at standard conditions and can be calculated by combining Equations 3.1 and 3.2.

$$V_m = \frac{V}{n} = \frac{RT}{p} = \frac{10.732 \times 519.67}{14.7} = 379.4 \text{ scf (or } 23.69 \text{ std m}^3) \quad (3.3)$$

Because the density is defined as the mass per unit volume of the substance, Equation 3.1 can be solved with respect to the density to yield:

$$\rho_g = \frac{m}{V} = \frac{pMW_a}{RT} \quad (3.4)$$

where  $\rho_g$  is the density of the gas mixture with units  $\text{lb/ft}^3$  (or  $\text{g/m}^3$ )

### 3.1.2. Specific Gravity of Gas

The gas specific gravity,  $\gamma_g$ , is defined as the ratio of the gas density to that of the air ( $\rho_{air}$ ). Both densities are referred to the same temperature and pressure, or:

$$\gamma_g = \frac{\rho_g}{\rho_{air}} \quad (3.5)$$

Assuming that the behavior of both the gas mixture and the air is described by the ideal gas equation, the gas specific gravity can be expressed as:

$$\gamma_g = \frac{\frac{pMW_a}{RT}}{\frac{pMW_{air}}{RT}} = \frac{MW_a}{MW_{air}} = \frac{MW_a}{28.96} \quad (3.6)$$

where,  $MW_{air}$  is the average molecular weight of dry air

### 3.1.3. Behavior of Real Gases

At low pressures and relatively high temperatures, the volume of most gases is so large that the volume of the molecules themselves may be neglected. Also, the distance between molecules is so great that the presence of even fairly strong attractive or repulsive forces is not sufficient to affect the behavior in the gas state. However, as the pressure is increased, the total volume occupied by the gas becomes small enough that the volume of the molecules themselves is appreciable and must be considered. Also, under these conditions, the distance between the molecules is decreased to the point at which the attractive or repulsive forces between the molecules become important. This behavior negates the assumptions required for ideal gas behavior, and serious errors are observed when comparing experimental volumes to those calculated with the ideal gas law. Consequently, a real gas law was formulated (in terms of a correction to the ideal gas law) by use of a proportionality term.

The volume of a real gas is usually less than what the volume of an ideal gas would be at the same temperature and pressure; hence, a real gas is said to be super compressible. The ratio of the real volume to the ideal volume, which is a measure of the amount that the gas deviates from perfect behavior, is called the **super-compressibility factor**, the **gas compressibility factor**, **gas deviation factor**, or simply the **Z-factor** and is given the symbol Z. The gas deviation factor is by definition the ratio of the volume actually occupied by a gas at a given pressure and temperature to the volume it would occupy if it behaved ideally, or:

$$Z = \frac{\text{Actual volume of gas at specified } T \text{ and } p}{\text{Ideal volume of gas at same } T \text{ and } p} \quad (3.7)$$

Note that the numerator and denominator of Equation 3.7 refer to the same mass. (This equation for the Z- factor is also used for liquids.) Thus, the real gas equation of state is written:

$$pV = nZRT \quad (3.8)$$

A typical relationship between Z-factor and pressure of a gas is depicted in Figure 3.1.

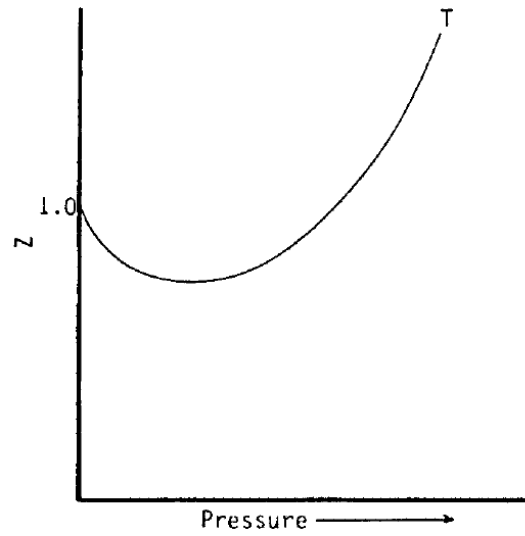


**Figure 3.1** Typical Z-factor versus pressure diagram

Then, the density of a real gas can be determined by the next equation:

$$\rho_g = \frac{pMW_a}{ZRT} \quad (3.9)$$

## ***3.2. Development of the Liquid Z-Factor based method***

### **3.2.1. Determination of bubble-point oil formation volume factor**

Following the definition of  $B_o$  at bubble-point pressure,  $B_{ob}$ , as expressed by the following equation:

$$B_{ob} = \frac{(V_o)_{p_b, T_{res}}}{(V_o)_{SC}} \quad (3.10)$$

the oil volume at reservoir temperature,  $T_{res}$ , and at bubble-point pressure,  $p_b$ , can be replaced with total mass of the hydrocarbon system divided by the density at bubble-point pressure and reservoir temperature.

$$B_{ob} = \frac{m_t}{\rho_{ob}(V_o)_{sc}} \quad (3.11)$$

where, the total mass of the hydrocarbon system is equal to the sum of the mass of the stock-tank oil,  $m_o$ , plus the mass of the solution gas,  $m_g$ , i.e.:

$$m_t = m_o + m_g \quad (3.12)$$

then, Equation 3.10 becomes:

$$B_{ob} = \frac{m_o + m_g}{\rho_{ob}(V_o)_{sc}} \quad (3.13)$$

As volume of stock-tank oil,  $(V_o)_{sc}$ , it is considered one barrel or, equivalently, 5.615 scf.

Given the bubble-point gas solubility,  $R_{sb}$ , per stock-tank oil and the specific gravity of the solution gas, the mass of  $R_{sb}$  scf of the gas, using Equation 3.2, is calculated as:

$$\frac{R_{sb}}{V_m} = \frac{m_g}{MW_a} \quad (3.14)$$

Combining Equation 3.6 with Equation 3.14 we end up with the following expression:

$$m_g = \frac{R_{sb}}{379.4} (28.96)(\gamma_g) \quad (3.15)$$

The mass of one barrel of the stock-tank oil is calculated as:

$$m_o = (1 \text{ bbl})\rho_{ob} \quad (3.16)$$

Substitution of 1 barrel of stock-tank oil in the above expression with the equivalent volume of 5.615 scf and of Equation 2.12, then, Equation 3.16 becomes:

$$m_o = (5.615)(62.4)(\gamma_o) \quad (3.17)$$

Substitution of Equations 3.15 and 3.17 in Equation 3.13 the next expression holds:

$$B_{ob} = \frac{(5.615)(62.4)\gamma_o + \frac{R_{sb}}{379.4}(28.96)(\gamma_g)}{(5.615)\rho_{ob}} \quad (3.18)$$

or, equivalently

$$B_{ob} = \frac{62.42796\gamma_o + 0.01363R_{sb}\gamma_g}{\rho_{ob}} \quad (3.19)$$

The above expression is a function of:

- Specific gravity of stock-tank oil,  $\gamma_o$
- Specific gravity of gas,  $\gamma_g$
- Bubble-point solution gas to oil ratio,  $R_{sb}$  (units: scf gas/STB oil)

which, are typical parameters measured during a surface well test

and a function of bubble-point oil density,  $\rho_{ob}$ , which depends on the value of the liquid Z-factor,  $Z_L$ . Methods of estimating  $Z_L$  utilizing an EOS model, based on the Standing and Katz (1942)<sup>[1]</sup> Z-factor chart, will be analyzed next.

The error in calculating the value of  $B_{ob}$  using Equation 3.19 depends only on the accuracy of the input variables ( $R_{sb}$ ,  $\gamma_g$  and  $\gamma_o$ ) and on the method for calculating  $\rho_{ob}$ .

### 3.2.1.1. Computation of bubble-point oil density based on the Standing-Katz $Z$ -factor chart

Equation 3.9, which applies for single phase gas, can be extended to single phase oil systems (assuming them in some way as high molecular weight hydrocarbon gases) for the calculation of oil density at bubble-point pressure and reservoir temperature,  $\rho_{ob}$ . Thus, Equation 3.9 is re-written as follows:

$$\rho_{ob} = \frac{p_b MW_o}{Z_L RT_{res}} \quad (3.20)$$

It is obvious that prior to the determination of oil density, computation of liquid  $Z$ -factor,  $Z_L$ , is required. Methods which have been developed for gas  $Z$ -factor estimation are used for this purpose.

Compressibility factors for gas mixtures are measured easily in a PVT cell. The gas deviation factor,  $Z$ , is determined by measuring the volume of a sample of the natural gas at a specific pressure and temperature, then measuring the volume of the same quantity of gas at atmospheric pressure and at ambient temperature. However, quite often experimental data is unavailable or PVT properties must be evaluated at conditions different than those examined by the laboratory studies. In these cases, gas deviation factor must be determined from correlations.

Since publication in 1942, the Standing and Katz (SK) gas  $Z$ -factor chart has become a standard correlation in the oil industry for the estimation of  $Z$ -factor for natural gas mixtures.

The gas  $Z$ -factor chart developed by Standing and Katz, shown in Figure 3.2, is based on van der Waals' principle of corresponding states. This principle states that two substances at the same conditions referenced to *critical pressure* and *critical temperature* will have similar properties. These conditions are referred to as *reduced pressure* and *reduced temperature*. Therefore, if two substances are compared at the same reduced conditions, the substances will have the same  $Z$ -factor. For mixtures, the critical properties are replaced with pseudo-critical properties. These values have no physical significance but serve as correlating parameters for corresponding-states calculations. Mathematically, the SK chart relates the  $Z$ -factor to pseudo-reduced pressure,  $p_{pr}$  and pseudo-reduced temperature,  $T_{pr}$ , which in turn depend on pseudo-critical pressure,  $p_{pc}$ , and pseudo-critical temperature,  $T_{pc}$ .

$$Z = f(p_{pr}, T_{pr}) \quad (3.21)$$

where

$$p_{pr} = \frac{p}{p_{pc}} \quad (3.22)$$

and

$$T_{pr} = \frac{T}{T_{pc}} \quad (3.23)$$

The pseudo-critical pressure and pseudo-critical temperature are defined as the molar average critical temperature and pressure of the mixture components. In an equation form, they are expressed as:

$$p_{pc} = \sum y_i p_{ci} \quad (3.24)$$

and

$$T_{pc} = \sum y_i T_{ci} \quad (3.25)$$

where

- $p_{ci}$ : Critical pressure of component  $i$  in the gas mixture
- $T_{ci}$ : Critical temperature of component  $i$  in the gas mixture
- $y_i$ : Mole fraction of component  $i$  in the gas mixture

These relations are known as Kay's rule after W.B. Kay,<sup>[2]</sup> who first suggested their use.

Equations 3.24 and 3.25 require the measurement of composition of the gas mixture. If the composition of the gas is unknown, then a correlation to estimate pseudo-critical temperature and pseudo-critical pressure values from the specific gravity is used. There are several different correlations available such the ones proposed by Sutton (1985, 2007)<sup>[2],[3]</sup>.

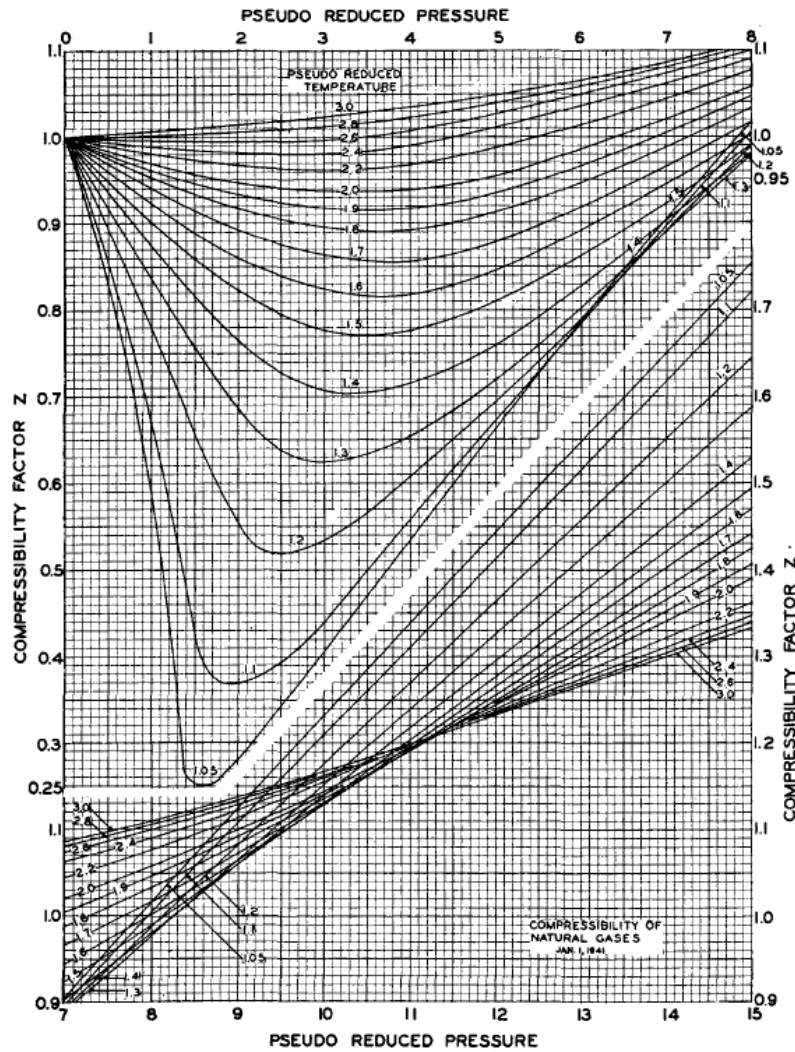


Figure 3.2 Standing and Katz (SK) gas Z-factor chart<sup>[1]</sup>

### ***Computation methods of Z-factor determination based on the SK Z-factor chart***

Several accurate methods have been developed to represent the SK chart digitally. The engineering community typically uses method published by Hall and Yarborough (1973,1974)<sup>[4],[5]</sup> (HY), Dranchuk, Purvis and Robinson (1974)<sup>[6]</sup> (DPR), Dranchuk and Abou-Kassem (1975)<sup>[7]</sup> (DAK) and by Brill and Beggs<sup>[8]</sup>. These methods all use some form of an equation of state that has been fitted specifically to selected digital Z-factor chart data published by Poettmann and Carpenter (1952)<sup>[9]</sup>. The geophysics community typically uses a method developed by Batzle and Wang (1992)<sup>[10]</sup> (BW). Londolno et al. (2002)<sup>[11]</sup> (LAB) refitted the chart with an expanded data set, resulting in a modified DAK method. They provided two equations: one to fit an expanded data set from the SK Z-

factor chart and another one that included pure-component data. Out of those five methods, the following four empirical correlations are described below:

- Hall-Yarborough
- Dranchuk-Abu-Kassem
- Dranchuk-Purvis-Robinson
- Brill and Beggs

### ***The Hall-Yarborough (HY) Method***

Hall and Yarborough (1973) presented an equation-of-state that accurately represents the Standing and Katz  $Z$ -factor chart. The proposed expression is based on the Starling-Carnahan equation-of-state. The coefficients of the correlation were determined by fitting them to data taken from the Standing and Katz  $Z$ -factor chart. Hall and Yarborough proposed the following mathematical form:

$$Z = \left[ \frac{0.06125 p_{pr} t}{y} \right] \text{EXP}[-1.2(1-t)^2] \quad (3.26)$$

where

- $t$ : Reciprocal of the pseudo-reduced temperature, i.e.  $T_{pc}/T$   
 $y$ : The reduced density, which is defined by Equation 3.28, that can be obtained as the solution of the following equation:

$$y = -0.06125 p_{pr} t \text{EXP}[-1.2(1-t)^2] + \frac{y + y^2 + y^3 - y^4}{(1-y)^3} - (14.76t - 9.76t^2 + 4.58t^3)y^2 - (90.7t - 242.2t^2 + 42.4t^3)y^{(2.18+2.82t)} \quad (3.27)$$

Since the reduced density,  $y$ , is a function of  $Z$ , the solution is thus obtained by iteration using a root finding technique such as the Newton-Raphson method.

The Hall and Yarborough equation is valid for  $0 \leq p_{pr} \leq 30$  and  $1.0 \leq T_{pr} \leq 3.0$ .

### ***The Dranchuk and Abu-Kassem (DAK) Method***

Dranchuk and Abu-Kassem (1975) derived an analytical expression for calculating the reduced gas density that can be used to estimate the gas compressibility factor. The reduced gas density,  $\rho_r$ , is defined as the ratio of the

gas density at a specified pressure and temperature to that of the gas at its critical pressure or temperature, or:

$$\rho_r = \frac{\rho}{\rho_c} = \frac{pMW_a/(ZRT)}{p_cMW_a/(Z_cRT_c)} = \frac{p/(ZT)}{p_c/(Z_cT_c)} \quad (3.28)$$

Assuming a value of 0.27 for the critical gas compressibility factor,  $Z_c$ , which is considered an appropriate value for mixtures comprised chiefly of methane<sup>[7]</sup>, Equation 3.28 leads to the following simplified expression for the reduced gas density:

$$\rho_r = \frac{0.27p_{pr}}{ZT_{pr}} \quad (3.29)$$

The DAK method uses a form of the Benedict-Webb-Rubin, eleven-constant, equation of state for calculating the reduced gas density,  $\rho_r$ :

$$f(\rho_r) = (R_1)\rho_r - \frac{R_2}{\rho_r} + (R_3)\rho_r^2 - (R_4)\rho_r^5 + (R_5)(1 + A_{11}\rho_r^2)\rho_r^2 \text{EXP}[-A_{11}\rho_r^2] + 1 = 0 \quad (3.30)$$

With the coefficients  $R_1$  through  $R_5$  as defined by the following relations:

$$R_1 = \left[ A_1 + \frac{A_2}{T_{pr}} + \frac{A_3}{T_{pr}^3} + \frac{A_4}{T_{pr}^4} + \frac{A_5}{T_{pr}^5} \right]$$

$$R_2 = \left[ \frac{0.27p_{pr}}{T_{pr}} \right]$$

$$R_3 = \left[ A_6 + \frac{A_7}{T_{pr}} + \frac{A_8}{T_{pr}^2} \right]$$

$$R_4 = A_9 \left[ + \frac{A_7}{T_{pr}} + \frac{A_8}{T_{pr}^2} \right]$$

$$R_5 = \left[ \frac{A_{10}}{T_{pr}^3} \right]$$

The constants  $A_1$  through  $A_{11}$  were determined by fitting the equation, using nonlinear regression models, to 1,500 data points from the SK Z-factor chart. The coefficients exhibit the following values:

$A_1=0.3265$	$A_2=-1.0700$	$A_3=-0.5339$	$A_4=0.01569$
$A_5=-0.05165$	$A_6=0.5475$	$A_7=-0.7361$	$A_8=0.1844$
$A_9=0.1056$	$A_{10}=0.6134$	$A_{11}=0.7210$	

Dranchuk and Abou-Kassem found an average absolute error of 0.486% in their equation, with a standard deviation of 0.00747. The data used for fitting the DAK equation encompassed the following ranges:  $0 \leq p_{pr} \leq 30$  and  $1.05 \leq T_{pr} \leq 3.0$ . In 2007, Sutton showed that the DAK equation could provide accurate results at pseudo-reduced pressures well beyond 30 (Sutton, 2007<sup>[12]</sup>) while in 2008, Sutton (Sutton, 2008<sup>[13]</sup>) was tried the DAK equation at pseudo-reduced pressures up to 80 and pseudo-reduced temperatures as low as 0.4.

The DAK EOS must be solved iteratively since the  $Z$ -factor appears on both sides of the Equation 3.30. The solution of this equation can be obtained by employing the Newton-Raphson iteration technique as summarized in the following steps:

*Step 1:* Make an initial guess of the unknown parameter,  $\rho_r^k$ , where  $k$  is an iteration counter. An appropriate initial guess of  $\rho_r^k$  is given by the following relationship:

$$\rho_r = \frac{0.27p_{pr}}{T_{pr}} \quad (3.30a)$$

*Step 2:* Substitute this initial value in Equation 3.30 and evaluate the nonlinear function. Unless the correct value of  $\rho_r^k$  has been initially selected, Equation 3.28 will have a nonzero value for the function  $f(\rho_r^k)$ .

*Step 3:* A new improved estimate of  $\rho_r$ , i.e.,  $\rho_r^{k+1}$ , is calculated from the following expression:

$$\rho_r^{k+1} = \rho_r^k - \frac{f(\rho_r^k)}{f'(\rho_r^k)} \quad (3.30b)$$

where

$$f'(\rho_r^k) = (R_1) + \frac{R_2}{\rho_r^2} + 2(R_3)\rho_r - 5(R_4)\rho_r^4 + 2(R_5)\rho_r \quad (3.30c)$$

$$EXP[-A_{11}\rho_r^2] [(1 + 2A_{11}\rho_r^3) - A_{11}\rho_r^2(1 + A_{11}\rho_r^2)]$$

*Step 4:* Steps 2 and 3 are repeated  $n$  times, until the error, i.e.,  $\text{abs}(\rho_r^k - \rho_r^{k+1})$ , becomes smaller than a preset tolerance, e.g.,  $10^{-12}$ .

*Step 5:* The correct value of  $\rho_r$  is then used to Equation 3.29 to evaluate the compressibility factor, i.e.:

$$Z = \frac{0.27p_{pr}}{\rho_r T_{pr}} \quad (3.30d)$$

### **The Dranchuk Purvis-Robinson (DPR) Method**

Dranchuk, Purvis, and Robinson (1974) developed a correlation based on the Benedict-Webb-Rubin type of equation-of-state. Fitting the equation to 1,500 data points from the Standing and Katz Z-factor chart optimized the eight coefficients of the proposed equations. The equation has the following form:

$$1 + T_1\rho_r + T_2\rho_r^2 + T_3\rho_r^5 + [T_4\rho_r^2(1 + A_8\rho_r^2)EXP(-A_8\rho_r^2)] - \frac{T_5}{\rho_r} = 0 \quad (3.31)$$

with

$$T_1 = \left[ A_1 + \frac{A_2}{T_{pr}} + \frac{A_3}{T_{pr}^3} \right]$$

$$T_2 = \left[ A_4 + \frac{A_5}{T_{pr}} \right]$$

$$T_3 = \left[ \frac{A_5 A_6}{T_{pr}} \right]$$

$$T_4 = \left[ \frac{A_7}{T_{pr}^3} \right]$$

$$T_5 = \left[ \frac{0.27 p_{pr}}{T_{pr}} \right]$$

where  $\rho_r$  is defined by Equation 3.28 and the coefficients  $A_1$  through  $A_8$  exhibit the following values:

$$\begin{array}{llll} A_1=0.31506237 & A_2=-1.0467099 & A_3=-0.57832720 & A_4=0.53530771 \\ A_5=-0.61232032 & A_6=-0.10488813 & A_7=0.68157001 & A_8=0.68446549 \end{array}$$

The method is valid within the following ranges of pseudo-reduced temperature and pressure:

- $1.05 < T_{pr} < 3.0$
- $0.2 < p_{pr} < 30$

### **The Brill and Beggs method**

For many petroleum engineering applications, the Brill and Beggs equation gives a satisfactory representation ( $\pm 1$  to 2%) of the original Standing-Katz Z-factor chart. The main limitations are that the reduced temperature must be

greater than 1.2 and less than 2 and the reduced pressure should be less than 15. This equation is the only one of the above that can be solved explicitly for  $Z$ .

$$Z = A + (1 - A)EXP(-B) + Cp_{pr}^D \quad (3.32)$$

where

$$A = 1.39(T_{pr} - 0.92)^{0.5} - 0.36T_{pr} - 0.101$$

$$B = (0.62 - 0.23T_{pr})p_{pr} + \left[ \left( \frac{0.066}{T_{pr} - 0.86} \right) - 0.037 \right] p_{pr}^2 + \left[ \frac{0.32}{10^9(T_{pr} - 1)} \right] p_{pr}^6$$

$$C = (0.132 - 0.321\log(T_{pr}))$$

$$D = 10^{0.3106 - 0.49T_{pr} + 0.1824T_{pr}^2}$$

### Comparison between Z-factor prediction methods

Figures 3.3 and 3.4<sup>[12]</sup> summarize the deviations of the predictions of the method error and their standard deviation respectively, against an expended methane data set obtained from NIST (National Institute of Standards and Technology) (Lemmon et al. 2005), for the various Z-factor methods. The DPR method shows the overall lowest error but a higher standard deviation. **The DAK method strikes a balance between low error and low standard deviation.**

Moreover, on the basis of Takacs<sup>[14]</sup> comparison of eight correlations representing the SK chart, the Hall and Yarborough and the Dranchuk and Abou-Kassem equations give the most accurate representation for a broad range of temperatures and pressures.

**For the above reasons the DAK equation is preferred among the other methods for the calculations presented in this work.**

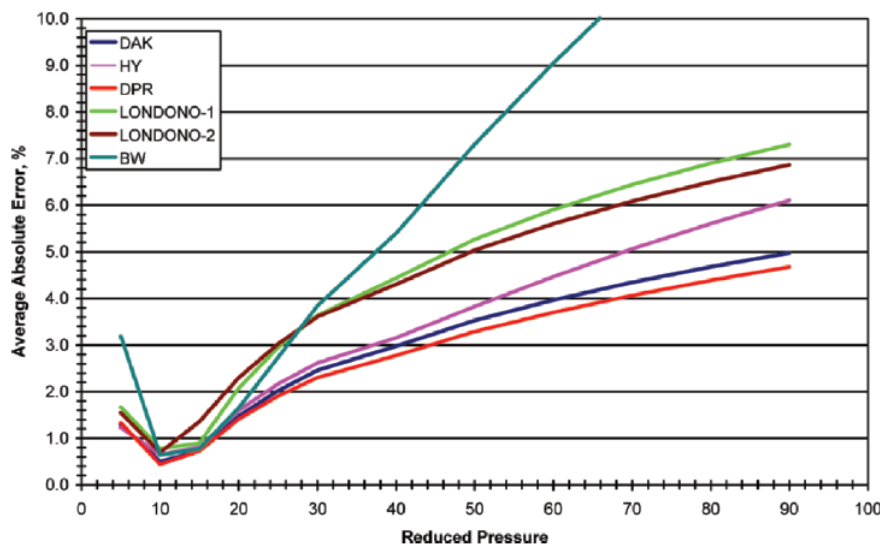


**Figure 3.3** Z-factor EOS methods predictions error (All isotherms –  $1.05 < T_r < 3.0$ )

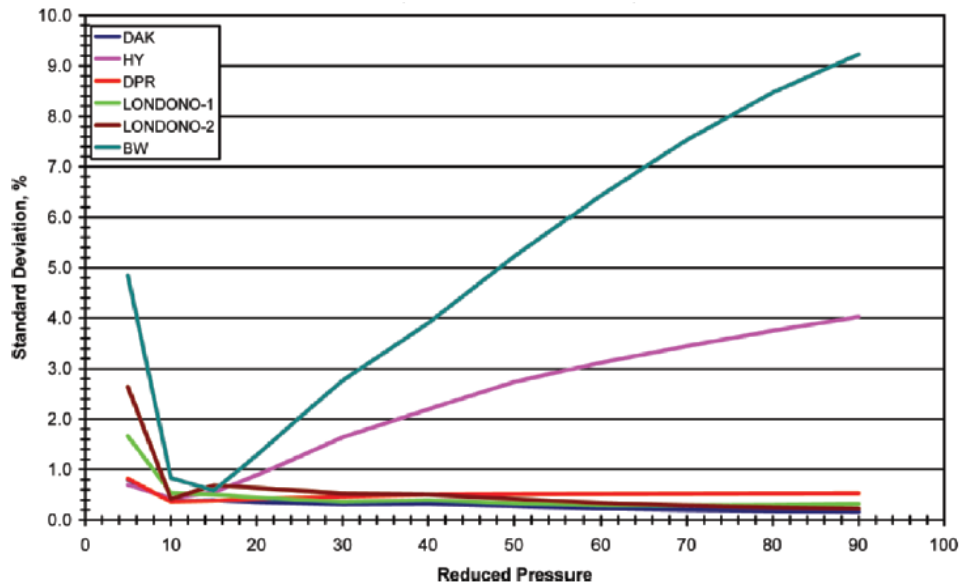


**Figure 3.4** Z-factor EOS methods predictions standard deviation (All isotherms –  $1.05 < T_r < 3.0$ )

In order to test the suitability of the DAK equation for determining liquid Z-factors, this quantity was determined by Sutton (Sutton, 2008) for n-decane across the range of  $0.40 \leq T_r \leq 1.05$  and  $0.6 \leq p_r \leq 90$ . Using data from the National Institute of Standards and Technology (NIST) as a standard (Lemmon et al. 2005), the prediction errors are shown in Figure 3.5<sup>[13]</sup>.

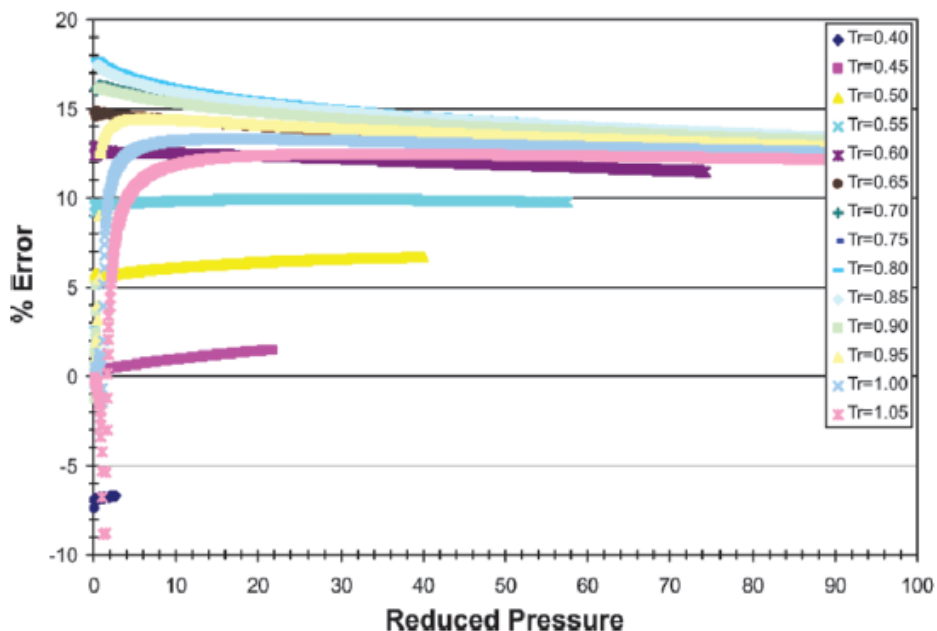


**Figure 3.5** DAK method Z-factor prediction error for n-decane

The DAK equation exhibits error typically in the range of 10 to 15% across the range of  $0.40 \leq T_r \leq 1.05$ . The errors are relatively constant as reduced pressures increases, making it ideal for correlating pseudo-critical properties

**The Sutton's (2008)<sup>[13]</sup> correlations for estimation of pseudo-critical properties**

A non-linear regression method was developed by Sutton (Sutton 1985<sup>[15]</sup>, 2007) to infer pseudo-critical properties from data measurements recorded for oil samples. The data were derived from internal reports accessed through the GeoMark database (Reservoir Fluid Database 2006) and from published sources (Kumar 1991<sup>[16]</sup>) representing samples from around the world and encompassing a wide range of properties. Liquid Z-factors were determined from CCE experiments using the well-stream molecular weight calculated from composition, pressure, temperature and density measurements.

The resulting pseudo-critical properties were plotted against the molecular weight of the well-stream fluid to determine a relationship (Figure 3.6). The pseudo-critical property data can be represented accurately by the following equations.

$$p_{pc} = 768.1 - 4.919MW_o + 1.302MW_o[\ln(MW_o) - 3.366] \quad (3.33)$$

$$T_{pc} = 135.6 + 10.864MW_o - 2.81MW_o[\ln(MW_o) - 3.366] \quad (3.34)$$

where  $MW_o$  represents the well-stream molecular weight of oil.

Equations 3.33 and 3.34, developed exclusively from oil data, perform in their extrapolation into the gas region and provide unified relationship for pseudo-critical properties for light gas, gas condensates, volatile oils and heavy oils.

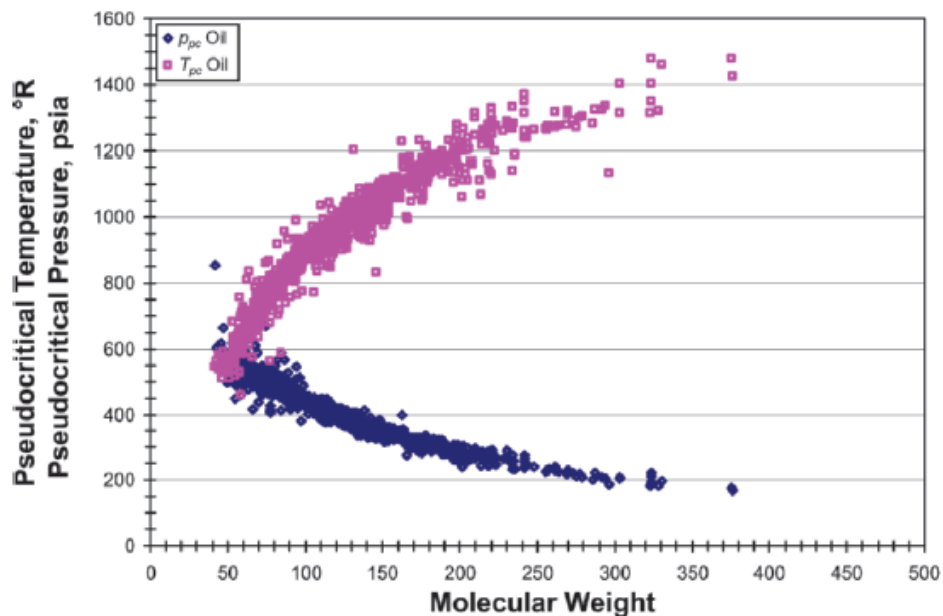


**Figure 3.6** Oil pseudo-critical property relationships from regression analysis<sup>[13]</sup>

Sutton (2008) in his work showed that the effects of non-hydrocarbons on crude oil systems do not need to be addressed in order to obtain accurate  $Z$ -factor calculations.

### **Wellstream molecular weight estimation<sup>[13]</sup>**

Figure 3.7 depicts Watson characterization factor,  $K_w$ , as a function of crude oil  $API$  gravity with data from a crude oil database and Sutton (2006)<sup>[17]</sup>.

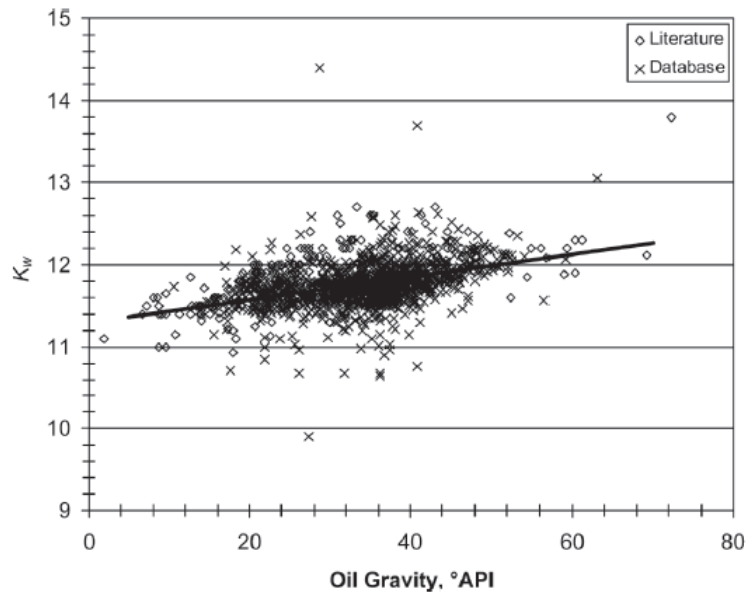


**Figure 3.7** Watson characterization factor relationship with crude oil  $API$  gravity<sup>[13]</sup>

From this figure the following expression can be derived:

$$K_w = 0.0143 \times API + 11.298 \quad (3.35)$$

The stock-tank oil molecular weight,  $MW_{\bar{o}}$ , is calculated by the following equation as a function of Watson characterization factor and oil specific gravity (Sutton 2008):

$$MW_{\bar{o}} = \left( \frac{K_w \gamma_o^{0.84573}}{4.5579} \right)^{6.58848} \quad (3.36)$$

The mole fraction of oil in the wellstream is obtained (Sutton 2008):

$$x_o = \left( 1 + \frac{7.521 \times 10^{-6} R_s MW_{\bar{o}}}{\gamma_o} \right)^{-1} \quad (3.37)$$

and the molecular weight of the wellstream can be calculated by:

$$MW_o = x_o MW_{\bar{o}} + 28.964(1 - x_o)\gamma_g \quad (3.38)$$

### 3.2.2. Determination of undersaturated oil formation volume factor

Having calculated the bubble-point oil formation volume factor,  $B_{ob}$ , then, the computation of  $B_o$  at any reservoir pressure greater than the bubble-point pressure can be done by utilizing the undersaturated isothermal oil compressibility,  $c_o$ , at the required reservoir pressure in the following equation:

$$B_o = B_{ob} \text{EXP}[-c_o(p_{res} - p_b)] \quad (3.39)$$

The derivation of the above expression has, already, been discussed in Chapter 1.

The computation of  $c_o$  used in Equation 3.39 can be done either with one of the correlations of Vasquez – Begg's, Ahmed's, Petrosky – Farshad's presented in Chapter 2 or by calculating the Z-factor at the desired  $p_{res}$  which is greater than  $p_b$  using the DAK equation (Equation 3.30). The question which one of the four methods is more accurate will be answered in Chapter 4. The second way will be analyzed in the following lines.

L. Mattar et al<sup>[18]</sup> showed an alternative way to obtain easily the  $c_o$ . By substitution of Equation 3.8 in Equation 1.5 we end up with the following expression:

$$c_o = \frac{1}{p} - \frac{1}{Z} \left( \frac{\partial Z}{\partial p} \right)_T \quad (3.40)$$

A pseudo-reduced compressibility,  $c_{pr}$ , may be defined by multiplying each term in Equation 3.40 by  $p_{pc}$ :

$$c_{pr} = c_o p_{pc} = \frac{1}{p_{pr}} - \frac{1}{Z} \left( \frac{\partial Z}{\partial p_{pr}} \right)_{T_{pr}} \quad (3.41)$$

Equation 330a may be differentiated to give:

$$\left( \frac{\partial Z}{\partial p_{pr}} \right) = \frac{0.27}{Z T_{pr}} \left[ \frac{\left( \frac{\partial Z}{\partial p_{pr}} \right)_{T_{pr}}}{1 + \frac{\rho_r}{Z} \left( \frac{\partial Z}{\partial p_{pr}} \right)_{T_{pr}}} \right] \quad (3.42)$$

Substitution of Equation 3.42 into Equation 3.41 leads to the following expression of the pseudo-reduced compressibility:

$$c_{pr} = \frac{1}{p_{pr}} - \frac{0.27}{Z^2 T_{pr}} \left[ \frac{\left( \frac{\partial Z}{\partial p_{pr}} \right)_{T_{pr}}}{1 + \frac{\rho_r}{Z} \left( \frac{\partial Z}{\partial p_{pr}} \right)_{T_{pr}}} \right] \quad (3.43)$$

the term  $\left( \frac{\partial Z}{\partial p_{pr}} \right)_{T_{pr}}$  can be calculated by differentiating the Equation 3.30 (DAK equation) as it has already been done (Equation 3.30c) since it is required for the determination of Z-factor.

Therefore, by substitution of Equation 3.43 in Equation 3.41 we obtain the value of  $c_o$  required for the estimation of the undersaturated oil formation volume factor.

The simplest way to obtain the  $c_o$  value is to substitute Equations 3.4 and 3.8 into the Equation 1.5, thus, the oil compressibility in terms of density is given by the following expression:

$$c_o = -\frac{1}{\rho_o} \left( \frac{\partial \rho_o}{\partial p} \right)_T \quad (3.44)$$

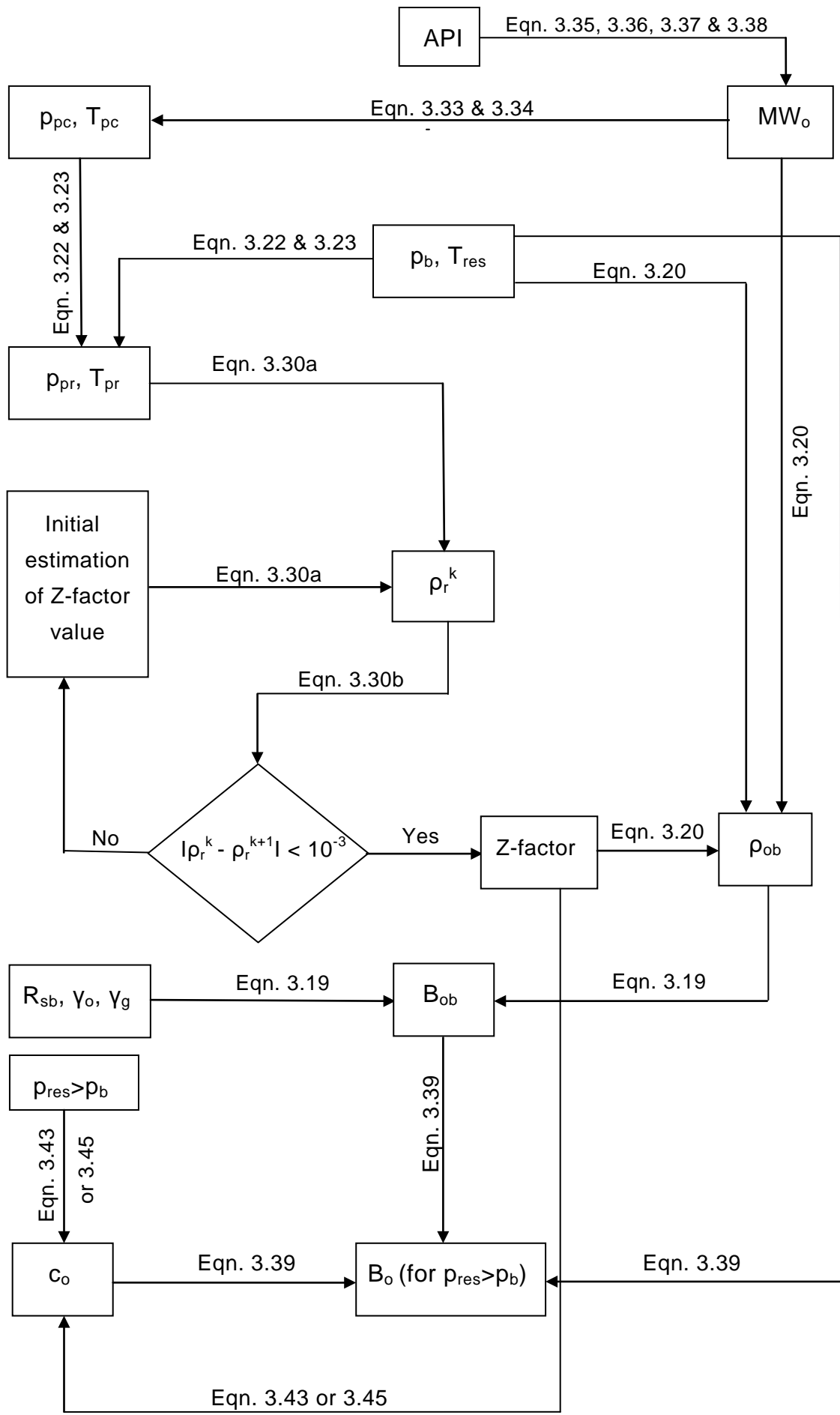
For small ranges of pressure, across which  $c_o$  is nearly constant, Equation 1.5 can be integrated to get:

$$c_o(p - p_b) = \ln \left( \frac{\rho_o}{\rho_{ob}} \right) \quad (3.45)$$

Then, the density of the liquid phase can be easily determined by Equation 3.4, using the DAK equation for the computation of Z-factor.

### ***3.3. Flow Chart of the Liquid Z-Factor Based $B_o$ prediction Method***

This section presents a summary (in the form of a flow chart) of the proposed method for predicting oil formation volume factor at pressures above bubble point pressure. As previously mentioned, the liquid Z-factor, necessary for the oil density at bubble point pressure estimation, is calculated from the DAK EOS in conjunction with the Sutton (2008)<sup>[13]</sup> correlations for the computation of pseudo-reduced properties. The data measured during a well test which are:  $\gamma_o$ ,  $\gamma_g$  and  $R_s$  in combination with  $MW_o$  constitute the required input parameters for the proposed method.



## C H A P T E R 4

# Evaluation Procedure – Comparison of Correlations

### 4.1. Error Analysis – Definitions

The field data of several reservoir oils from all over the world, together with their  $B_o$  values at bubble point and at elevated reservoir pressures measured in the PVT lab, were used for testing the performance of the developed correlation as well as some of the most widely used correlations which are presented in Chapter 2.

#### 4.1.1. Statistical Error Analysis

The accuracy of correlations relative to the experimental values is determined by various statistical indices. The criteria used in this study include: average percent relative error (APRE), average absolute percent relative error (AAPRE), minimum/maximum absolute percent error ( $E_{min}$  and  $E_{max}$  respectively), standard deviation ( $SD$ ) and the correlation coefficient ( $r^2$ ). Equations for those parameters are given below:

##### 1. Average Percent Relative Error (APRE):

It is the measure of the relative deviation from the experimental data, defined by:

$$E_r = \left(\frac{1}{n_d}\right) \sum_{i=1}^{n_d} E_i \quad (4.1)$$

Where  $E_i$  is the relative deviation of an estimated value,  $x_{est}$ , from an experimental value,  $x_{exp}$  and is defined by the following expression:

$$E_i = \left( \frac{x_{est} - x_{exp}}{x_{exp}} \right) \times 100, i = 1, 2, \dots, n_d \quad (4.2)$$

## 2. Average Absolute Percent Relative Error (AAPRE):

It measures the relative absolute deviation from the experimental values, defined by:

$$E_a = \left( \frac{1}{n_d} \right) \sum_{i=1}^{n_d} |E_i| \quad (4.3)$$

## 3. Minimum and Maximum Absolute Percent Relative Error:

To define the range of error for each correlation, the calculated absolute percent relative error values are scanned to determine the minimum and maximum values. They are defined by:

$$E_{max} = \max_{i=1}^{n_d} [E_i] \quad (4.4)$$

and

$$E_{min} = \min_{i=1}^{n_d} [E_i] \quad (4.5)$$

The lower the value of the  $E_{max}$ , the higher the accuracy of the correlation is.

## 4. Standard Deviation:

Standard deviation,  $SD$ , of the estimated relative to the experimental values is a measure of dispersion and can be calculated using the following equation:

$$SD^2 = \left( \frac{1}{n_d - 1} \right) \sum_{i=1}^{n_d} E_i^2 \quad (4.6)$$

A lower value of standard deviation means a smaller degree of scattering. The accuracy of the correlation is determined by the value of the standard deviation, where small value indicates higher accuracy. The value of standard deviation is usually expressed in percent.

## 5. The Correlation Coefficient:

It represents the degree of success in reducing the standard deviation by regression analysis, defined by:

$$r^2 = 1 - \frac{\sum_{i=1}^{n_d} (x_{exp} - x_{est})_i^2}{\sum_{i=1}^{n_d} (x_{exp} - x_{bar})_i^2} \quad (4.7)$$

where,  $x_{bar}$  represents the average of the experimental data points.

The correlation coefficient lies between 0 and 1. A value of 1 indicates a perfect correlation, whereas a value of 0 implies no correlation at all, among the given independent variables.

### 4.1.2. Evaluation Using Crossplots

In this technique, all the estimated values are plotted versus the experimental values, and thus a crossplot is formed. A 45° [0.79-rad] straight line is drawn on the crossplot on which estimated value is equal to experimental value. The closer the plotted data points are to this line, the more accurate the correlation is proved to be.

## 4.2. Results of the Error Analysis

The experimental data used for testing the performance of each one of the presented correlations, was derived from four different databases. Each one database contains laboratory measurements performed on crude oil samples collected from the following regions worldwide:

- 1) Malaysia - 93 crude oil samples<sup>[1]</sup>
- 2) Middle East - 110 crude oil samples<sup>[2]</sup>
- 3) North Sea - 41 crude oil samples<sup>[3]</sup>
- 4) Worldwide - 202 crude oil samples<sup>[4]</sup>

All the experimental data are presented in Appendix A and the comparison between the experimental and estimated values are depicted in Appendix B. Totally, 446 data points used for comparison.

The experimental data contained in the fourth database will be called TUC database.

The performance of each correlation, initially, was tested **against each individual database** for the prediction of bubble-point oil FVF,  $B_{ob}$ .

The TUC database, which contains crude oil samples of worldwide origin, does not contain measurements of  $B_{ob}$ , but rather measurements of density at the bubble-point pressure. For this reason, the experimental  $B_{ob}$  was generated, utilizing Equation 3.19.

At a second stage, given the estimated  $B_{ob}$  values of each one correlation, and applying the Petrosky-Farshad correlation for the calculation of  $c_o$  (the reason why this method was selected, will be clarified in the following section), the undersaturated  $B_o$  values was estimated, using Equation 3.39.

For the generation of the experimental undersaturated  $B_o$  values, the same procedure was performed, using the experimental  $c_o$  values, contained in the TUC database, as well as the experimental  $B_{ob}$  values. The elevated pressure at which the undersaturated  $B_o$ , as well as the undersaturated  $c_o$ , values were evaluated, was decided to be set at **500 psi above the bubble-point pressure**.

According to the above, the data points against which the accuracy of the predicted undersaturated  $B_o$  value was tested were the experimental data points of the fourth database (equal to 202 data points).

The error analysis for the accuracy of the undersaturated value of  $c_o$ , based on the methods presented in Chapter 2 and 3 (Vasquez-Begg's, Petrosky-Farshad's, Ahmed's, using densities, using Mattar's et al equation), are presented below.

## 4.2.1. Error analysis for the prediction of the undersaturated $c_o$

Tables 4.1 - 4.5 illustrate the results of the statistical error analysis performed for the undersaturated oil isothermal compressibility coefficient,  $c_o$  according to the type of crude oil. The Petrosky-Farshad correlation exhibited the lowest errors and standard deviation, with the highest correlation coefficient accuracy of 0.870, as presented in Table 4.2. The undersaturated  $c_o$  prediction using densities (Equation 3.45) stood second in accuracy. Vasquez-Beggs correlation as well as Mattar's equation showed even poor accuracy, with a correlation coefficient of 0.719 and 0.643 (Tables 4.1 and 4.4), respectively. Finally, Ahmed's correlation, as shown in Table 4.3, proved totally inaccurate since the correlation coefficient has a negative value.

As indicated by the crossplots of Vasquez-Beggs and Mattar correlations (Figures 4.1 and 4.4, respectively), both methods can be applied for  $c_o$  values up to  $2 \times 10^{-5} \text{ psi}^{-1}$ .

Most of the plotted points of Petrosky-Farshad's correlation, shown in Figure 4.2, fall very closely to the diagonal. This is the reason why this correlation was preferred for the estimation of  $c_o$  required in Equation 3.39 for the undersaturated  $B_o$  determination.

Conversely, the plotted points of Ahmed's correlation (Figure 4.3) deviate considerably from the diagonal.

The fact that the Petrosky-Farshad correlation provides the most accurate results was selected out of the five available methods for the estimation of undersaturated  $c_o$  used

It also should be pointed out that the statistical indices of all methods reveal higher accuracy for **light** crude oils than in the case of Heavy or Medium crudes.

### 4.2.1.1. Vasquez and Begg's Correlation

**Table 4.1** Statistical error analysis for the prediction of undersaturated  $c_o$  using Vasquez and Begg's correlation

Crude Oil Type	$r^2$	SD	$E_{\min}$	$E_{\max}$	APRE (%)	AAPRE (%)
All Types	0.643	50.03	0.08	340.01	16.02	29.11
Heavy	<0.000	91.35	8.99	213.57	58.45	29.01
Medium	<0.000	107.04	7.84	340.01	2.80	56.79
Light	0.661	41.03	0.08	200.44	15.08	25.70

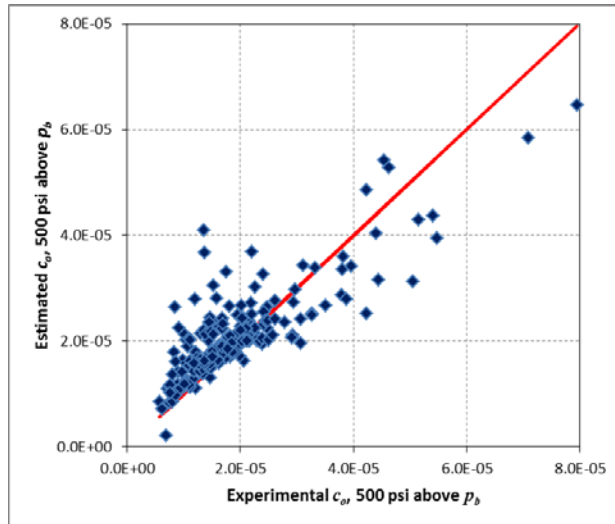


Figure 4.1 Crossplot for undersaturated  $c_o$  (Vasquez and Begg's Correlation)

#### 4.2.1.2. Petrosky and Farshad's Correlation

Table 4.2 Statistical error analysis for the prediction of undersaturated  $c_o$  using Petrosky and Farshad's correlation

Crude Oil Type	$r^2$	SD	$E_{min}$	$E_{max}$	APRE (%)	AAPRE (%)
All Types	<b>0.870</b>	25.53	0.03	132.96	7.09	16.17
Heavy	<0.000	20.36	3.05	38.47	-3.05	16.20
Medium	<0.000	31.33	0.62	88.48	-7.31	20.41
Light	0.860	25.28	0.03	132.96	8.58	15.95

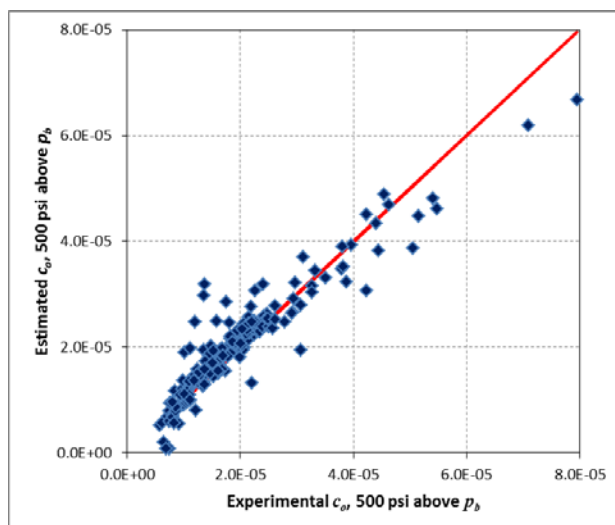
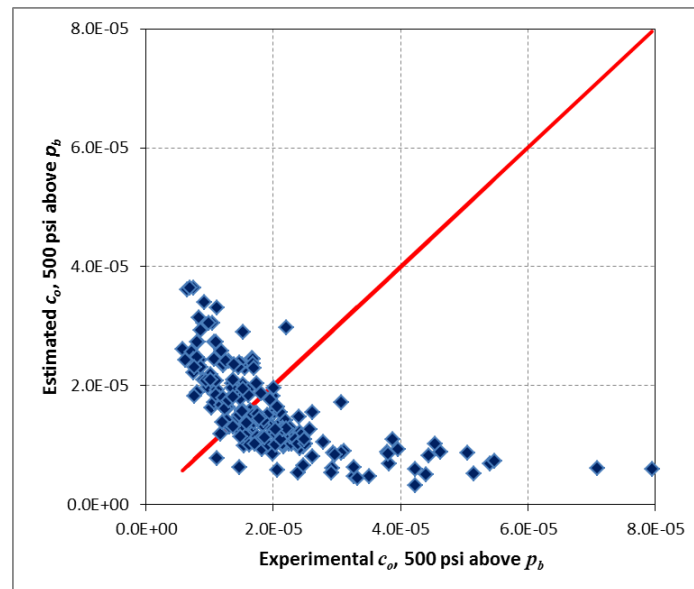


Figure 4.2 Crossplot for undersaturated  $c_o$  (Petrosky - Farshad's Correlation)

### 4.2.1.3. Ahmed's Correlation

**Table 4.3** Statistical error analysis for the prediction of undersaturated  $c_o$  using Ahmed's correlation

Crude Oil Type	$r^2$	SD	$E_{min}$	$E_{max}$	APRE (%)	AAPRE (%)
All Types	<0.000	105.17	0.21	455.84	19.23	71.94
Heavy	<0.000	256.38	92.47	352.28	228.47	70.54
Medium	<0.000	186.13	57.31	389.70	147.37	156.25
Light	<0.000	85.93	0.21	455.84	0.67	58.90



**Figure 4.3** Crossplot for undersaturated  $c_o$  (Ahmed's Correlation)

### 4.2.1.4. Mattar's Correlation

**Table 4.4** Statistical error analysis for the prediction of undersaturated  $c_o$  using Mattar's correlation

Crude Oil Type	$r^2$	SD	$E_{min}$	$E_{max}$	APRE (%)	AAPRE (%)
All Types	0.719	20.31	0.20	71.18	-13.68	16.73
Heavy	<0.000	32.94	5.45	71.18	-5.49	23.28
Medium	<0.000	22.80	1.52	36.38	-19.59	19.59
Light	0.692	19.59	0.20	61.53	-13.61	16.23

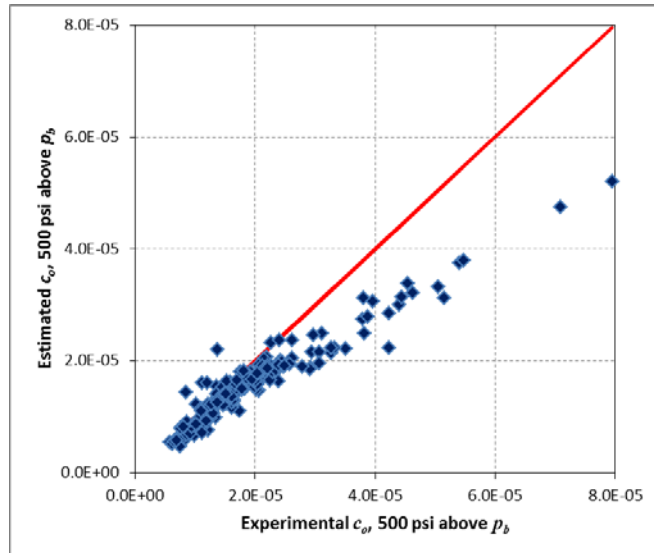


Figure 4.4 Crossplot for undersaturated  $c_o$  (Using Mattar's correlation)

#### 4.2.1.5. Undersaturated $c_o$ prediction using densities (Equation 3.45)

Table 4.5 Statistical error analysis for the prediction of undersaturated  $c_o$  using densities (Equation 3.45)

Crude Oil Type	$r^2$	SD	$E_{min}$	$E_{max}$	APRE (%)	AAPRE (%)
All Types	0.857	30.26	0.12	213.23	11.42	17.37
Heavy	<0.000	90.11	2.33	213.23	30.38	17.45
Medium	<0.000	28.18	0.62	75.02	-4.52	18.88
Light	0.866	25.40	0.12	197.97	11.73	15.91

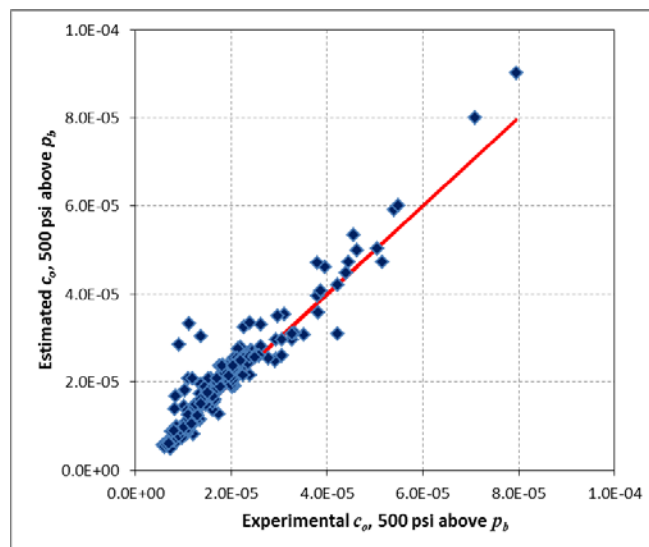


Figure 4.5 Crossplot for undersaturated  $c_o$  [using densities (Equation 3.45)]

In the next section, the statistical and graphic error analysis performed on the presented correlations for the prediction of the  $B_{ob}$  and for the undersaturated  $B_o$  is illustrated.

#### **4.2.2. Error analysis for the prediction of the $B_o$ at bubble-point and at undersaturated conditions**

As mentioned in the introduction of this chapter, each one of the presented methods was tested against each individual database, for the estimation of  $B_{ob}$ . For each one correlation, a table showing the calculated statistical parameters and the crossplot for each database, separately, are presented.

##### **4.2.2.1. Standing's Correlation**

- ***Accuracy of  $B_{ob}$***

As Table 4.6 shows, the Standing's correlation proved very accurate for the estimation of  $B_{ob}$ , especially for Middle East crude oils with a correlation coefficient of 0.957.

**Table 4.6** Accuracy of Standing's Correlation for the determination of  $B_{ob}$

Region of oil samples	Range of $B_{ob}$	$r^2$	SD	$E_{min}$	$E_{max}$	APRE (%)	AAPRE (%)
Worldwide	All Range	0.940	6.16	0.00	20.49	2.01	4.81
	$1 < B_{ob} < 2$	0.864	5.64	0.00	20.49	1.61	4.38
	$B_{ob} > 2$	0.743	8.97	1.07	15.82	4.57	7.57
North Sea	All Range	0.920	7.15	0.01	28.31	4.25	4.88
	$1 < B_{ob} < 1.5$	0.799	4.64	0.01	13.13	1.62	2.98
	$B_{ob} > 1.5$	0.768	6.39	1.40	14.62	5.49	5.49
Middle East	All Range	<b>0.957</b>	2.84	0.00	10.84	1.58	1.94
	$1 < B_{ob} < 1.5$	0.970	1.79	0.00	5.01	0.93	1.35
	$B_{ob} > 1.5$	0.323	6.65	2.97	10.84	5.99	5.99
Malaysia	All Range	0.951	2.987	0.022	8.845	-0.016	2.308

According to the crossplots illustrated in Figures 4.6 - 4.9, the Standing's correlation is suggested to be used only in the  $B_{ob}$  range of  $1 < B_{ob} < 1.5$ , since, beyond this interval the data points fall irregularly with respect to the diagonal.

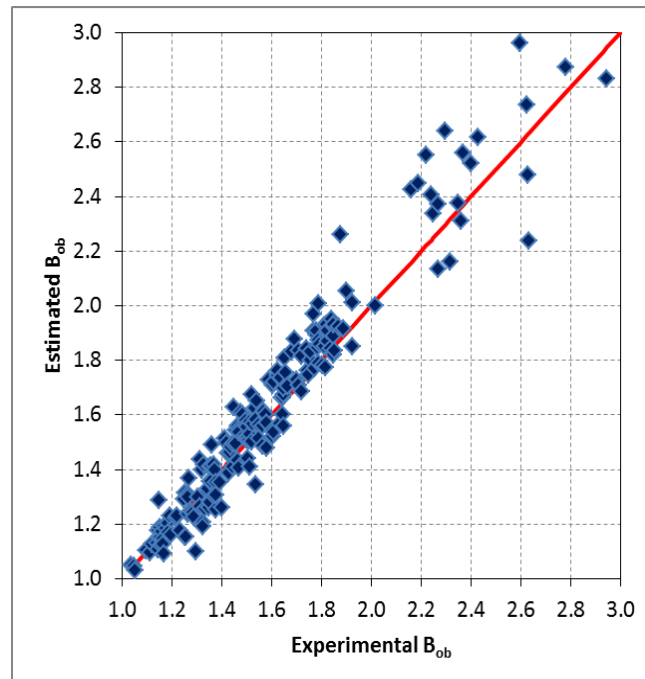


**Figure 4.6** Crossplot for  $B_{ob}$  using Standing's Correlation – TUC database

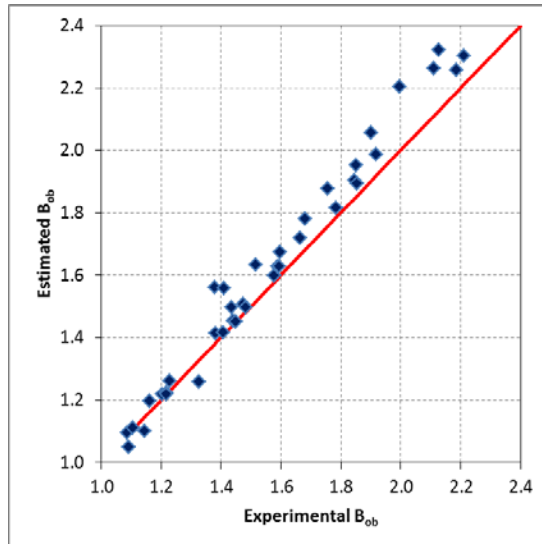


**Figure 4.7** Crossplot for  $B_{ob}$  using Standing's Correlation - North Sea oil samples

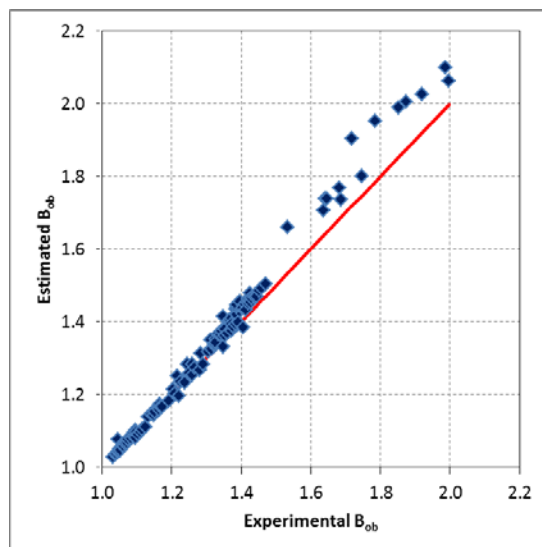


**Figure 4.8** Crossplot for  $B_{ob}$  using Standing's Correlation - Middle East oil samples

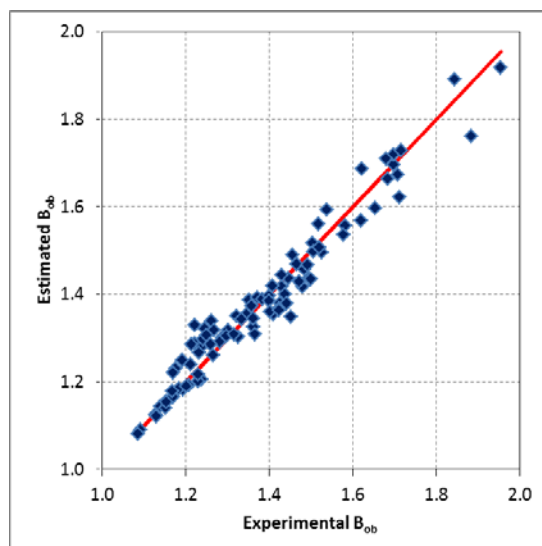


**Figure 4.9** Crossplot for  $B_{ob}$  using Standing's Correlation - Malaysian oil samples

- **Accuracy of undersaturated  $B_o$**

The accuracy of the prediction of  $B_{ob}$  by Standing's correlation is illustrated in the precise estimation of  $B_o$  for pressure 500 psi above the bubble-point pressure, as shown in Table 4.7, with a correlation coefficient of 0.960.

**Table 4.7** Accuracy of undersaturated  $B_o$  using Standing's Correlation for the estimation of the  $B_{ob}$  and Petrosky-Farshad's method for the  $c_o$  calculation

Crude Oil Type	$r^2$	SD	$E_{min}$	$E_{max}$	APRE (%)	AAPRE (%)
All Types	0.960	4.07	0.01	16.34	1.67	2.90
Heavy	<0.000	5.01	0.14	11.89	0.54	2.94
Medium	0.944	2.67	0.21	5.96	0.14	1.90
Light	0.957	4.11	0.01	16.34	1.83	2.97

The plotted points in the crossplot of Figure 4.10 are consistent with the results of the above table, indicating a slight overestimation of the undersaturated  $B_o$ , for values more than 1.5.

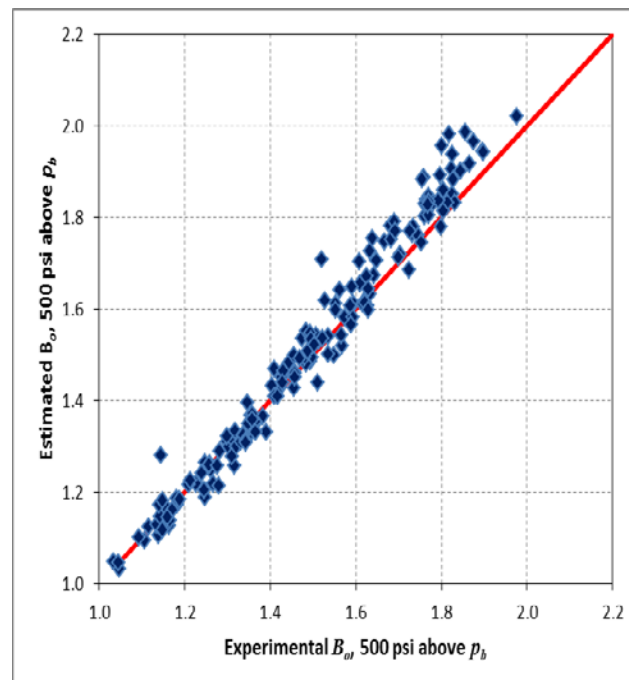


**Figure 4.10** Crossplot for undersaturated  $B_o$  at 500psi above  $p_b$  - Standing's Correlation

#### 4.2.2.2. Vasquez and Begg's Correlation

- **Accuracy of  $B_{ob}$**

As it is depicted by Table 4.8, the  $B_{ob}$  prediction provided by the Vasquez and Begg's correlation is less accurate than the Standing's correlation for the Malaysian, North Sea and for TUC database. On the other hand, the results are more precise than the Standing's method compared with the Middle East oil samples.

**Table 4.8** Accuracy of Vasquez-Begg's Correlation for the determination of  $B_{ob}$

Region of Oil Samples	Range of $B_{ob}$	$r^2$	SD	$E_{min}$	$E_{max}$	APRE (%)	AAPRE (%)
Worldwide	All Range	0.896	6.51	0.04	22.62	-4.02	4.89
	$1 < B_{ob} < 2$	0.913	4.57	0.04	13.71	-2.74	3.75
	$B_{ob} > 2$	<0.500	13.73	0.36	22.62	-12.25	12.25
North Sea	All Range	0.957	4.01	0.05	11.93	-1.87	3.01
Middle East	All Range	0.980	2.08	0.01	6.90	-0.26	1.66
Malaysia	All Range	0.945	2.81	0.01	10.25	0.02	2.13

From the crossplots given in Figures 4.11 and 4.12, the  $B_{ob}$  prediction using Vasquez and Begg's correlation is excellent for  $B_{ob}$  values **less than 2.0**. Beyond this value the data points are scattered abnormally, expressing low degree of correlation.

However, Figures 4.13 and 4.14 indicate that the maximum allowed  $B_{ob}$  value that this method can be applied, is equal to **1.5**.

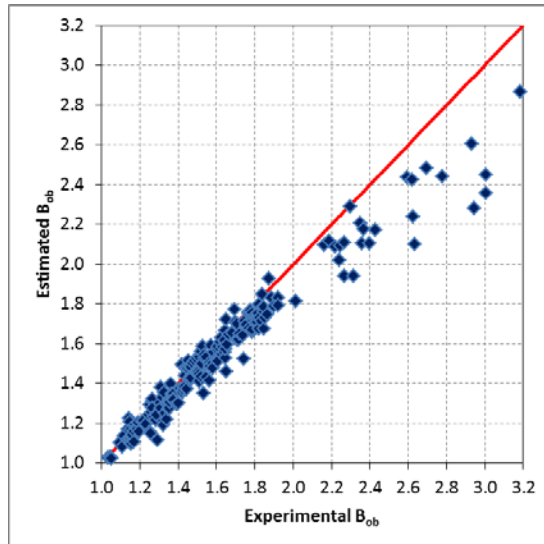


**Figure 4.11** Crossplot for  $B_{ob}$  using Vasquez-Begg's Correlation – TUC database

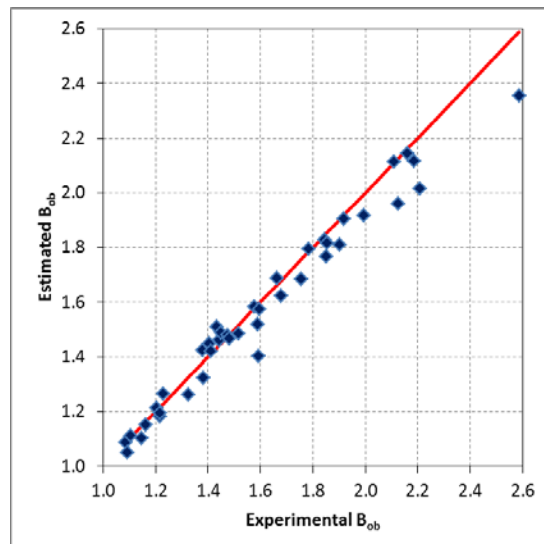


**Figure 4.12** Crossplot for  $B_{ob}$  using Vasquez-Begg's Correlation – North Sea oil samples

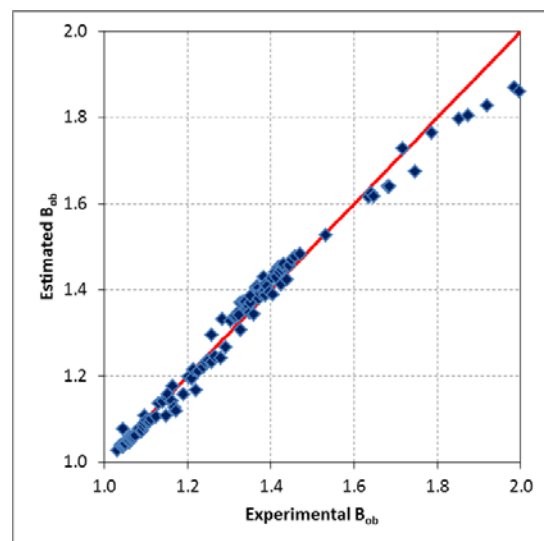


**Figure 4.13** Crossplot for  $B_{ob}$  using Vasquez-Begg's Correlation, Middle East oil samples

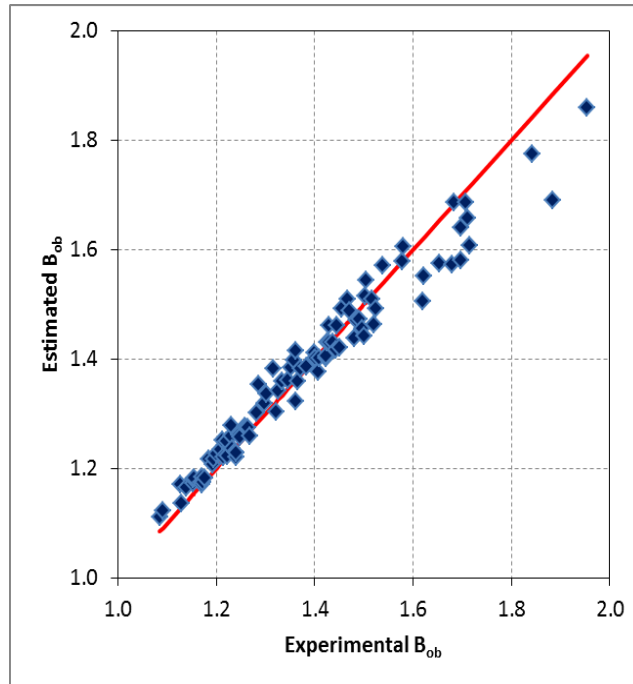


**Figure 4.14** Crossplot for  $B_{ob}$  using Vasquez-Begg's Correlation, Malaysian oil samples

- **Accuracy of undersaturated  $B_o$**

Based on a correlation coefficient of 0.910, presented in Table 4.9, and on the slight deviation of the data points from the diagonal, as depicted in Figure 4.15, the undersaturated  $B_o$  prediction, utilizing Vasquez-Begg's correlation, is satisfactory.

**Table 4.9** Accuracy of undersaturated  $B_o$  using Vasquez-Begg's Correlation for the estimation of the  $B_{ob}$  and Petrosky-Farshad's method for the  $c_o$  calculation

Crude Oil Type	$r^2$	SD	$E_{min}$	$E_{max}$	APRE (%)	AAPRE (%)
All Range	0.910	6.07	0.00	22.75	-4.05	4.57
Heavy	<0.000	4.41	0.88	7.73	-1.76	3.57
Medium	0.870	4.29	0.69	7.79	-1.88	3.41
Light	0.903	6.23	0.00	22.75	-4.31	4.69

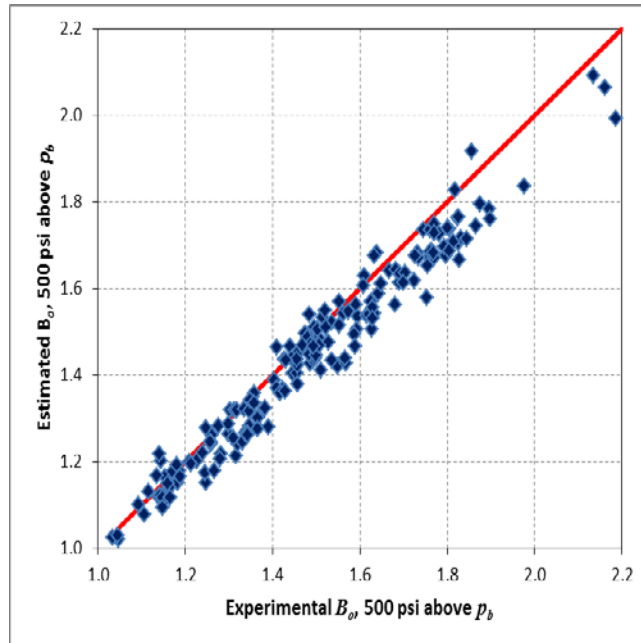


Figure 4.15 Crossplot for undersaturated  $B_o$  at 500psi above  $p_b$  - Vasquez and Begg's Correlation

### 4.2.2.3. Glaso's Correlation

- **Accuracy of  $B_{ob}$**

With a correlation coefficient of 0.947 and a standard deviation equal to 5.34, as presented in Table 4.10, Glaso's correlation constitutes a more accurate method of predicting the  $B_{ob}$  than the Standing's and the Vasquez–Begg's correlations, as far as the TUC database is concerned.

Table 4.10 Accuracy of Glaso's Correlation for the determination of  $B_{ob}$

Region of Oil Samples	Range of $B_{ob}$	$r^2$	SD	$E_{min}$	$E_{max}$	APRE (%)	AAPRE (%)
Worldwide	All Range	0.947	5.34	0.003	18.23	-1.33	4.14
	$1 < B_{ob} < 2$	0.903	4.94	0.003	16.89	-0.74	3.90
	$B_{ob} > 2$	0.684	7.58	0.478	18.23	-5.11	5.67
North Sea	All Range	0.972	3.79	0.013	11.30	0.84	2.69
Middle East	All Range	0.974	2.42	0.01	9.15	0.01	1.90
	$1 < B_{ob} < 1.5$	0.971	1.91	0.01	4.71	-0.53	1.64
	$B_{ob} > 1.5$	0.674	4.73	0.23	9.15	3.68	3.71
Malaysia	All Range	0.921	3.62	0.03	9.48	-2.05	2.98

As depicted in Figures 4.16 - 4.18, the Glaso's correlation is appropriate for  $B_{ob}$  values **up to 1.5**. Above this value the plotted data points deviate considerably from the diagonal.

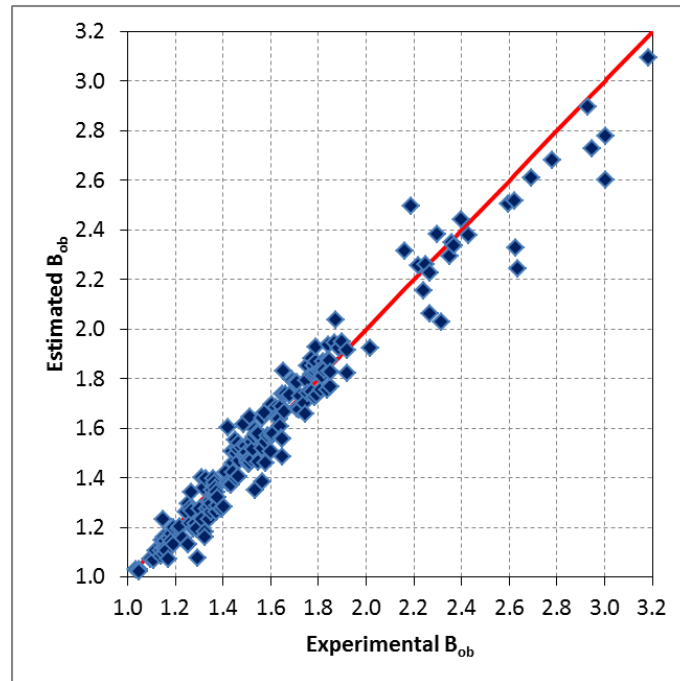


Figure 4.16 Crossplot for  $B_{ob}$  using Glaso's Correlation – TUC database

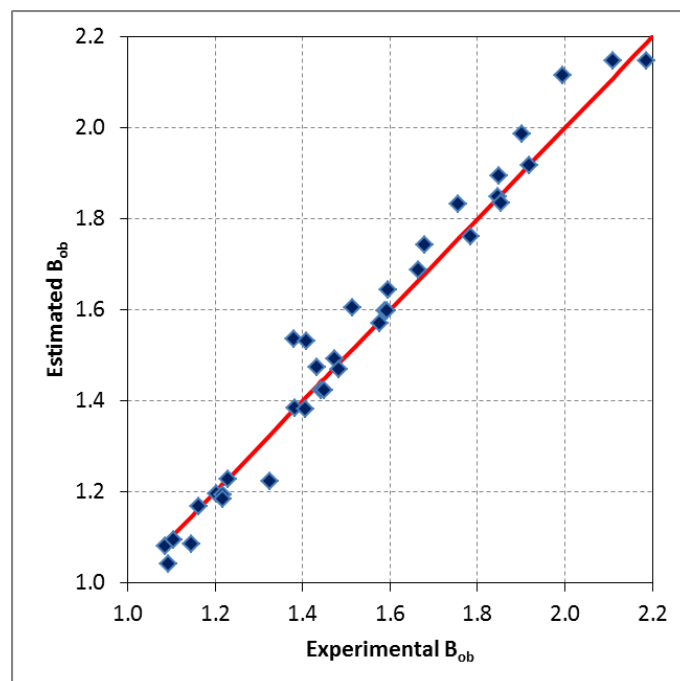
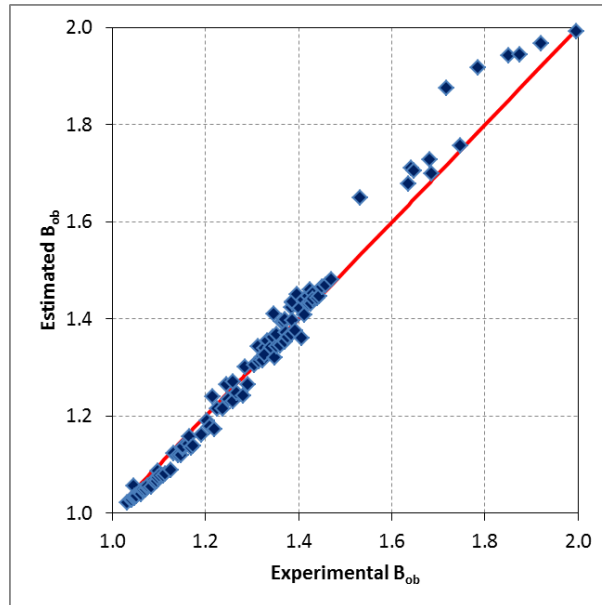
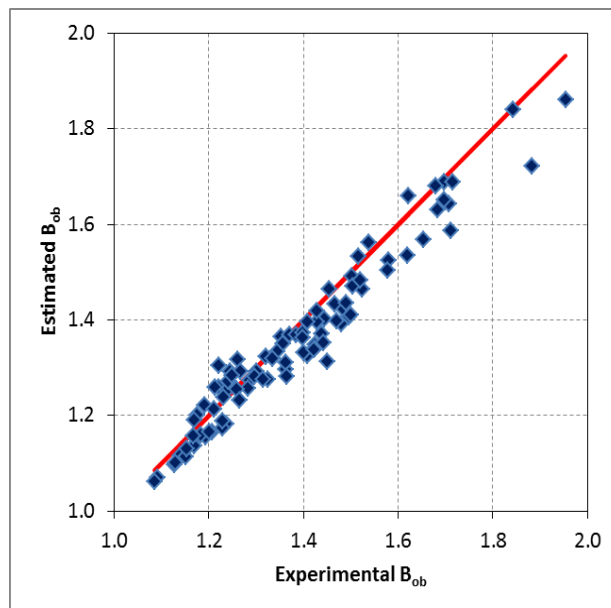


Figure 4.17 Crossplot for  $B_{ob}$  using Glaso's Correlation – North Sea oil samples



**Figure 4.18** Crossplot for  $B_{ob}$  using Glaso's Correlation – Middle East oil samples



**Figure 4.19** Crossplot for  $B_{ob}$  using Glaso's Correlation – Malaysian oil samples

- ***Accuracy of undersaturated  $B_o$***

The statistical error analysis performed on undersaturated  $B_o$  based on Glaso's correlation for the estimation of  $B_{ob}$  is presented in Table 4.11.

**Table 4.11** Accuracy of undersaturated  $B_o$  using Glaso's Correlation for the estimation of the  $B_{ob}$  and Petrosky-Farshad's method for the  $c_o$  calculation

Crude Oil Type	$r^2$	SD	$E_{min}$	$E_{max}$	APRE (%)	AAPRE (%)
All Range	0.974	3.67	0.00	14.31	-1.54	2.74
Heavy	<0.000	4.79	1.19	7.25	-2.13	3.91
Medium	0.927	3.41	0.58	7.64	-2.09	2.73
Light	0.973	3.63	0.00	14.31	-1.47	2.69

The crossplot depicted in Figure 4.20 indicates the satisfactorily estimation of the undersaturated  $B_o$ , since, the most data points fall very close to the diagonal.

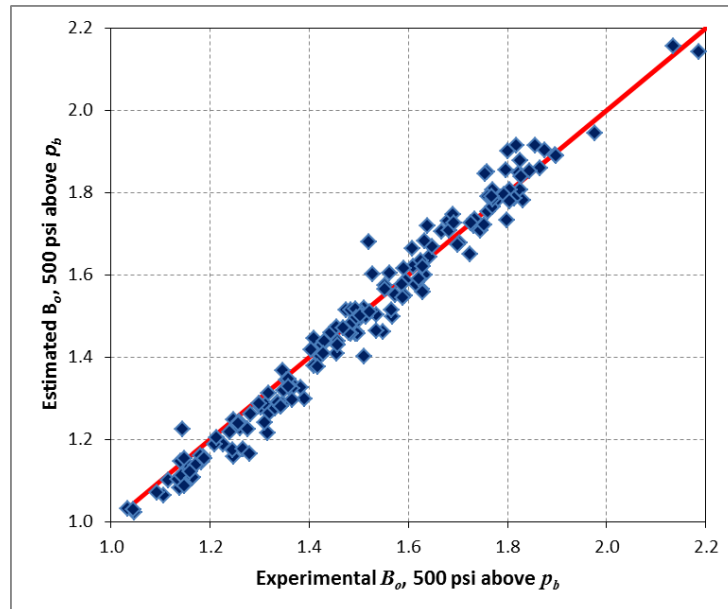


**Figure 4.20** Crossplot for undersaturated  $B_o$  at 500psi above  $p_b$  - Glaso's Correlation

#### 4.2.2.4. Al-Mahroun's Correlation

- **Accuracy of  $B_{ob}$**

This correlation constitutes the most accurate of all methods presented in this study for the prediction of the  $B_{ob}$ , when compared against **the Middle East and the North Sea oils**, with a correlation coefficient of 0.961 and 0.994,

respectively (Table 4.12). The former statement is reasonable, as this method was developed especially for Middle East oils.

**Table 4.12** Accuracy of Al-Mahroun's Correlation for the determination of  $B_{ob}$

Region of Oil Samples	Range of $B_{ob}$	$r^2$	SD	$E_{min}$	$E_{max}$	APRE (%)	AAPRE (%)
Worldwide	All Range	0.948	5.62	0.00	22.81	-1.54	4.28
	$1 < B_{ob} < 2$	0.923	4.55	0.00	16.63	-0.50	3.62
	$B_{ob} > 2$	0.716	10.28	0.67	22.81	-8.24	8.49
North Sea	All Range	<b>0.961</b>	3.97	0.03	13.95	0.12	2.83
Middle East	All Range	<b>0.994</b>	1.20	0.01	4.00	-0.18	0.92
Malaysia	All Range	0.943	3.202	0.116	9.076	0.255	2.421

From the crossplots illustrated in Figures 4.21 – 4.24 it is obvious that the Al-Mahroun's correlation provides accurate estimation for  $B_{ob}$  range  $1 < B_{ob} < 2$ .

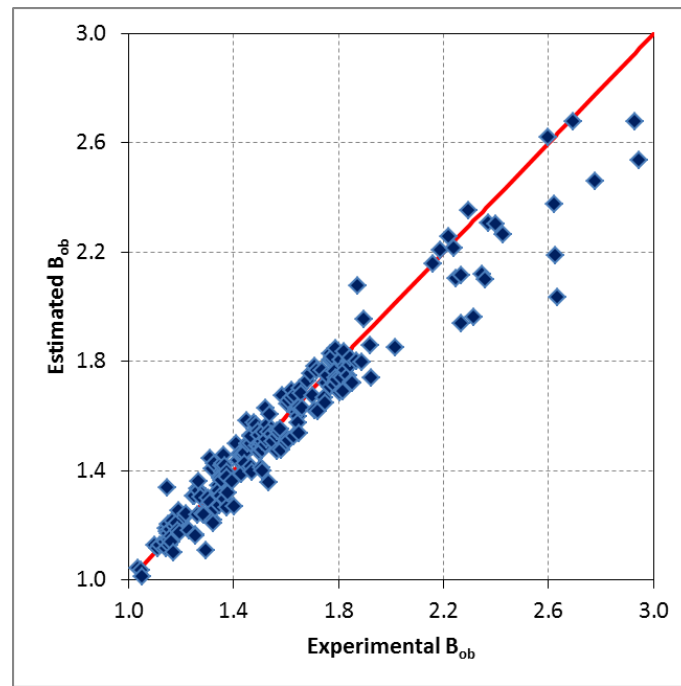


**Figure 4.21** Crossplot for  $B_{ob}$  using Al-Mahroun's Correlation – TUC database

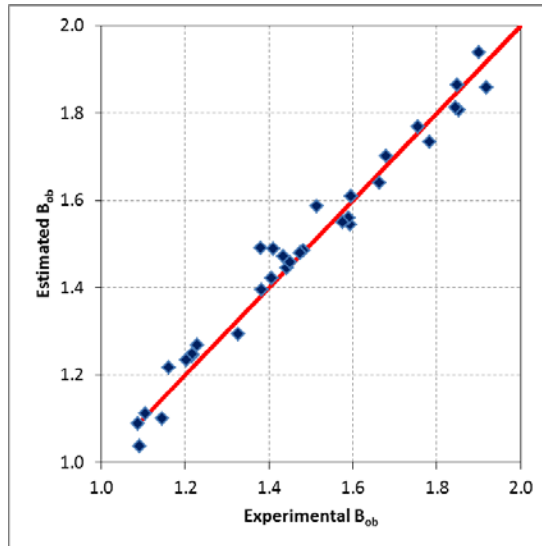


**Figure 4.22** Crossplot for  $B_{ob}$  using Al-Mahroun's Correlation – North Sea oil samples

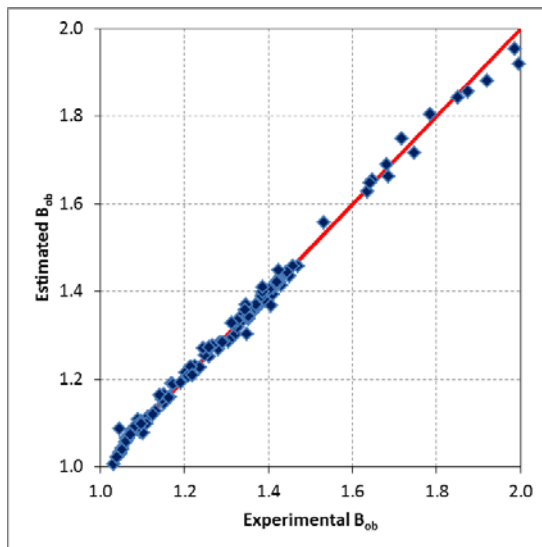


**Figure 4.23** Crossplot for  $B_{ob}$  using Al-Mahroun's Correlation – Middle East oil samples

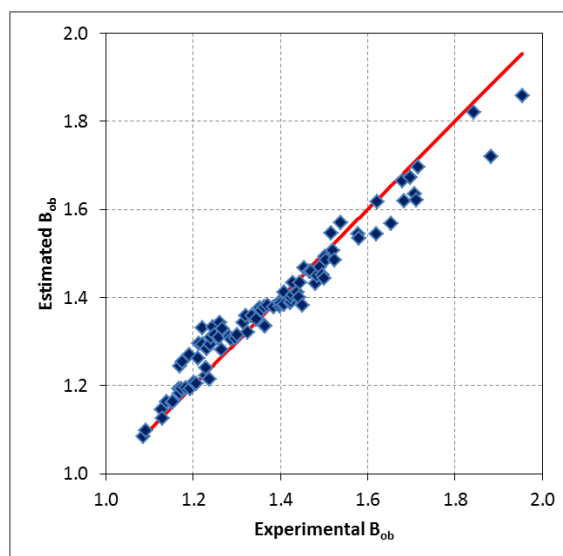


**Figure 4.24** Crossplot for  $B_{ob}$  using Al-Mahroun's Correlation - Malaysian oil samples

- **Accuracy of undersaturated  $B_o$**

The results from the statistical error analysis performed for the undersaturated  $B_o$ , as shown in Table 4.13, are comparable with the results arising from the Standing's and Glaso's correlations, providing sufficient precision.

**Table 4.13** Accuracy of undersaturated  $B_o$  using Al-Mahroun's Correlation for the estimation of the  $B_{ob}$  and Petrosky-Farshad's method for the  $c_o$  calculation

Crude Oil Type	$r^2$	SD	$E_{min}$	$E_{max}$	APRE (%)	AAPRE (%)
All Range	0.963	4.04	0.01	16.68	-1.68	2.66
Heavy	<0.000	6.50	0.10	16.44	1.88	3.37
Medium	0.971	2.32	0.03	4.11	0.09	1.77
Light	0.961	4.01	0.01	16.68	-1.96	2.69

The crossplot for the undersaturated  $B_o$ , shown in Figure 4.25, indicates the adequate performance of Al-Mahroun's correlation for the  $B_{ob}$  calculation, used in Equation 3.39.

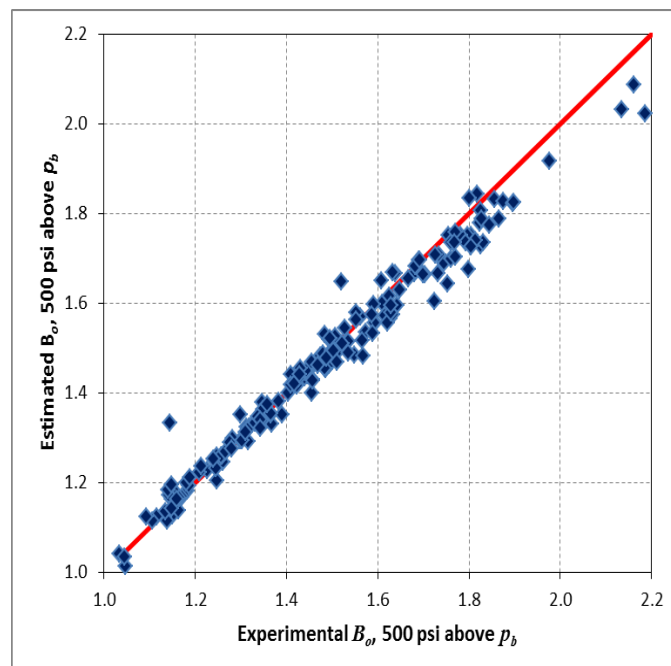


**Figure 4.25** Crossplot for undersaturated  $B_o$  at 500psi above  $p_b$  – Al-Mahroun's Correlation

#### 4.2.2.5. Sulaimon's Correlation

- **Accuracy of  $B_{ob}$**

The statistical accuracy of  $B_{ob}$ , based on Sulaimon's method, as illustrated in Table 4.14, implements the highest errors, out of all the presented correlations for all the databases.

**Table 4.14** Accuracy of Sulaimon's Correlation for the determination of  $B_{ob}$

Region of Oil Samples	Range of $B_{ob}$	$r^2$	SD	$E_{min}$	$E_{max}$	APRE (%)	AAPRE (%)
Worldwide	All Range	0.653	12.27	0.00	36.31	-3.42	9.35
	$1 < B_{ob} < 2$	<b>0.838</b>	8.16	0.00	19.90	0.29	6.71
	$B_{ob} > 2$	0.586	25.23	12.34	36.31	-23.92	23.92
North Sea	All Range	0.608	11.31	0.44	22.26	-1.03	9.09
Middle East	All Range	0.558	12.62	0.58	23.28	9.06	10.60
Malaysia	All Range	0.702	8.54	0.14	16.93	2.53	7.21

The crossplots for the  $B_{ob}$  estimation, based on of Sulaimon's correlation, are depicted in Figures 4.26 - 4.29. As shown in Figure 4.26, for  $B_{ob}$  values more than 2.0, the data points fall far away from the diagonal, indicating poor accuracy.

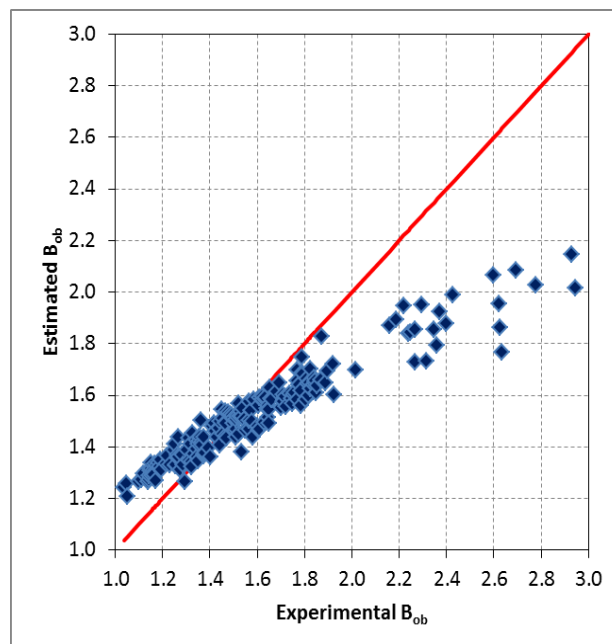


**Figure 4.26** Crossplot for  $B_{ob}$  using Sulaimon's Correlation – TUC database

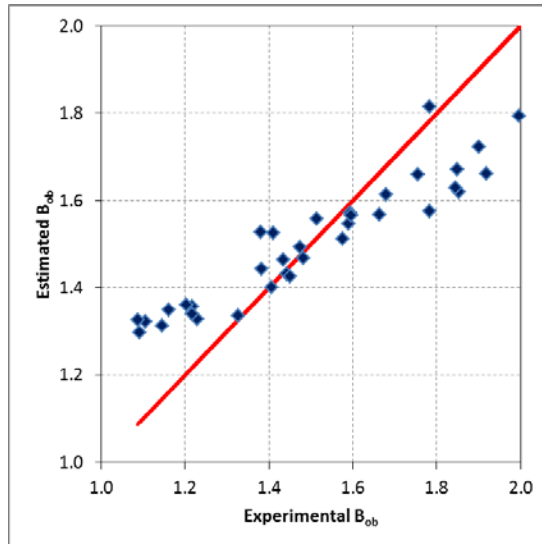


**Figure 4.27** Crossplot for  $B_{ob}$  using Sulaimon's Correlation – North Sea oil samples

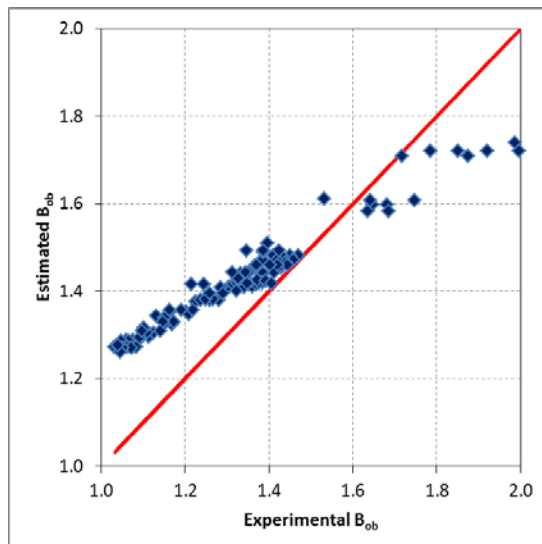


**Figure 4.28** Crossplot for  $B_{ob}$  using Sulaimon's Correlation – Middle East oil samples

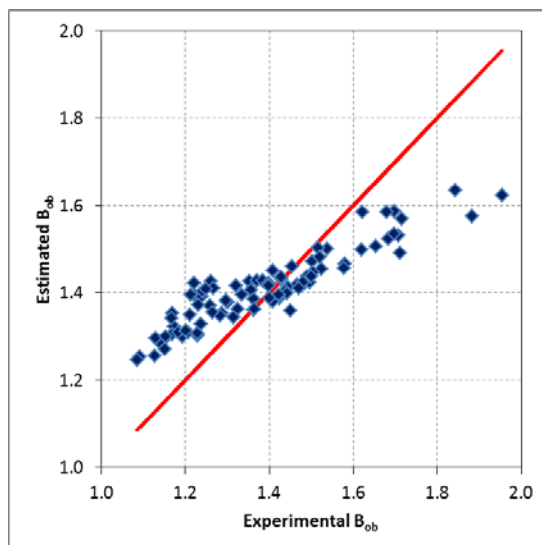


**Figure 4.29** Crossplot for  $B_{ob}$  using Sulaimon's Correlation - Malaysian oil samples

- **Accuracy of undersaturated  $B_o$**

The very low accurate estimation of  $B_{ob}$  using the Sulaimon's correlation, resulted in a low precision prediction of undersaturated  $B_o$ , as shown in Table 4.15.

**Table 4.15** Accuracy of undersaturated  $B_o$  using Sulaimon's Correlation for the estimation of the  $B_{ob}$  and Petrosky-Farshad's method for the  $c_o$  calculation

Crude Oil Type	$r^2$	SD	$E_{min}$	$E_{max}$	APRE (%)	AAPRE (%)
All Range	0.654	11.91	0.01	36.29	-3.35	9.12
Heavy	<0.000	13.52	6.51	15.80	12.37	12.37
Medium	0.321	11.35	1.21	15.96	9.07	10.04
Light	0.628	11.88	0.01	36.29	-4.96	8.91

The crossplot for the  $B_o$  at pressure 500psi above  $p_b$  is presented in Figure 4.30, affirming the low accuracy of the  $B_{ob}$  estimation.

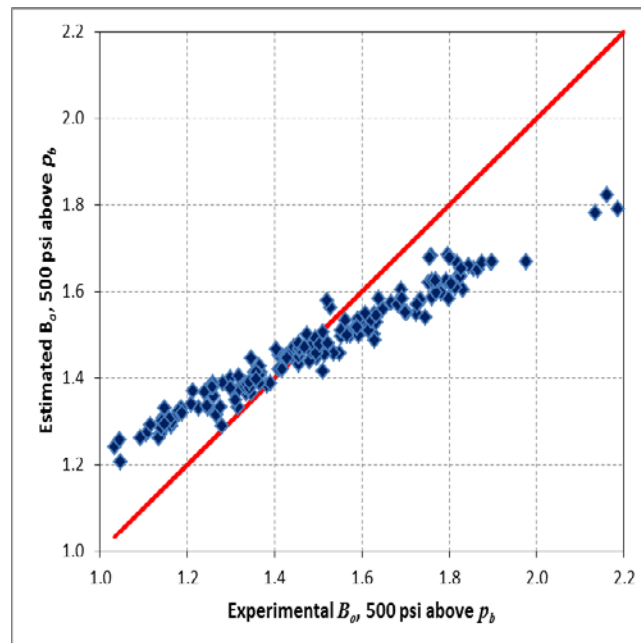


**Figure 4.30** Crossplot for undersaturated  $B_o$  at 500psi above  $p_b$  – Sulaimon's Correlation

#### 4.2.2.6. Liquid Z-factor Based $B_o$ Prediction Method

- **Accuracy of  $\rho_{ob}$**

It is interesting to present the accuracy of the density at the bubble-point,  $\rho_{ob}$ , since the TUC database, as mentioned previously, contains measurements of  $\rho_{ob}$  rather than of  $B_{ob}$ . The estimated  $\rho_{ob}$  was determined by the Equation 3.20, utilizing the DAK equation for the calculation of the liquid Z-factor.

The sufficient precision of the  $\rho_{ob}$  as illustrated by the correlation coefficient accuracy of 0.938 (Table 4.16) indicates that the  $B_{ob}$  determination utilizing the liquid Z-factor based method (which requires the  $\rho_{ob}$  as input variable), will be sufficient as well.

**Table 4.16** Accuracy of the  $\rho_{ob}$

$r^2$	SD	$E_{min}$	$E_{max}$	APRE (%)	AAPRE (%)
0.955	3.11	0.01	12.29	-0.55	2.23

The scattering of data points, presented in the crossplot in Figure 4.31, verify the high precision of the  $\rho_{ob}$ .

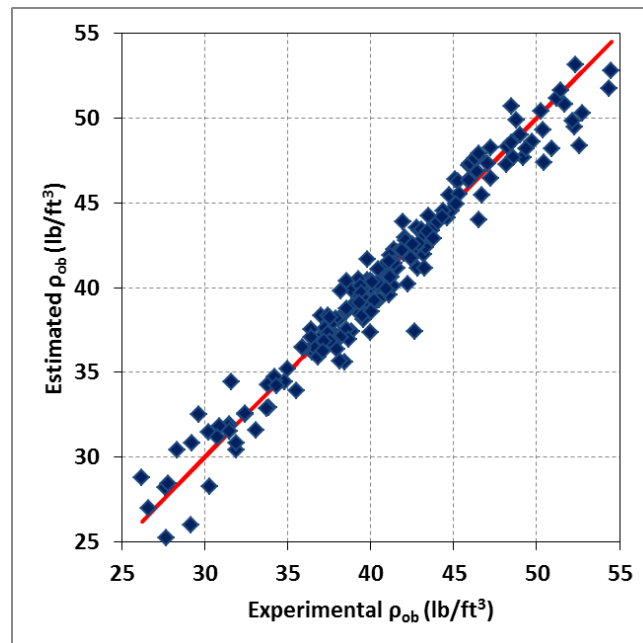


**Figure 4.31** Crossplot for the  $\rho_{ob}$

- **Accuracy of  $B_{ob}$**

The results of the statistical accuracy, using the proposed method, are presented in the table below and show adequate accuracy compared to the four databases.

**Table 4.17** Accuracy of Liquid Z-factor based Correlation for the determination of  $B_{ob}$

Region of oil samples	Range of $B_{ob}$	$r^2$	SD	$E_{min}$	$E_{max}$	APRE (%)	AAPRE (%)
Worldwide	All Range	<b>0.980</b>	3.70	0.01	26.36	0.78	2.38
	$1 < B_{ob} < 2$	0.963	3.41	0.01	26.36	0.94	2.13
	$B_{ob} > 2$	0.904	5.29	0.18	12.26	-0.28	4.00
North Sea	All Range	0.972	4.10	0.06	10.70	0.74	3.08
Middle East	All Range	0.979	2.67	0.02	7.60	0.02	1.55
Malaysia	All Range	<b>0.960</b>	2.71	0.03	6.73	0.11	2.23

As presented in the crossplots in Figures 4.32 - 4.35, the liquid Z-factor based method can be applied, in contrast to the other correlations, for  $B_{ob}$  values of **more than 2.0**.

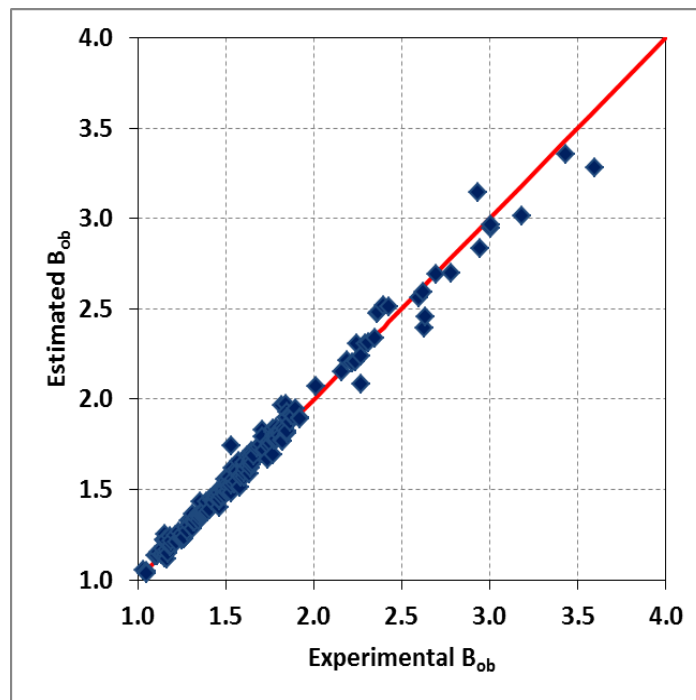


**Figure 4.32** Crossplot for  $B_{ob}$  using the liquid Z-factor based Correlation – TUC database

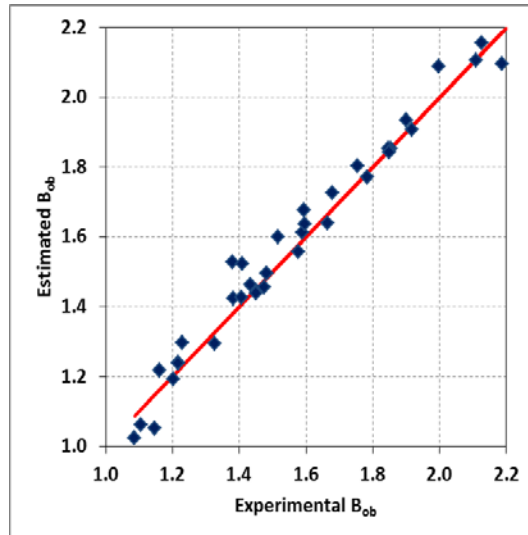


**Figure 4.33** Crossplot for  $B_{ob}$  using the liquid Z-factor based Correlation – North Sea oil samples

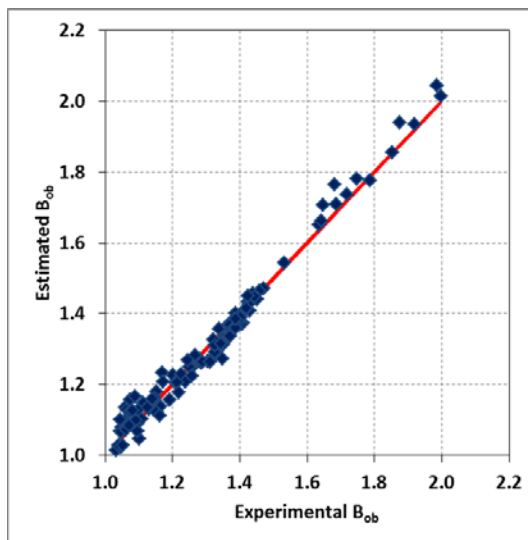


**Figure 4.34** Crossplot for  $B_{ob}$  using the liquid Z-factor based Correlation – Middle East oil samples

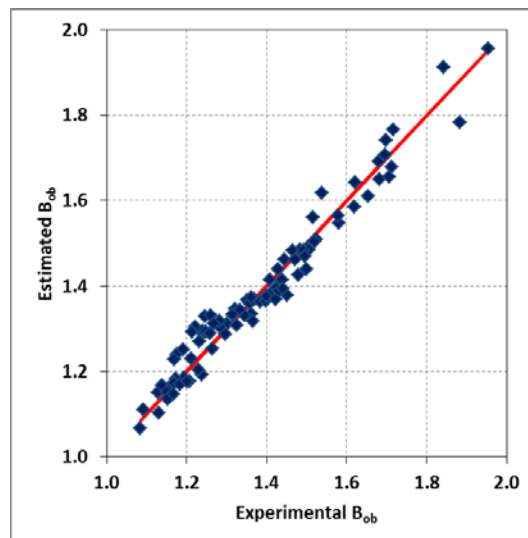


**Figure 4.35** Crossplot for  $B_{ob}$  using the liquid Z-factor based Correlation - Malaysian oil samples

- **Accuracy of undersaturated  $B_o$**

The undersaturated  $B_o$  estimation, utilizing the liquid Z-factor based method and the Petrosky-Farshad correlation for the estimation of  $c_o$  is presented in the table below.

**Table 4.18** Accuracy of undersaturated  $B_o$  using the liquid Z-factor based Correlation for the estimation of the  $B_{ob}$  and Petrosky-Farshad's method for the  $c_o$  calculation

Crude Oil Type	$r^2$	SD	$E_{min}$	$E_{max}$	APRE (%)	AAPRE (%)
All Range	0.979	3.66	0.01	26.15	0.75	2.35
Heavy	<0.000	11.19	0.19	26.15	7.35	7.35
Medium	0.953	2.91	0.07	6.59	1.68	2.04
Light	0.979	3.06	0.01	12.98	0.39	2.15

The satisfactory results of the statistical accuracy presented in the above table, are verified in the following crossplot (Figure 4.36), in which almost all data points are located on the diagonal.

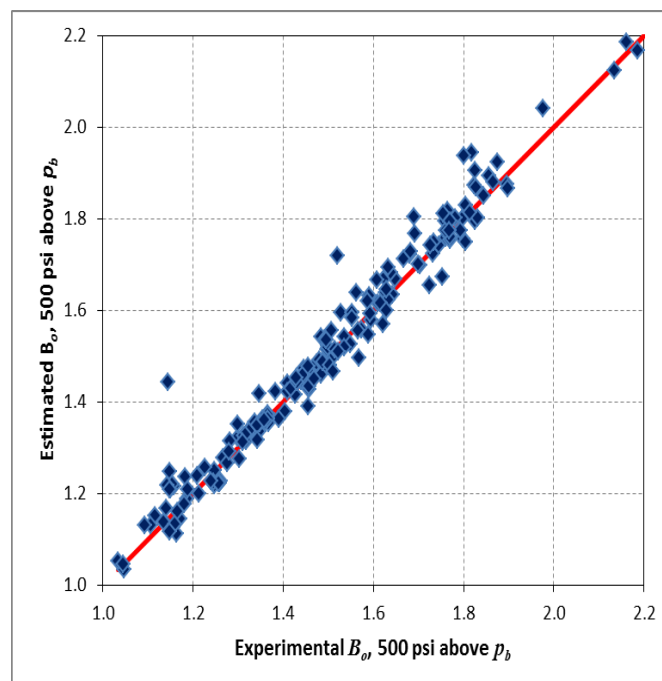


**Figure 4.36** Crossplot for undersaturated  $B_o$  at 500psi above  $p_b$  – Liquid Z-factor Based Correlation

### 4.2.3. Effect of the wellstream molecular weight on the accuracy of the $B_{ob}$ and of the undersaturated $B_o$

Given the fact that the determination of the wellstream molecular weight,  $MW_o$ , even in the laboratory, cannot be done precisely ( $\pm 8\%$  commonly accepted deviations), it is noteworthy to examine the effect of the  $MW_o$ , in the performance of the liquid Z-factor based method for the  $B_o$  prediction at bubble-point and at undersaturated conditions. For this reason, Tables 4.19 and 4.20 present the variation of the  $B_{ob}$  and of the undersaturated  $B_o$ , respectively, as the  $MW_o$  encompasses the following range:  $-8\% \leq MW_o \leq 8\%$ .

It should be mentioned, that this method was tested against the TUC database, since, it contains experimental data of oil samples collected from Worldwide origin.

**Table 4.19** Effect of  $MW_o$  on the accuracy of the  $B_{ob}$

Change in $MW_o$ (%)	$r^2$	SD	$E_{min}$	$E_{max}$	APRE (%)	AAPRE (%)
<b>-8</b>	<b>0.944</b>	<b>5.89</b>	<b>0.010</b>	<b>27.35</b>	<b>4.36</b>	<b>4.57</b>
-7	0.952	5.47	0.099	27.20	3.86	4.16
-6	0.959	5.09	0.041	27.06	3.38	3.77
-5	0.965	4.75	0.009	26.92	2.92	3.41
-4	0.970	4.44	0.003	26.80	2.46	3.08
-3	0.974	4.19	0.029	26.68	2.03	2.81
-2	0.977	3.97	0.029	26.56	1.60	2.60
-1	0.979	3.81	0.029	26.46	1.18	2.46
<b>0</b>	<b>0.980</b>	<b>3.70</b>	<b>0.013</b>	<b>26.36</b>	<b>0.78</b>	<b>2.38</b>
<b>1</b>	0.981	3.64	0.019	26.26	0.38	2.37
<b>2</b>	<b>0.981</b>	<b>3.63</b>	<b>0.002</b>	<b>26.17</b>	<b>-0.01</b>	<b>2.38</b>
<b>3</b>	0.981	3.67	0.012	26.08	-0.39	2.47
<b>4</b>	0.980	3.75	0.045	26.00	-0.75	2.60
<b>5</b>	0.978	3.87	0.025	25.93	-1.11	2.72
<b>6</b>	0.976	4.00	0.034	25.86	-1.44	2.88
<b>7</b>	0.974	4.17	0.003	25.79	-1.77	3.06
<b>8</b>	0.971	4.36	0.076	25.73	-2.10	3.27

From the above Table, it seems that decreasing by 8% the  $MW_o$  of all samples, the liquid Z-factor based method will provide less accurate results, since, the correlation coefficient of the will be decreased by 3.7%.

On the other hand, the increment by 2% of the  $MW_o$  will cause an increment of  $B_{ob}$  accuracy by 1%.

**Table 4.20** Effect of  $MW_o$  on the accuracy of the undersaturated  $B_o$ 

Change in $MW_o$ (%)	$r^2$	SD	$E_{min}$	$E_{max}$	APRE (%)	AAPRE (%)
-8	<b>0.945</b>	6.04	0.01	27.14	4.42	4.64
-7	0.953	5.62	0.02	26.99	3.92	4.23
-6	0.959	5.23	0.05	26.85	3.44	3.85
-5	0.965	4.88	0.03	26.71	2.97	3.50
-4	0.970	4.57	0.01	26.59	2.52	3.18
-3	0.974	4.30	0.00	26.47	2.08	2.91
-2	0.977	4.08	0.02	26.36	1.65	2.70
-1	0.979	3.91	0.00	26.25	1.24	2.56
<b>0</b>	<b>0.979</b>	<b>3.66</b>	<b>0.01</b>	<b>26.15</b>	<b>0.75</b>	<b>2.35</b>
1	0.981	3.71	0.01	26.05	0.43	2.44
2	<b>0.982</b>	3.69	0.01	25.96	0.04	2.45
3	0.981	3.71	0.04	25.88	-0.34	2.53
4	0.981	3.78	0.00	25.80	-0.70	2.65
5	0.979	3.87	0.09	25.72	-1.05	2.75
6	0.978	4.00	0.02	25.65	-1.39	2.89
7	0.975	4.16	0.02	25.58	-1.72	3.07
8	0.973	4.34	0.01	25.52	-2.05	3.25

The results from the above Table match with those of Table 4.19.

### ***4.3. Comparison of Correlations***

#### **4.3.1. Comparison of correlations for the $B_o$ prediction at bubble-point**

In Tables 4.21 – 4.24 is illustrated a comparison between the presented correlations for the  $B_o$  prediction at bubble-point.

**Table 4.21** Comparison of the presented correlations for the  $B_{ob}$  prediction against the TUC database

Method	$r^2$	SD	$E_{min}$	$E_{max}$	APRE (%)	AAPRE (%)
<b>Liquid Z-factor based</b>	<b>0.980</b>	<b>3.70</b>	<b>0.01</b>	<b>26.36</b>	<b>0.78</b>	<b>2.38</b>
Standing	0.940	6.16	0.00	20.49	2.01	4.81
Vasquez & Beggs	0.896	6.51	0.04	22.62	-4.02	4.89
Glaso	0.947	5.34	0.00	18.23	-1.33	4.14
Al-Mahroun	0.948	5.62	0.00	22.81	-1.54	4.28
Sulaimon	0.653	12.27	0.00	36.31	-3.42	9.35

**Table 4.22** Comparison of the presented correlations for the  $B_{ob}$  prediction against the North Sea oil samples

Method	$r^2$	SD	$E_{min}$	$E_{max}$	APRE (%)	AAPRE (%)
<b>Liquid Z-factor based</b>	0.972	4.10	0.06	10.70	0.74	3.08
Standing	0.920	7.15	0.01	28.31	4.25	4.88
Vasquez & Beggs	0.957	4.01	0.05	11.93	-1.87	3.01
Glaso	0.972	3.79	0.01	11.30	0.84	2.69
Al-Mahroun	<b>0.961</b>	<b>3.97</b>	<b>0.03</b>	<b>13.95</b>	<b>0.12</b>	<b>2.83</b>
Sulaimon	0.608	11.31	0.44	22.26	-1.03	9.09

**Table 4.23** Comparison of the presented correlations for the  $B_{ob}$  prediction against the Middle East oil Samples

Method	$r^2$	SD	$E_{min}$	$E_{max}$	APRE (%)	AAPRE (%)
Liquid Z-factor based	0.979	2.67	0.02	7.60	0.02	1.55
Standing	0.957	2.84	0.00	10.84	1.58	1.94
Vasquez & Beggs	0.980	2.08	0.01	6.90	-0.26	1.66
Glaso	0.974	2.42	0.01	9.15	0.01	1.90
Al-Mahroun	<b>0.994</b>	<b>1.20</b>	<b>0.01</b>	<b>4.00</b>	<b>-0.18</b>	<b>0.92</b>
Sulaimon	0.558	12.62	0.58	23.28	9.06	10.60

**Table 4.24** Comparison of the presented correlations for the  $B_{ob}$  prediction against the Malaysian oil Samples

Method	$r^2$	SD	$E_{min}$	$E_{max}$	APRE (%)	AAPRE (%)
Liquid Z-factor based	<b>0.960</b>	<b>2.71</b>	<b>0.03</b>	<b>6.73</b>	<b>0.11</b>	<b>2.23</b>
Standing	0.951	2.99	0.02	8.85	-0.02	2.31
Vasquez & Beggs	0.945	2.81	0.01	10.25	0.02	2.13
Glaso	0.921	3.62	0.03	9.48	-2.05	2.98
Al-Mahroun	0.943	3.20	0.12	9.08	0.26	2.42
Sulaimon	0.702	8.54	0.14	16.93	2.53	7.21

### 4.3.2. Comparison of correlations for the $c_o$ prediction 500 psi above $p_b$

The Table below presents a comparison of each method for the  $c_o$  prediction 500 psi above  $p_b$

**Table 4.25** Comparison of the presented correlations for the  $c_o$  prediction, 500 psi above  $p_b$

Method	$r^2$	SD	$E_{\min}$	$E_{\max}$	APRE (%)	AAPRE (%)
Using densities	0.857	30.26	0.12	213.23	11.42	17.37
Vasquez & Beggs	0.643	50.03	0.08	340.01	16.02	29.11
Petrosky & Farshad	0.870	25.53	0.03	132.96	7.09	16.17
Ahmed	<0.000	105.17	0.21	455.84	19.23	71.94
Mattar's equation	0.719	20.31	0.20	71.18	-13.68	16.73

### 4.3.3. Comparison of correlations for the $B_o$ prediction 500 psi above $p_b$

In Table 4.26 is illustrated a comparison between the presented correlations for the  $B_o$  prediction, 500 psi above  $p_b$ .

**Table 4.26** Comparison of the presented correlations for the  $B_o$  prediction 500 psi above  $p_b$

Method	$r^2$	SD	$E_{\min}$	$E_{\max}$	APRE (%)	AAPRE (%)
Liquid Z-factor based	<b>0.979</b>	<b>3.66</b>	<b>0.01</b>	<b>26.15</b>	<b>0.75</b>	<b>2.35</b>
Standing	0.960	4.07	0.01	16.34	1.67	2.90
Vasquez & Beggs	0.910	6.07	0.03	22.75	-4.05	4.57
Glaso	0.974	3.67	0.02	14.31	-1.54	2.74
Al-Mahroun	0.963	4.04	0.01	16.68	-1.68	2.66
Sulaimon	0.654	11.91	0.01	36.29	-3.35	9.12

Having investigated, in this Chapter, the performance of the proposed method against five well-known empirical correlations, used from the oil industry, for the determination of the oil formation volume factor, Chapter 5 deals with the useful conclusions that came out from this study.

# C H A P T E R 5

## Conclusions

1. Using fundamental relationships a simple method was developed which is called liquid  $Z$ -factor based correlation, for the prediction of the  $B_o$  at the bubble-point and at undersaturated conditions.
2. The correlation expresses the  $B_o$  as a function of data that are measured in the field during the Well Test ( $GOR$ ,  $API$ ,  $S_g$ ,  $T_{res}$ ) and the reservoir density at reservoir pressure. The DAK representation of the Standing-Katz  $Z$ -factor chart was used to calculate the crude oil density.
3. A literature review was conducted to qualify the most popular correlations for the  $B_{ob}$  prediction, currently used by the oil industry. These correlations include:
  - the Standing's (1947) correlation
  - the Vasquez-Begg's (1980) correlation
  - the Glaso's (1980) correlation
  - the Al-Mahrour's (1988) correlation, and
  - the Sulaimon's (2014) correlation
4. The accuracy of each method, including the developed correlation, was tested against four databases including experimental data of oil samples collected from all around the world.
5. The statistical error analysis performed for  $B_o$  at bubble-point pressure showed that the developed correlation exhibits the lowest errors for two out of the four databases. Hence, **the Liquid  $Z$ -factor based method provides accurate results for the  $B_{ob}$  prediction.**

6. Moreover, the empirical correlations proved inadequate for predicting  $B_{ob}$  values greater than 2, in contrast with the precise estimation of the proposed method for that  $B_o$  range.
7. The undersaturated  $c_o$  estimation was performed using the following correlations:
  - Vasquez-Begg's correlation
  - Petrosky-Farshad's correlation
  - Ahmed's correlation
  - Mattar's correlation
  - Correlation using densities

The most precise  $c_o$  determination is done using the Petrosky-Farshad's correlation

8. The estimation of  $B_o$  at pressure 500 psi above  $p_b$ , using the liquid  $Z$ -factor based correlation, exhibits the lowest statistical errors out of the five, well-known empirical correlations.
9. Finally, we recommend the use of the proposed method for  $B_o$  estimations in the field, since, it is accurate for a wide  $B_o$  range as well as valid for origins located all around the world.

## APPENDIX **A**

Experimental data of samples used for testing the performance of  
the correlations

**Table A.1 Experimental data of samples collected from Worldwide origin (TUC database)**

No	API Gravity	Specific gravity of stock-tank oil	Bubble-point pressure	Reservoir pressure 500psi above $p_b$	$c_o$ 500psi above $p_b$	Reservoir Temperature	Bubble-point solution gas to oil ratio	Gas specific gravity	Bubble-point oil density
	$^{\circ}$ API	$\gamma_o$	$p_b$ (psia)	$p_{res}$ (psi)	$c_o$ (1/psia)	$T_{res}$ ( $^{\circ}$ R)	$R_{sb}$ (scf/STB)	$\gamma_g$	$\rho_{ob}$ (lb/ft <sup>3</sup> )
1	14.0	0.972	1344.0	1841.45	5.77E-06	629.7	173.9	0.846	51.70
2	18.5	0.943	1345.0	1842.37	7.22E-06	644.7	202.5	0.869	50.29
3	19.2	0.939	1475.0	1973.58	7.43E-06	645.7	255.5	0.922	52.33
4	19.4	0.938	1592.9	2093.17	6.18E-06	600.4	226.1	0.784	49.23
5	19.9	0.935	1555.0	2058.66	8.44E-06	835.7	234.1	0.908	48.64
6	21.0	0.928	585.0	1090.22	9.08E-06	669.7	136.6	1.445	54.51
7	21.5	0.925	1687.0	2190.72	8.30E-06	647.7	259.8	0.807	51.24
8	22.2	0.921	1777.0	2272.57	1.21E-05	670.8	237.9	1.059	51.47
9	23.2	0.915	1105.0	1609.64	8.17E-06	617.7	161.2	0.761	50.41
10	23.7	0.912	2077.5	2578.53	9.08E-06	657.3	343.2	0.836	53.30
11	25.3	0.902	2009.0	2505.64	7.41E-06	610.7	249.0	0.59	50.48
12	25.4	0.902	2000.0	2497.49	1.00E-05	643.4	344.7	0.891	52.58
13	25.9	0.899	1970.4	2470.73	9.76E-06	636.7	517.9	0.958	50.90
14	26.5	0.896	596.0	1100.39	1.04E-05	684.7	134.9	1.133	54.35
15	27.0	0.893	2825.3	3328.51	1.03E-05	641.9	609.2	0.883	45.10
16	28.3	0.886	6560.0	7059.54	1.47E-05	715.7	1343.7	0.762	52.29
17	29.5	0.879	38.5	539.59	7.43E-06	590.7	3.2	2.029	52.75
18	29.7	0.878	2637.0	3132.44	8.10E-06	614.7	352.9	0.595	47.25
19	29.8	0.878	1357.0	1853.36	1.07E-05	626.7	294.6	0.921	48.47
20	30.8	0.872	1476.0	1974.5	1.30E-05	744.9	283.0	0.981	47.07

No	API Gravity	Specific gravity of stock-tank oil	Bubble-point pressure	Reservoir pressure 500psi above $p_b$	$c_o$ 500psi above $p_b$	Reservoir Temperature	Bubble-point solution gas to oil ratio	Gas specific gravity	Bubble-point oil density
	$^{\circ}$ API	$\gamma_o$	$p_b$ (psia)	$p_{res}$ (psi)	$c_o$ (1/psia)	$T_{res}$ ( $^{\circ}$ R)	$R_{sb}$ (scf/STB)	$\gamma_g$	$\rho_{ob}$ (lb/ft <sup>3</sup> )
21	31.1	0.87	418.0	921.49	9.88E-06	651.7	197.2	1.627	48.78
22	31.2	0.87	1511.0	2018.56	8.08E-06	605.6	218.3	0.789	48.22
23	31.4	0.869	1676.0	2180.71	8.64E-06	605.3	294.7	0.774	52.15
24	31.4	0.868	1825.0	2327.64	1.74E-05	674.0	505.8	1.161	49.02
24	31.4	0.868	1825.0	2327.64	1.74E-05	674.0	505.8	1.161	49.02
25	31.9	0.866	2645.0	3139.57	1.52E-05	674.7	743.6	0.955	47.22
26	32.0	0.865	3949.0	4449.59	1.17E-05	645.8	865.6	0.76	49.74
27	32.1	0.865	5687.0	6187.7	2.93E-05	759.7	1970.9	0.843	46.39
28	32.3	0.864	1886.0	2382.99	1.53E-05	739.7	501.0	0.907	49.40
29	32.3	0.864	3342.0	3844.06	1.63E-05	701.7	1006.5	0.921	45.86
30	32.4	0.863	6157.0	6657.12	2.91E-05	764.7	2077.5	0.806	46.56
31	32.4	0.863	2086.0	2586.22	1.61E-05	684.7	517.4	1.007	44.74
32	32.4	0.863	1366.0	1861.6	1.21E-05	681.7	370.8	1.24	48.51
33	32.5	0.863	2200.0	2699.82	1.11E-05	605.1	475.8	0.79	45.94
34	32.7	0.862	1406.0	1910.54	1.02E-05	686.7	515.2	1.308	45.97
35	33.0	0.86	2714.1	3210.78	1.64E-05	670.7	786.1	0.936	46.31
36	33.1	0.86	2218.9	2716.8	1.16E-05	642.7	635.0	0.861	46.54
37	33.6	0.857	1636.3	2132.75	7.68E-06	624.7	310.3	0.851	42.57
38	33.9	0.856	3966.7	4464.58	2.02E-05	693.3	1302.3	0.823	42.98
39	33.9	0.855	3113.9	3610.41	2.13E-05	752.7	872.8	0.955	46.68
40	33.9	0.855	4055.0	4552.98	1.65E-05	679.7	1158.9	0.828	40.80
41	33.9	0.855	2604.9	3103.74	1.07E-05	612.7	578.4	0.751	48.21

No	API Gravity	Specific gravity of stock-tank oil	Bubble-point pressure	Reservoir pressure 500psi above $p_b$	$c_o$ 500psi above $p_b$	Reservoir Temperature	Bubble-point solution gas to oil ratio	Gas specific gravity	Bubble-point oil density
	$^{\circ}$ API	$\gamma_o$	$p_b$ (psia)	$p_{res}$ (psi)	$c_o$ (1/psia)	$T_{res}$ ( $^{\circ}$ R)	$R_{sb}$ (scf/STB)	$\gamma_g$	$\rho_{ob}$ (lb/ft <sup>3</sup> )
42	34.0	0.855	6356.0	6855.74	2.07E-05	711.7	1715.3	0.727	42.82
43	34.0	0.855	280.0	778.99	9.16E-06	673.5	43.7	1.087	45.26
44	34.1	0.855	4305.0	4801.25	1.53E-05	704.7	1191.7	0.883	44.65
45	34.2	0.854	51.9	552.06	6.51E-06	614.7	9.5	1.79	42.31
46	34.2	0.854	2372.0	2875.34	1.10E-05	675.3	513.2	0.797	43.97
47	34.2	0.854	950.0	1454.1	1.07E-05	674.7	225.0	1.012	45.32
48	34.3	0.853	4560.0	5058.65	1.83E-05	699.7	1264.2	0.822	43.10
49	34.4	0.853	6138.0	6637.42	3.27E-05	754.7	2696.8	0.795	42.97
50	34.5	0.852	639.7	1140.77	8.33E-06	671.7	67.2	0.893	43.66
51	34.6	0.852	5454.0	5953.56	1.11E-05	754.5	1270.9	0.725	42.84
52	34.6	0.852	2288.7	2790.14	1.35E-05	626.7	581.8	0.878	42.76
53	34.6	0.852	4789.0	5291.89	1.99E-05	698.7	1363.8	0.782	42.38
54	34.7	0.852	2578.0	3079.77	1.19E-05	636.0	648.6	0.844	46.53
55	34.7	0.851	4022.7	4518.92	1.51E-05	719.7	881.3	0.781	43.06
56	34.7	0.851	2545.1	3050.42	1.22E-05	701.7	489.4	0.821	43.25
57	34.7	0.851	5970.0	6469.19	3.51E-05	749.7	2833.4	0.821	44.89
58	34.7	0.851	6195.0	6695.56	2.39E-05	706.1	2116.3	0.781	44.36
59	34.9	0.85	839.7	1339.12	8.55E-06	671.7	132.3	1.106	42.19
60	35.2	0.849	3694.7	4196.39	1.59E-05	666.3	1114.3	0.885	45.91
61	35.4	0.848	2631.0	3127.08	2.05E-05	734.0	706.4	0.977	42.02
62	35.5	0.847	2534.9	3031.32	1.35E-05	697.7	483.5	0.828	44.32
63	36.1	0.844	3434.0	3932.28	1.51E-05	707.6	743.6	0.812	45.16

No	API Gravity	Specific gravity of stock-tank oil	Bubble-point pressure	Reservoir pressure 500psi above $p_b$	$c_o$ 500psi above $p_b$	Reservoir Temperature	Bubble-point solution gas to oil ratio	Gas specific gravity	Bubble-point oil density
	$^{\circ}$ API	$\gamma_o$	$p_b$ (psia)	$p_{res}$ (psi)	$c_o$ (1/psia)	$T_{res}$ ( $^{\circ}$ R)	$R_{sb}$ (scf/STB)	$\gamma_g$	$\rho_{ob}$ (lb/ft <sup>3</sup> )
64	36.1	0.844	39.2	540.2	6.93E-06	617.7	2.1	1.567	43.17
65	36.4	0.843	3242.0	3740.01	1.32E-05	620.0	955.3	0.848	41.43
66	36.6	0.842	3289.4	3789.89	3.12E-05	713.7	2149.0	1.118	43.50
67	36.6	0.842	2354.7	2859.82	7.61E-06	581.7	528.4	0.801	43.33
68	36.7	0.841	2902.4	3406	1.28E-05	694.7	535.5	0.85	41.44
69	36.8	0.841	3953.6	4453.47	2.16E-05	709.7	1430.2	0.882	41.09
70	36.8	0.841	3684.0	4187.2	1.59E-05	673.5	991.2	0.812	42.42
71	36.9	0.84	3026.0	3524.15	1.83E-05	688.7	994.1	0.923	42.03
72	36.9	0.84	2462.0	2966.14	1.28E-05	614.7	767.4	0.859	41.43
73	36.9	0.84	1874.0	2372.11	9.45E-06	601.5	445.0	1.012	41.26
74	37.0	0.84	2697.0	3195.59	1.61E-05	647.2	809.2	0.895	43.46
75	37.0	0.84	3289.9	3790.26	1.35E-05	638.7	852.1	0.78	42.81
76	37.1	0.839	3843.0	4345.31	1.78E-05	687.7	1130.9	0.887	43.77
77	37.1	0.839	5275.0	5774.36	4.22E-05	740.1	2306.5	0.809	41.94
78	37.2	0.839	3519.0	4014.03	1.43E-05	671.0	863.0	0.756	42.42
79	37.2	0.839	2697.8	3196.3	1.46E-05	628.5	922.8	0.901	42.08
80	37.3	0.838	894.2	1402.79	1.11E-05	679.7	244.9	1.118	41.57
81	37.3	0.838	2852.0	3352.13	1.74E-05	730.7	717.9	0.955	42.13
82	37.3	0.838	1865.0	2363.94	1.10E-05	603.3	449.7	0.949	41.59
83	37.4	0.838	969.0	1471.6	8.09E-06	626.7	213.7	0.92	42.87
84	37.5	0.837	3738.0	4240.99	2.25E-05	709.7	1404.2	0.935	40.55
85	37.6	0.837	1827.0	2329.46	1.02E-05	605.1	445.7	0.958	41.10

No	API Gravity	Specific gravity of stock-tank oil	Bubble-point pressure	Reservoir pressure 500psi above $p_b$	$c_o$ 500psi above $p_b$	Reservoir Temperature	Bubble-point solution gas to oil ratio	Gas specific gravity	Bubble-point oil density
	$^{\circ}$ API	$\gamma_o$	$p_b$ (psia)	$p_{res}$ (psi)	$c_o$ (1/psia)	$T_{res}$ ( $^{\circ}$ R)	$R_{sb}$ (scf/STB)	$\gamma_g$	$\rho_{ob}$ (lb/ft <sup>3</sup> )
86	37.6	0.837	3423.0	3922.72	2.25E-05	665.7	1364.4	0.919	41.18
87	37.7	0.836	2583.9	3084.99	1.51E-05	671.7	774.2	0.916	42.54
88	38.0	0.835	2900.0	3403.85	1.72E-05	734.7	710.6	0.931	41.39
89	38.1	0.834	3828.2	4325.47	2.94E-05	689.7	1948.7	0.897	40.69
90	38.1	0.834	2438.0	2934.53	1.25E-05	626.7	794.1	0.888	41.10
91	38.2	0.834	2455.0	2959.87	2.20E-05	711.7	1149.1	1.043	41.33
92	38.2	0.834	3903.0	4403.51	2.47E-05	709.7	1496.5	0.907	40.09
93	38.3	0.833	3935.0	4437.71	2.17E-05	709.7	1360.7	0.869	40.46
94	38.4	0.833	3689.0	4191.5	2.15E-05	711.7	1436.8	0.925	41.19
95	38.5	0.832	2622.0	3119.05	1.65E-05	646.5	816.6	0.868	40.46
96	38.5	0.832	1220.0	1727.89	1.26E-05	630.7	372.4	1.034	41.87
97	38.6	0.832	3730.0	4226.71	1.53E-05	713.7	790.3	0.795	40.53
98	38.6	0.832	4030.0	4531.88	1.56E-05	714.7	898.8	0.78	39.99
99	38.6	0.832	1841.0	2342.16	1.45E-05	645.7	702.9	1.038	42.64
100	38.7	0.832	2595.0	3094.95	1.64E-05	692.7	781.1	0.972	37.02
101	38.7	0.831	4350.0	4850.9	1.62E-05	678.2	1134.3	0.77	39.72
102	38.7	0.831	2717.0	3213.39	1.52E-05	648.6	863.8	0.863	43.27
103	38.8	0.831	2531.0	3027.87	1.51E-05	659.3	792.9	0.952	40.43
104	38.8	0.831	5436.9	5937.36	3.32E-05	666.3	3659.5	0.825	39.84
105	38.8	0.831	3961.1	4459.86	2.29E-05	710.7	1311.8	0.874	39.84
106	38.8	0.831	2903.8	3407.21	1.63E-05	653.7	1006.1	0.909	39.94
107	38.8	0.831	844.9	1343.87	1.36E-05	624.7	954.6	1.131	39.98

No	API Gravity	Specific gravity of stock-tank oil	Bubble-point pressure	Reservoir pressure 500psi above $p_b$	$c_o$ 500psi above $p_b$	Reservoir Temperature	Bubble-point solution gas to oil ratio	Gas specific gravity	Bubble-point oil density
	$^{\circ}$ API	$\gamma_o$	$p_b$ (psia)	$p_{res}$ (psi)	$c_o$ (1/psia)	$T_{res}$ ( $^{\circ}$ R)	$R_{sb}$ (scf/STB)	$\gamma_g$	$\rho_{ob}$ (lb/ft <sup>3</sup> )
108	38.9	0.83	3939.0	4434.12	2.41E-05	709.7	1549.7	0.869	42.28
109	38.9	0.83	3390.9	3894.81	2.26E-05	709.7	1272.9	0.947	39.81
110	39.0	0.83	3048.0	3552.43	1.94E-05	709.7	940.7	0.91	39.35
111	39.0	0.83	4627.0	5129.81	2.48E-05	645.7	2423.7	0.821	40.00
112	39.0	0.83	1697.0	2199.79	1.36E-05	667.7	649.4	1.013	39.33
113	39.1	0.829	2080.0	2580.8	1.30E-05	597.7	759.1	0.934	38.85
114	39.1	0.829	1391.0	1884.49	1.55E-05	709.7	428.7	1.077	39.85
115	39.2	0.829	4116.9	4618.4	1.49E-05	699.7	892.2	0.761	39.99
116	39.3	0.828	1188.0	1685.82	1.66E-05	714.7	354.9	1.171	38.58
117	39.3	0.828	3014.7	3514.21	1.92E-05	709.7	1016.3	0.945	39.59
118	39.5	0.828	1178.0	1676.64	1.68E-05	714.7	369.8	1.188	39.32
119	39.6	0.827	5141.6	5639.08	3.27E-05	731.1	2227.2	0.809	38.93
120	39.7	0.826	2989.0	3491.51	1.27E-05	627.4	872.9	0.829	39.27
121	39.8	0.826	3952.8	4452.85	1.76E-05	716.7	969.2	0.829	39.49
122	39.8	0.826	2790.9	3288.55	1.70E-05	639.3	1026.0	0.902	39.40
123	39.8	0.826	3964.0	4462.31	1.71E-05	644.7	1302.8	0.817	39.37
124	39.9	0.826	1307.0	1807.57	1.51E-05	714.7	399.9	1.137	39.44
125	40.0	0.825	1253.0	1758.11	1.47E-05	714.7	392.9	1.085	38.85
126	40.0	0.825	2208.0	2707.02	1.20E-05	621.7	1362.0	1.063	36.50
127	40.1	0.824	769.0	1273.93	1.52E-05	759.3	176.5	1.178	39.99
128	40.1	0.824	3000.0	3501.22	2.01E-05	656.7	1291.7	0.923	40.11
129	40.2	0.824	2217.0	2715.14	1.59E-05	621.7	1370.6	1.061	39.73

No	API Gravity	Specific gravity of stock-tank oil	Bubble-point pressure	Reservoir pressure 500psi above $p_b$	$c_o$ 500psi above $p_b$	Reservoir Temperature	Bubble-point solution gas to oil ratio	Gas specific gravity	Bubble-point oil density
	$^{\circ}\text{API}$	$\gamma_o$	$p_b$ (psia)	$p_{res}$ (psi)	$c_o$ (1/psia)	$T_{res}$ ( $^{\circ}\text{R}$ )	$R_{sb}$ (scf/STB)	$\gamma_g$	$\rho_{ob}$ (lb/ft <sup>3</sup> )
130	40.2	0.824	1360.0	1856.1	1.46E-05	714.7	414.1	1.12	40.30
131	40.2	0.824	2790.8	3288.51	1.47E-05	629.7	800.5	0.823	40.91
132	40.3	0.824	2666.0	3167.97	1.78E-05	640.0	1062.6	0.921	38.59
133	40.3	0.824	1247.0	1752.62	1.38E-05	672.8	423.5	1.109	40.00
134	40.3	0.824	1933.0	2436.84	2.02E-05	617.1	1162.9	1.063	38.68
135	40.3	0.823	2842.0	3343.28	1.91E-05	726.4	781.6	0.962	37.42
136	40.4	0.823	1416.7	1920.3	1.68E-05	724.7	334.4	0.998	37.08
137	40.4	0.823	1906.0	2401.14	1.49E-05	645.7	803.0	1.05	38.23
138	40.4	0.823	2860.0	3359.23	2.42E-05	668.7	1381.8	0.983	37.05
139	40.5	0.823	3866.5	4365.34	3.79E-05	769.7	1814.5	0.962	38.56
140	40.6	0.822	947.0	1451.34	1.18E-05	617.7	336.7	1.152	37.42
141	40.6	0.822	3604.0	4103.13	2.16E-05	710.7	1155.1	0.909	37.45
142	40.6	0.822	3914.9	4413.59	2.61E-05	655.7	2120.0	0.864	40.26
143	40.7	0.822	2747.0	3249.59	1.69E-05	692.7	815.0	0.986	40.05
144	40.8	0.821	5515.0	6015.89	4.23E-05	664.5	5474.4	0.771	38.56
145	40.9	0.821	2888.4	3384.39	1.82E-05	682.7	1018.8	0.918	37.74
146	41.0	0.82	2202.0	2701.62	2.00E-05	702.2	593.1	0.96	38.07
147	41.4	0.818	3161.0	3660.46	2.44E-05	691.5	1312.2	0.896	38.23
148	41.4	0.818	3350.0	3851.02	1.84E-05	717.7	828.9	0.833	37.89
149	41.5	0.818	4223.0	4720.32	1.92E-05	709.7	1178.5	0.807	37.53
150	41.5	0.818	3299.2	3798.42	1.37E-05	635.7	926.4	0.804	37.60
151	41.5	0.818	4130.0	4629.44	3.06E-05	709.7	1739.3	0.871	36.65

No	API Gravity	Specific gravity of stock-tank oil	Bubble-point pressure	Reservoir pressure 500psi above $p_b$	$c_o$ 500psi above $p_b$	Reservoir Temperature	Bubble-point solution gas to oil ratio	Gas specific gravity	Bubble-point oil density
	$^{\circ}$ API	$\gamma_o$	$p_b$ (psia)	$p_{res}$ (psi)	$c_o$ (1/psia)	$T_{res}$ ( $^{\circ}$ R)	$R_{sb}$ (scf/STB)	$\gamma_g$	$\rho_{ob}$ (lb/ft <sup>3</sup> )
152	41.5	0.818	2937.5	3437	2.15E-05	712.7	1145.6	0.966	36.72
153	41.6	0.817	2344.1	2850.28	1.62E-05	689.7	522.2	0.944	39.35
154	41.7	0.817	3804.9	4305.52	2.03E-05	638.7	1447.8	0.824	37.26
155	41.7	0.817	1760.0	2257.11	1.75E-05	630.7	1315.1	1.109	37.44
156	41.8	0.817	4640.9	5141.01	4.40E-05	704.7	3659.8	0.87	38.43
157	41.8	0.816	1974.9	2474.8	1.37E-05	682.7	382.4	0.809	36.41
158	42.0	0.816	731.0	1238.89	2.20E-05	797.7	138.2	1.003	37.35
159	42.0	0.816	3748.0	4249.54	2.35E-05	709.7	1201.4	0.899	36.56
160	42.0	0.816	3728.1	4225.11	1.83E-05	714.7	1112.9	0.883	38.14
161	42.1	0.815	2900.0	3403.85	1.85E-05	692.7	906.5	0.953	37.80
162	42.1	0.815	1932.5	2436.42	1.53E-05	709.7	565.0	1.017	37.54
163	42.3	0.814	3852.0	4352.98	1.86E-05	709.7	1065.4	0.924	37.98
164	42.4	0.814	3912.8	4411.81	2.38E-05	712.7	1302.2	0.868	36.86
165	42.4	0.814	3150.0	3650.81	2.05E-05	658.5	1330.1	0.923	36.44
166	42.4	0.814	2503.4	3003.21	2.11E-05	704.7	869.2	0.952	37.43
167	42.5	0.813	3910.0	4409.47	3.82E-05	658.7	2846.6	0.904	37.54
168	42.7	0.812	1679.0	2183.44	1.80E-05	687.7	778.2	1.081	37.17
169	42.8	0.812	3835.0	4331.29	5.05E-05	794.1	1928.7	0.913	37.16
170	42.8	0.812	3415.0	3915.76	2.78E-05	665.1	1503.4	0.9	35.95
171	42.8	0.812	2812.8	3308.01	1.78E-05	650.7	914.3	0.828	35.88
172	43.0	0.811	2219.7	2717.53	2.06E-05	704.7	868.2	1.049	33.89
173	43.1	0.811	2670.0	3171.54	1.52E-05	659.7	752.0	0.892	35.02

No	API Gravity	Specific gravity of stock-tank oil	Bubble-point pressure	Reservoir pressure 500psi above $p_b$	$c_o$ 500psi above $p_b$	Reservoir Temperature	Bubble-point solution gas to oil ratio	Gas specific gravity	Bubble-point oil density
	$^{\circ}$ API	$\gamma_o$	$p_b$ (psia)	$p_{res}$ (psi)	$c_o$ (1/psia)	$T_{res}$ ( $^{\circ}$ R)	$R_{sb}$ (scf/STB)	$\gamma_g$	$\rho_{ob}$ (lb/ft <sup>3</sup> )
174	43.1	0.81	1820.0	2323.11	2.01E-05	699.7	599.7	1.098	34.84
175	43.6	0.808	3739.0	4241.84	2.97E-05	688.2	2097.7	0.89	34.21
176	43.7	0.808	2489.0	2990.31	2.26E-05	686.7	1409.7	1.018	34.20
177	43.9	0.807	4415.0	4916.62	5.15E-05	691.7	3783.3	0.876	33.76
178	44.0	0.806	3747.1	4248.74	2.12E-05	712.7	1186.8	0.884	33.83
179	44.0	0.806	2780.0	3278.91	2.15E-05	652.7	1313.0	0.938	31.59
180	44.0	0.806	277.0	776.2	1.12E-05	658.7	92.2	1.414	34.36
181	44.0	0.806	3971.7	4475.78	2.50E-05	712.7	1295.4	0.87	32.47
182	44.1	0.806	2705.0	3202.71	2.20E-05	651.7	1309.9	0.94	32.43
183	44.2	0.805	1427.9	1930.51	1.70E-05	716.7	403.3	1.061	33.07
184	44.3	0.805	3207.7	3709.98	2.58E-05	709.7	1074.0	0.929	31.88
185	44.4	0.804	3267.0	3770.3	2.49E-05	665.7	1455.1	0.946	35.54
186	44.6	0.803	1796.0	2301.33	1.94E-05	652.7	863.6	1.036	31.89
187	45.0	0.802	2737.0	3240.71	2.04E-05	636.0	1327.0	0.905	31.48
188	45.4	0.8	3302.0	3800.88	3.96E-05	731.7	2036.9	1.013	31.43
189	45.8	0.798	1350.6	1847.49	1.37E-05	666.8	1035.2	1.094	29.62
190	46.6	0.795	2467.0	2970.63	4.63E-05	653.7	2857.4	1.101	28.36
191	46.6	0.794	3564.1	4060.91	3.80E-05	731.7	2149.3	0.95	31.49
192	47.1	0.792	3852.0	4352.98	4.45E-05	747.7	2110.1	0.906	30.89
193	47.1	0.792	1997.0	2494.77	2.40E-05	676.7	1266.0	1.084	30.30
194	47.3	0.792	3225.0	3725.12	7.95E-05	727.7	4262.0	1.028	30.24
195	47.5	0.791	3262.0	3765.93	3.87E-05	739.7	1489.7	0.933	27.65

No	API Gravity	Specific gravity of stock-tank oil	Bubble-point pressure	Reservoir pressure 500psi above $p_b$	$c_o$ 500psi above $p_b$	Reservoir Temperature	Bubble-point solution gas to oil ratio	Gas specific gravity	Bubble-point oil density
	$^{\circ}$ API	$\gamma_o$	$p_b$ (psia)	$p_{res}$ (psi)	$c_o$ (1/psia)	$T_{res}$ ( $^{\circ}$ R)	$R_{sb}$ (scf/STB)	$\gamma_g$	$\rho_{ob}$ (lb/ft <sup>3</sup> )
196	47.5	0.791	3376.0	3873.69	7.09E-05	726.7	3977.6	1.014	30.76
197	47.6	0.79	2547.1	3052.2	2.62E-05	749.7	831.7	0.96	29.21
198	47.9	0.789	2576.0	3077.99	3.06E-05	749.7	573.1	0.972	27.83
199	48.4	0.787	2107.9	2606	4.55E-05	661.7	2526.5	1.162	29.16
200	48.4	0.787	3595.2	4095.55	5.41E-05	714.7	3061.1	0.951	26.22
201	48.4	0.786	3695.0	4196.65	5.48E-05	739.7	2701.9	0.923	27.67

**Table A.2 Experimental data of samples collected from Malaysia**

Sample Number	API Gravity	Bubble-point pressure	Reservoir Temperature	Bubble-point solution gas to oil ratio	Gas specific gravity	Bubble-point Oil FVF
	$^{\circ}$ API	$p_b$ (psia)	$T_{res}$ ( $^{\circ}$ F)	$R_{sb}$ (scf/STB)	$\gamma_g$	$B_{ob}$ (bbl/STB)
1	26.6	1818	152	285	0.704	1.153
2	26.9	952	146	142	0.667	1.092
3	28.9	2106	161	344	0.648	1.194
4	29.1	1085	187	169	0.638	1.128
5	29.2	1271	187	198	0.775	1.139
6	31	1760	211	372	1.195	1.222
7	31.2	3063	180	577	0.737	1.301
8	31.4	1220	174	267	0.884	1.173
9	31.4	1302	180	242	0.824	1.170
10	31.9	1195	180	214	0.664	1.152
11	31.9	935	125	150	0.612	1.085
12	32.2	3063	180	586	0.628	1.287
13	32.3	1058	127	220	0.790	1.130
14	32.5	2368	235	440	0.756	1.282
15	32.6	1910	152	384	0.733	1.238
16	33.3	3142	247	761	0.723	1.484

Sample Number	API Gravity	Bubble-point pressure	Reservoir Temperature	Bubble-point solution gas to oil ratio	Gas specific gravity	Bubble-point Oil FVF
	°API	p <sub>b</sub> (psia)	T <sub>res</sub> (°F)	R <sub>sb</sub> (scf/STB)	γ <sub>g</sub>	B <sub>ob</sub> (bbl/STB)
17	33.4	1390	141	287	0.718	1.154
18	34	1765	151	345	0.695	1.184
19	34.1	3851	243	819	0.663	1.466
20	34.6	2970	239	737	0.707	1.445
21	34.8	1838	153	366	0.664	1.208
22	35	1530	209	355	1.228	1.240
23	35.4	1450	208	359	1.250	1.214
24	36.1	1982	224	415	1.140	1.246
25	36.6	1700	206	364	1.028	1.232
26	37	2350	169	680	0.818	1.352
27	37.1	1660	203	421	1.298	1.221
28	37.1	2168	164	544	0.789	1.297
29	37.4	3440	192	863	0.764	1.455
30	37.4	1492	159	341	0.716	1.201
31	37.5	1951	173	367	0.627	1.230
32	37.7	2616	177	667	0.842	1.371
33	37.8	1780	205	509	0.853	1.362
34	38	1225	211	267	1.263	1.176
35	38	1225	211	260	1.168	1.170
36	38.2	1370	205	313	1.174	1.192
37	38.2	2480	171	686	0.737	1.357
38	38.3	2310	161	636	0.801	1.345
39	38.6	2408	166	683	0.821	1.384
40	38.6	2692	179	393	0.631	1.230
41	38.9	1562	196	463	1.181	1.261
42	39	1570	207	366	1.315	1.241
43	39.2	2020	211	491	1.051	1.321
44	39.3	3449	195	899	0.769	1.503
45	39.6	2611	225	810	0.789	1.525
46	39.8	1593	203	421	1.181	1.268
47	39.8	790	150	274	1.005	1.168
48	40	2423	169	713	0.765	1.399
49	40	2360	167	694	0.765	1.399
50	40	2470	166	760	0.758	1.429
51	40	1698	193	646	0.964	1.408
52	40.2	3780	209	1023	0.658	1.581
53	40.4	2609	198	1019	1.038	1.622
54	40.4	2344	184	791	0.743	1.429
55	40.5	1744	190	524	0.727	1.325

Sample Number	API Gravity	Bubble-point pressure	Reservoir Temperature	Bubble-point solution gas to oil ratio	Gas specific gravity	Bubble-point Oil FVF
	°API	p <sub>b</sub> (psia)	T <sub>res</sub> (°F)	R <sub>sb</sub> (scf/STB)	γ <sub>g</sub>	B <sub>ob</sub> (bbl/STB)
56	40.7	2402	242	844	0.919	1.619
57	41	1414	185	425	1.155	1.249
58	41.4	1658	186	368	0.865	1.212
59	41.4	3387	194	919	0.673	1.505
60	41.8	1728	215	397	0.941	1.259
61	42	2562	234	741	0.795	1.491
62	42.3	3420	194	1212	0.685	1.683
63	42.9	2194	214	664	0.750	1.438
64	42.9	1620	188	404	0.847	1.265
65	43.1	2290	208	990	0.801	1.653
66	43.2	2390	226	956	0.811	1.538
67	44.5	2081	230	494	0.677	1.315
68	45.2	2274	245	546	0.689	1.451
69	45.2	1530	185	566	0.817	1.334
70	45.3	2193	214	634	0.717	1.425
71	45.3	2221	238	547	0.693	1.362
72	45.4	3160	186	1213	0.705	1.707
73	46.6	2165	211	856	0.916	1.517
74	46.8	2822	280	1006	0.876	1.698
75	47.1	1790	224	686	0.800	1.496
76	47.8	1510	189	522	0.730	1.365
77	47.9	2145	216	1022	1.045	1.697
78	48.1	1805	204	599	0.767	1.424
79	48.2	2090	210	1011	1.050	1.680
80	48.4	1741	217	563	0.759	1.409
81	48.4	1758	199	628	0.762	1.442
82	48.4	2360	267	993	1.014	1.716
83	48.7	1750	189	714	0.820	1.500
84	48.8	2058	205	765	0.939	1.520
85	48.8	2500	228	1355	0.877	1.843
86	48.9	2550	231	1170	0.858	1.884
87	49.1	1769	204	585	0.765	1.401
88	49.3	2632	228	888	0.730	1.578
89	49.5	1755	190	694	0.790	1.480
90	50.3	3148	250	1440	0.788	1.954
91	50.4	2540	239	1020	0.730	1.712
92	50.5	1810	189	606	0.770	1.423
93	53.2	2111	220	692	0.740	1.471

**Table A.3 Experimental data of samples collected from Middle East**

Sample Number	Bubble-point pressure	API Gravity	Reservoir Temperature	Bubble-point solution gas to oil ratio	Gas specific gravity	Bubble-point Oil FVF
	$p_b$ (psia)	$^{\circ}$ API	$T_{res}$ ( $^{\circ}$ F)	$R_{sb}$ (scf/STB)	$\gamma_g$	$B_{ob}$ (bbl/STB)
1	205	19.4	160	39	1.251	1.061
2	179	19.4	120	39	1.251	1.045
3	246	21.8	160	45	1.123	1.065
4	231	21.8	130	45	1.123	1.051
5	847	22.8	100	265	1.058	1.132
6	186	23.6	190	29	1.185	1.075
7	174	23.6	160	29	1.185	1.061
8	161	23.6	130	29	1.185	1.047
9	148	23.6	100	29	1.185	1.032
10	584	25.1	160	127	1.025	1.114
11	515	25.1	120	127	1.025	1.096
12	236	25.4	190	61	1.356	1.090
13	211	25.4	160	61	1.356	1.075
14	186	25.4	130	61	1.356	1.059
15	1,630	26.1	165	347	0.933	1.203
16	1,405	26.1	100	347	0.933	1.165
17	240	26.2	140	61	1.272	1.066
18	214	26.2	100	61	1.272	1.047
19	477	27.1	220	158	1.308	1.169
20	874	27.2	160	232	0.989	1.152
21	408	27.4	160	104	1.126	1.098
22	545	27.5	155	141	1.072	1.125
23	508	27.5	130	141	1.072	1.110
24	697	27.9	80	189	1.031	1.102
25	1,437	28.2	150	389	1.002	1.226
26	1,377	28.4	160	331	0.921	1.210
27	236	28.5	155	80	1.297	1.091
28	1,061	28.9	100	302	0.931	1.152
29	163	29.2	200	26	1.182	1.083
30	147	29.2	160	26	1.182	1.062
31	130	29.2	120	26	1.182	1.041
32	3,090	29.7	175	680	0.755	1.360
33	2,687	29.7	100	680	0.755	1.304
34	238	30.2	165	44	1.050	1.072
35	214	30.2	125	44	1.050	1.052
36	444	30.5	205	168	1.367	1.173
37	392	30.5	165	168	1.367	1.148

Sample Number	Bubble-point pressure	API Gravity	Reservoir Temperature	Bubble-point solution gas to oil ratio	Gas specific gravity	Bubble-point Oil FVF
	$p_b$ (psia)	$^{\circ}$ API	$T_{res}$ ( $^{\circ}$ F)	$R_{sb}$ (scf/STB)	$\gamma_g$	$B_{ob}$ (bbl/STB)
38	3,003	30.8	175	665	0.766	1.340
39	2,588	30.8	100	665	0.766	1.284
40	1,480	31	180	412	0.973	1.280
41	1,405	31	160	412	0.973	1.259
42	1,292	31	130	412	0.973	1.238
43	1,472	31.2	185	417	0.980	1.267
44	1,378	31.2	160	417	0.980	1.250
45	966	31.2	150	433	1.188	1.245
46	804	31.2	100	433	1.188	1.215
47	421	31.6	170	62	0.875	1.045
48	3,223	32	175	750	0.800	1.387
49	3,057	32	175	679	0.778	1.371
50	2,751	32	100	750	0.800	1.333
51	2,607	32	100	679	0.778	1.315
52	854	32.1	175	196	0.942	1.141
53	696	32.1	100	196	0.942	1.097
54	3,155	32.2	185	700	0.774	1.384
55	3,101	32.2	175	700	0.774	1.376
56	2,901	32.2	140	700	0.774	1.352
57	2,639	32.2	100	700	0.774	1.323
58	3,204	32.6	160	742	0.752	1.372
59	2,865	32.6	100	742	0.752	1.327
60	3,571	32.7	175	898	0.802	1.471
61	3,426	32.7	150	898	0.802	1.451
62	3,279	32.7	125	898	0.802	1.430
63	3,127	32.7	100	898	0.802	1.411
64	2,558	33	170	602	0.803	1.323
65	3,180	33.1	175	730	0.757	1.392
66	2,925	33.2	175	693	0.774	1.406
67	2,530	33.2	100	693	0.774	1.349
68	3,354	34.2	185	825	0.779	1.431
69	3,311	34.2	175	825	0.779	1.425
70	3,155	34.2	170	818	0.789	1.427
71	2,900	34.2	100	818	0.789	1.365
72	2,871	34.2	100	825	0.779	1.368
73	3,228	34.4	175	775	0.783	1.413
74	2,789	34.4	100	775	0.783	1.352
75	3,297	35.4	180	867	0.799	1.458
76	3,066	35.4	140	867	0.799	1.420
77	2,804	35.4	100	867	0.799	1.384

Sample Number	Bubble-point pressure	API Gravity	Reservoir Temperature	Bubble-point solution gas to oil ratio	Gas specific gravity	Bubble-point Oil FVF
	p <sub>b</sub> (psia)	°API	T <sub>res</sub> (°F)	R <sub>sb</sub> (scf/STB)	γ <sub>g</sub>	B <sub>ob</sub> (bbl/STB)
78	2,521	36.1	200	746	0.907	1.440
79	1,631	36.2	100	803	1.013	1.397
80	3,057	36.5	185	811	0.812	1.445
81	2,941	36.5	160	811	0.812	1.421
82	2,836	36.5	140	811	0.812	1.403
83	2,617	36.5	100	811	0.812	1.371
84	1,282	36.5	155	469	0.960	1.291
85	642	37.3	165	266	1.192	1.220
86	601	37.3	145	266	1.192	1.191
87	518	37.3	105	266	1.192	1.163
88	1,766	38	100	1,087	1.056	1.533
89	1,890	38.1	100	580	0.802	1.259
90	1,477	38.6	150	560	1.002	1.327
91	174	38.9	100	46	1.105	1.039
92	1,847	39.1	100	805	0.929	1.387
93	3,573	39.3	225	1,507	0.951	1.875
94	2,652	39.3	100	1,507	0.951	1.718
95	1,834	39.3	170	755	1.004	1.425
96	1,603	39.3	125	755	1.004	1.387
97	1,367	39.3	80	755	1.004	1.347
98	2,845	39.4	240	1,143	0.951	1.682
99	2,636	39.4	200	1,143	0.951	1.647
100	3,218	39.9	220	1,151	0.894	1.686
101	3,030	39.9	180	1,151	0.894	1.636
102	3,250	40.2	240	1,203	0.925	1.747
103	2,831	40.2	160	1,203	0.925	1.642
104	1,824	41.9	115	692	0.876	1.344
105	1,641	41.9	80	692	0.876	1.313
106	3,405	42.8	235	1,579	0.930	1.997
107	3,201	42.8	190	1,579	0.930	1.920
108	2,896	42.8	145	1,579	0.930	1.852
109	2,559	42.8	100	1,579	0.930	1.786
110	3,198	44.6	230	1,602	0.960	1.986

**Table A.4 Experimental data of samples collected from North Sea**

Sample Number	Bubble-point pressure	API Gravity	Reservoir Temperature	Bubble-point solution gas to oil ratio	Gas specific gravity	Bubble-point Oil FVF
	$p_b$ (psia)	$^{\circ}$ API	$T_{res}$ ( $^{\circ}$ F)	$R_{sb}$ (scf/STB)	$\gamma_g$	$B_{ob}$ (bbl/STB)
1	3,814	22.3	211	459	0.650	1.230
2	1,361	27.9	240	840	1.248	1.593
3	4,215	28.1	200	891	0.975	1.380
4	4,210	28.4	200	887	0.968	1.410
5	2,695	29.9	220	620	0.973	1.382
6	3501	31.7	230	950	0.980	1.589
7	5545	32.5	270	1950	0.894	1.784
8	931	32.6	200	228	1.276	1.162
9	3546	33.2	200	648	0.695	-
10	5405	33.6	250	2216	0.909	2.160
11	6641	34.8	254	2637	0.889	2.588
12	1,126	34.8	210	267	1.173	1.217
13	3501	35.1	230	756	0.759	1.442
14	7127	36.2	280	2036	0.760	2.110
15	3,395	36.6	242	688	0.710	1.406
16	1,525	37.2	253	326	0.863	1.326
17	5545	37.3	270	1361	0.721	1.784
18	4011	37.4	193	1052	0.767	1.577
19	1169	37.4	225	256	1.049	1.218
20	5232	37.5	180	1417	0.755	-
21	500	37.6	100	181	1.024	1.146
22	150	37.6	80	90	1.269	1.092
23	3683	37.6	192	860	0.758	-
24	4497	38	245	1924	0.935	2.210
25	3796	38	180	909	0.732	1.434
26	500	38.2	100	200	1.054	1.105
27	4810	38.2	180	1328	0.750	-
28	6641	38.5	254	2060	0.753	2.186
29	4735	38.6	180	1280	0.756	1.664
30	5405	39	250	1623	0.761	1.918
31	3158	39.2	210	1039	0.946	1.596
32	4,186	40.3	223	1,850	1.053	2.126
33	2,620	40.4	220	780	0.868	1.483
34	3,748	40.8	230	1,258	1.033	1.755
35	3,493	41.5	230	1,124	1.023	1.680
36	2,850	41.7	230	853	1.158	1.515
37	4,005	42.4	235	1,718	1.000	1.996

Sample Number	Bubble-point pressure	API Gravity	Reservoir Temperature	Bubble-point solution gas to oil ratio	Gas specific gravity	Bubble-point Oil FVF
	$p_b$ (psia)	$^{\circ}\text{API}$	$T_{\text{res}}$ ( $^{\circ}\text{F}$ )	$R_{\text{sb}}$ (scf/STB)	$\gamma_g$	$B_{\text{ob}}$ (bbl/STB)
38	4494	42.5	260	1409	0.799	1.854
39	250	42.5	80	169	1.265	1.087
40	4498	42.9	245	1450	0.793	1.846
41	1000	42.9	155	338	0.998	1.204
42	2,420	43.3	147	889	0.849	1.474
43	3,247	44.8	210	770	0.729	1.450
44	4,432	47.7	249	1,452	1.034	1.901
45	4,620	48.1	248	1,344	0.985	1.850

## APPENDIX **B**

Comparison between estimated end experimental values

**Table B.1 Comparison of methods for  $B_{ob}$  prediction against Experimental data of oils collected from Malaysia**

Malaysian oils						
Experimental	Estimated					
	Liquid Z-factor Based Method	Standing's	Vasquez-Begg's	Glaso's	Al-Mahroun's	Sulaimon's
Bob (bbl/STB)						
1.085	1.067	1.081	1.172	1.063	1.161	1.246
1.092	1.111	1.091	1.123	1.070	1.097	1.254
1.128	1.151	1.124	1.171	1.096	1.145	1.255
1.130	1.103	1.120	1.137	1.100	1.126	1.294
1.139	1.167	1.144	1.166	1.116	1.164	1.286
1.152	1.152	1.141	1.112	1.113	1.084	1.271
1.153	1.160	1.156	1.180	1.131	1.163	1.296
1.154	1.134	1.154	1.182	1.131	1.164	1.300
1.168	1.146	1.179	1.260	1.156	1.328	1.341
1.170	1.174	1.164	1.176	1.137	1.192	1.306
1.170	1.229	1.220	1.183	1.190	1.254	1.353
1.173	1.183	1.177	1.170	1.151	1.182	1.322
1.176	1.239	1.231	1.185	1.201	1.245	1.363
1.184	1.169	1.184	1.218	1.160	1.196	1.310
1.192	1.252	1.249	1.207	1.221	1.269	1.372
1.194	1.185	1.182	1.217	1.156	1.193	1.299
1.201	1.177	1.191	1.492	1.166	1.466	1.313
1.208	1.177	1.191	1.234	1.167	1.204	1.308
1.212	1.231	1.240	1.251	1.213	1.263	1.348
1.214	1.293	1.285	1.222	1.258	1.296	1.395
1.221	1.325	1.329	1.250	1.305	1.332	1.422
1.222	1.304	1.287	1.224	1.259	1.293	1.395
1.230	1.194	1.201	1.259	1.174	1.222	1.300
1.230	1.203	1.217	1.386	1.189	1.379	1.308
1.232	1.269	1.266	1.237	1.237	1.283	1.372
1.238	1.193	1.206	1.232	1.182	1.214	1.327
1.240	1.289	1.281	1.220	1.253	1.293	1.392
1.241	1.295	1.298	1.228	1.272	1.310	1.403
1.246	1.328	1.321	1.261	1.292	1.332	1.404
1.249	1.292	1.306	1.257	1.283	1.315	1.409
1.259	1.288	1.285	1.277	1.255	1.309	1.370
1.261	1.331	1.340	1.275	1.316	1.343	1.425
1.265	1.252	1.260	1.431	1.233	1.412	1.355
1.268	1.313	1.318	1.174	1.293	1.193	1.411
1.282	1.317	1.290	1.302	1.256	1.311	1.347
1.287	1.301	1.300	1.354	1.273	1.304	1.352

Malaysian oils						
Experimental	Estimated					
	Liquid Z-factor Based Method	Standing's	Vasquez-Begg's	Glaso's	Al-Mahroun's	Sulaimon's
	Bob (bbl/STB)					
1.297	1.286	1.305	1.319	1.282	1.307	1.382
1.301	1.312	1.317	1.336	1.292	1.315	1.378
1.315	1.332	1.309	1.382	1.276	1.343	1.343
1.321	1.346	1.351	1.304	1.324	1.358	1.417
1.325	1.309	1.303	1.342	1.276	1.320	1.362
1.334	1.343	1.343	1.421	1.319	1.382	1.395
1.345	1.331	1.355	1.362	1.334	1.350	1.410
1.352	1.368	1.387	1.384	1.366	1.375	1.426
1.357	1.360	1.374	1.398	1.351	1.370	1.407
1.362	1.334	1.325	1.323	1.297	1.337	1.386
1.362	1.372	1.345	1.430	1.311	1.400	1.360
1.365	1.317	1.308	1.360	1.281	1.335	1.363
1.371	1.369	1.392	1.382	1.369	1.382	1.428
1.384	1.364	1.389	1.279	1.368	1.240	1.428
1.399	1.376	1.396	1.411	1.374	1.390	1.421
1.399	1.364	1.384	1.400	1.362	1.380	1.416
1.401	1.375	1.360	1.402	1.332	1.386	1.388
1.408	1.414	1.419	1.432	1.396	1.406	1.450
1.409	1.379	1.355	1.402	1.325	1.384	1.380
1.423	1.368	1.363	1.402	1.338	1.388	1.394
1.424	1.381	1.367	1.405	1.339	1.390	1.392
1.425	1.395	1.379	1.414	1.349	1.377	1.388
1.429	1.396	1.417	1.376	1.396	1.411	1.432
1.429	1.440	1.443	1.552	1.419	1.616	1.436
1.438	1.415	1.400	1.275	1.371	1.283	1.404
1.442	1.393	1.378	1.416	1.352	1.400	1.398
1.445	1.463	1.437	1.462	1.403	1.434	1.411
1.451	1.378	1.348	1.359	1.313	1.359	1.359
1.455	1.468	1.491	1.226	1.465	1.207	1.461
1.466	1.482	1.468	1.510	1.433	1.460	1.419
1.471	1.461	1.428	1.488	1.399	1.458	1.409
1.480	1.426	1.417	1.439	1.393	1.432	1.423
1.484	1.485	1.458	1.471	1.423	1.450	1.422
1.491	1.484	1.467	1.473	1.436	1.470	1.437
1.496	1.469	1.436	1.455	1.407	1.452	1.423
1.500	1.439	1.434	1.441	1.411	1.444	1.436
1.503	1.491	1.517	1.516	1.491	1.492	1.472
1.505	1.485	1.497	1.545	1.470	1.485	1.446

<b>Malaysian oils</b>						
<b>Experimental</b>	<b>Estimated</b>					
	<b>Liquid Z-factor Based Method</b>	<b>Standing's</b>	<b>Vasquez-Begg's</b>	<b>Glaso's</b>	<b>Al-Mahroun's</b>	<b>Sulaimon's</b>
	<b>Bob (bbl/STB)</b>					
<b>1.517</b>	1.561	1.560	1.509	1.534	1.546	1.502
<b>1.520</b>	1.503	1.507	1.464	1.483	1.506	1.480
<b>1.525</b>	1.509	1.495	1.492	1.465	1.484	1.454
<b>1.538</b>	1.617	1.594	1.572	1.562	1.570	1.500
<b>1.578</b>	1.564	1.537	1.578	1.505	1.544	1.457
<b>1.581</b>	1.548	1.556	1.606	1.525	1.533	1.467
<b>1.619</b>	1.585	1.568	1.506	1.535	1.544	1.499
<b>1.622</b>	1.643	1.686	1.462	1.659	1.434	1.584
<b>1.653</b>	1.611	1.597	1.576	1.568	1.568	1.506
<b>1.680</b>	1.693	1.710	1.572	1.681	1.664	1.585
<b>1.683</b>	1.650	1.663	1.686	1.631	1.618	1.523
<b>1.697</b>	1.708	1.720	1.581	1.689	1.673	1.587
<b>1.698</b>	1.741	1.696	1.640	1.652	1.673	1.534
<b>1.707</b>	1.655	1.674	1.686	1.643	1.634	1.531
<b>1.712</b>	1.679	1.622	1.658	1.587	1.621	1.491
<b>1.716</b>	1.767	1.729	1.607	1.689	1.696	1.570
<b>1.843</b>	1.914	1.890	1.774	1.841	1.819	1.635
<b>1.884</b>	1.783	1.761	1.691	1.721	1.720	1.575
<b>1.954</b>	1.957	1.918	1.859	1.860	1.859	1.623

**Table B.2 Comparison of methods for  $B_{ob}$  prediction against Experimental data of oils collected from Middle East**

Middle East Oils						
Experimental	Estimated					
	Liquid Z-factor Based Method	Standing's	Vasquez-Begg's	Glaso's	Al-Mahroun's	Sulaimon's
Bob (bbl/STB)						
1.032	1.157	1.028	1.028	1.022	1.085	1.272
1.039	0.973	1.036	1.039	1.028	1.022	1.276
1.041	1.126	1.037	1.040	1.027	1.092	1.271
1.045	1.136	1.043	1.035	1.032	1.065	1.277
1.045	1.100	1.077	1.078	1.055	1.087	1.262
1.047	1.099	1.043	1.039	1.031	1.059	1.272
1.047	1.088	1.044	1.043	1.034	1.064	1.286
1.051	1.128	1.050	1.045	1.036	1.068	1.275
1.052	1.083	1.047	1.043	1.034	1.074	1.271
1.059	1.164	1.061	1.052	1.045	1.108	1.287
1.061	1.067	1.064	1.046	1.045	1.030	1.277
1.061	1.065	1.059	1.050	1.041	1.033	1.272
1.062	1.073	1.058	1.058	1.040	1.058	1.271
1.065	1.079	1.066	1.056	1.047	1.042	1.275
1.066	1.024	1.065	1.058	1.048	1.030	1.286
1.072	1.027	1.068	1.057	1.048	1.039	1.271
1.075	1.013	1.075	1.061	1.051	1.007	1.272
1.075	1.123	1.077	1.062	1.057	1.082	1.287
1.083	1.029	1.080	1.077	1.054	1.023	1.271
1.090	1.077	1.094	1.072	1.068	1.056	1.287
1.091	1.097	1.084	1.074	1.064	1.090	1.294
1.096	1.146	1.082	1.084	1.065	1.113	1.296
1.097	1.157	1.102	1.108	1.086	1.163	1.309
1.098	1.129	1.096	1.090	1.074	1.105	1.296
1.102	1.046	1.090	1.097	1.078	1.077	1.316
1.110	1.136	1.096	1.095	1.078	1.119	1.304
1.114	1.088	1.105	1.100	1.082	1.079	1.296
1.125	1.102	1.111	1.106	1.088	1.097	1.304
1.132	1.131	1.140	1.136	1.124	1.126	1.343
1.141	1.066	1.146	1.141	1.120	1.098	1.309
1.148	1.206	1.143	1.107	1.119	1.188	1.329
1.152	1.178	1.156	1.148	1.132	1.164	1.325
1.152	1.122	1.152	1.158	1.136	1.144	1.339
1.163	1.177	1.158	1.142	1.143	1.209	1.357
1.165	1.226	1.173	1.176	1.157	1.216	1.353
1.169	1.233	1.167	1.127	1.135	1.191	1.323

<b>Middle East Oils</b>						
<b>Experimental</b>	<b>Estimated</b>					
	<b>Liquid Z-factor Based Method</b>	<b>Standing's</b>	<b>Vasquez-Begg's</b>	<b>Glaso's</b>	<b>Al-Mahroun's</b>	<b>Sulaimon's</b>
<b>Bob (bbl/STB)</b>						
<b>1.173</b>	1.161	1.167	1.119	1.138	1.154	1.329
<b>1.191</b>	1.157	1.183	1.158	1.162	1.191	1.357
<b>1.203</b>	1.136	1.214	1.198	1.190	1.160	1.353
<b>1.210</b>	1.206	1.203	1.194	1.179	1.207	1.346
<b>1.215</b>	1.282	1.251	1.216	1.239	1.277	1.382
<b>1.220</b>	1.111	1.196	1.166	1.172	1.157	1.357
<b>1.226</b>	1.229	1.235	1.211	1.214	1.230	1.376
<b>1.238</b>	1.272	1.234	1.221	1.215	1.269	1.379
<b>1.245</b>	1.250	1.284	1.232	1.266	1.255	1.382
<b>1.250</b>	1.269	1.257	1.235	1.235	1.271	1.415
<b>1.259</b>	1.246	1.253	1.233	1.231	1.252	1.379
<b>1.259</b>	1.223	1.284	1.296	1.271	1.272	1.395
<b>1.267</b>	1.204	1.273	1.246	1.248	1.228	1.415
<b>1.280</b>	1.207	1.266	1.241	1.241	1.226	1.379
<b>1.284</b>	1.356	1.313	1.332	1.300	1.349	1.409
<b>1.291</b>	1.447	1.284	1.266	1.264	1.444	1.460
<b>1.304</b>	1.363	1.317	1.327	1.304	1.350	1.410
1.313	1.313	1.351	1.336	1.344	1.358	1.444
<b>1.315</b>	1.400	1.324	1.339	1.312	1.393	1.440
<b>1.323</b>	1.383	1.334	1.349	1.322	1.377	1.420
<b>1.323</b>	1.325	1.338	1.341	1.315	1.330	1.401
<b>1.327</b>	1.369	1.351	1.370	1.339	1.370	1.425
<b>1.327</b>	1.310	1.343	1.308	1.325	1.333	1.430
<b>1.333</b>	1.362	1.367	1.371	1.355	1.360	1.415
<b>1.340</b>	1.260	1.365	1.371	1.341	1.284	1.409
1.344	1.263	1.375	1.359	1.363	1.328	1.444
<b>1.347</b>	1.940	1.414	1.363	1.410	1.857	1.708
<b>1.349</b>	1.370	1.332	1.346	1.320	1.368	1.418
<b>1.352</b>	1.372	1.362	1.371	1.344	1.368	1.420
<b>1.352</b>	1.408	1.379	1.385	1.368	1.408	1.443
<b>1.360</b>	1.267	1.369	1.344	1.345	1.285	1.410
<b>1.365</b>	1.445	1.403	1.405	1.392	1.436	1.455
<b>1.368</b>	1.432	1.404	1.409	1.393	1.427	1.455
<b>1.371</b>	1.304	1.376	1.380	1.353	1.328	1.440
<b>1.371</b>	1.415	1.409	1.403	1.399	1.422	1.460
<b>1.372</b>	1.291	1.393	1.404	1.372	1.318	1.425
<b>1.376</b>	1.329	1.386	1.390	1.363	1.338	1.420
<b>1.384</b>	1.276	1.393	1.396	1.369	1.303	1.420

<b>Middle East Oils</b>						
<b>Experimental</b>	<b>Estimated</b>					
	<b>Liquid Z-factor Based Method</b>	<b>Standing's</b>	<b>Vasquez-Begg's</b>	<b>Glaso's</b>	<b>Al-Mahroun's</b>	<b>Sulaimon's</b>
<b>Bob (bbl/STB)</b>						
<b>1.384</b>	1.464	1.435	1.429	1.424	1.458	1.472
<b>1.387</b>	1.267	1.419	1.412	1.397	1.295	1.415
<b>1.387</b>	1.359	1.440	1.399	1.433	1.399	1.490
1.387	1.737	1.446	1.387	1.435	1.749	1.708
<b>1.392</b>	1.382	1.399	1.408	1.376	1.380	1.423
<b>1.397</b>	1.374	1.456	1.394	1.450	1.402	1.509
<b>1.403</b>	1.389	1.437	1.428	1.421	1.405	1.460
<b>1.406</b>	1.273	1.384	1.389	1.361	1.303	1.418
<b>1.411</b>	1.472	1.449	1.441	1.438	1.457	1.481
<b>1.413</b>	1.311	1.432	1.430	1.409	1.343	1.443
<b>1.420</b>	1.414	1.463	1.453	1.447	1.423	1.472
<b>1.421</b>	1.335	1.452	1.440	1.432	1.371	1.460
<b>1.425</b>	1.427	1.457	1.454	1.435	1.422	1.456
1.425	1.450	1.479	1.411	1.460	1.448	1.492
<b>1.427</b>	1.333	1.453	1.446	1.431	1.361	1.456
<b>1.430</b>	1.441	1.467	1.455	1.452	1.436	1.481
<b>1.431</b>	1.335	1.465	1.460	1.440	1.363	1.455
<b>1.440</b>	1.458	1.467	1.424	1.442	1.443	1.467
<b>1.445</b>	1.264	1.469	1.455	1.446	1.284	1.395
<b>1.451</b>	1.408	1.485	1.469	1.466	1.414	1.481
<b>1.458</b>	1.360	1.492	1.477	1.469	1.389	1.472
<b>1.471</b>	1.374	1.503	1.483	1.480	1.392	1.481
<b>1.533</b>	1.542	1.659	1.528	1.650	1.558	1.611
<b>1.636</b>	1.709	1.705	1.614	1.678	1.663	1.582
<b>1.642</b>	1.781	1.737	1.624	1.712	1.716	1.607
<b>1.647</b>	1.766	1.737	1.617	1.706	1.689	1.598
<b>1.682</b>	1.706	1.769	1.640	1.728	1.655	1.598
<b>1.686</b>	1.651	1.736	1.640	1.700	1.629	1.582
<b>1.718</b>	1.385	1.904	1.728	1.875	1.410	1.492
<b>1.747</b>	1.662	1.800	1.675	1.756	1.647	1.607
<b>1.786</b>	2.014	1.953	1.765	1.918	1.920	1.721
<b>1.852</b>	1.934	1.989	1.796	1.943	1.881	1.721
<b>1.875</b>	1.317	2.005	1.805	1.944	1.371	1.492
<b>1.920</b>	1.856	2.026	1.828	1.968	1.843	1.721
<b>1.986</b>	2.045	2.099	1.869	2.025	1.954	1.740
<b>1.997</b>	1.776	2.063	1.859	1.992	1.804	1.721

**Table B.3 Comparison of methods for  $B_{ob}$  prediction against Experimental data of oils collected from North Sea**

North Sea Oils						
Experimental	Estimated					
	Liquid Z-factor Based Method	Standing's	Vasquez-Begg's	Glaso's	Al-Mahroun's	Sulaimon's
Bob (bbl/STB)						
1.087	2.089	1.093	1.916	2.115	2.018	1.793
1.092	1.238	1.050	1.582	1.571	1.248	1.340
1.105	1.462	1.111	2.014	2.191	1.471	1.463
1.146	1.052	1.100	1.049	1.041	1.099	1.314
1.162	2.172	1.198	2.026	2.174	2.033	1.815
1.204	1.024	1.219	1.816	1.835	1.089	1.327
1.217	2.309	1.222	2.144	2.327	2.161	1.901
1.218	1.771	1.218	1.793	1.761	1.734	1.575
1.230	1.297	1.261	1.266	1.228	1.268	1.327
1.326	1.427	1.259	1.448	1.382	1.423	1.400
1.380	1.528	1.561	1.423	1.536	1.491	1.527
1.382	1.424	1.413	1.324	1.385	1.394	1.443
1.406	2.105	1.416	2.113	2.146	2.049	1.769
1.410	1.524	1.557	1.421	1.532	1.489	1.524
1.434	0.985	1.498	1.103	1.085	1.036	1.298
1.442	1.239	1.455	2.355	2.548	1.244	1.356
1.450	1.457	1.452	1.478	1.492	1.479	1.493
1.474	1.193	1.508	1.827	1.848	1.234	1.360
1.483	2.156	1.498	1.960	2.214	2.083	1.858
1.515	1.727	1.632	1.624	1.743	1.700	1.614
1.577	1.558	1.599	1.195	1.186	1.549	1.512
1.589	1.612	1.629	1.519	1.597	1.559	1.547
1.593	1.676	1.628	1.403	1.598	1.544	1.570
1.596	1.907	1.674	1.904	1.918	1.859	1.660
1.664	2.097	1.719	2.117	2.147	2.055	1.771
1.680	1.804	1.781	1.685	1.832	1.769	1.659
1.755	1.497	1.878	1.467	1.469	1.484	1.467
1.784	1.293	1.815	1.260	1.222	1.294	1.336
1.846	1.852	1.904	1.212	1.197	1.813	1.628
1.850	1.936	1.951	1.811	1.987	1.938	1.722
1.854	1.853	1.893	1.087	1.082	1.806	1.619
1.901	1.439	2.056	1.489	1.423	1.458	1.426
1.918	1.640	1.986	1.686	1.687	1.641	1.568
1.996	1.599	2.205	1.484	1.604	1.586	1.558
2.110	1.456	2.262	1.459	1.423	1.445	1.431
2.126	1.637	2.322	1.573	1.644	1.610	1.565

North Sea Oils						
Experimental	Estimated					
	Liquid Z-factor Based Method	Standing's	Vasquez-Begg's	Glaso's	Al-Mahroun's	Sulaimon's
<b>Bob (bbl/STB)</b>						
<b>2.160</b>	1.217	2.476	1.151	1.169	1.216	1.349
<b>2.186</b>	1.062	2.258	1.112	1.096	1.111	1.323
<b>2.210</b>	2.185	2.303	1.511	1.474	2.068	1.827
<b>2.588</b>	2.483	2.771	1.181	1.193	2.375	2.012

**Table B.4 Comparison of methods for  $B_{ob}$  prediction against TUC database**

TUC database						
Experimental	Estimated					
	Liquid Z-factor Based Method	Standing's	Vasquez-Begg's	Glaso's	Al-Mahroun's	Sulaimon's
<b>Bob (bbl/STB)</b>						
<b>1.036</b>	1.054	1.048	1.275	1.234	1.042	1.242
<b>1.049</b>	1.046	1.045	1.299	1.276	1.035	1.257
<b>1.050</b>	1.034	1.032	1.223	1.151	1.013	1.206
<b>1.098</b>	1.133	1.104	1.754	1.724	1.127	1.265
<b>1.111</b>	1.134	1.096	1.641	1.702	1.117	1.274
<b>1.118</b>	1.155	1.127	1.134	1.105	1.127	1.294
<b>1.138</b>	1.140	1.130	1.157	1.133	1.139	1.264
<b>1.142</b>	1.139	1.109	1.209	1.193	1.117	1.274
<b>1.144</b>	1.170	1.176	1.168	1.144	1.187	1.289
<b>1.149</b>	1.452	1.288	1.207	1.232	1.340	1.315
<b>1.149</b>	1.224	1.151	1.370	1.421	1.177	1.307
<b>1.153</b>	1.254	1.151	1.099	1.120	1.169	1.316
<b>1.153</b>	1.218	1.189	1.142	1.106	1.203	1.340
<b>1.154</b>	1.212	1.123	1.109	1.097	1.129	1.289
<b>1.155</b>	1.123	1.121	1.752	1.808	1.147	1.300
<b>1.159</b>	1.224	1.173	1.168	1.144	1.185	1.308
<b>1.162</b>	1.220	1.147	1.134	1.119	1.159	1.301
<b>1.164</b>	1.117	1.128	1.105	1.071	1.138	1.292
<b>1.169</b>	1.164	1.191	1.619	1.678	1.217	1.333
<b>1.170</b>	1.149	1.092	1.414	1.519	1.100	1.268
<b>1.176</b>	1.182	1.184	1.715	1.757	1.197	1.325

<b>TUC database</b>						
<b>Experimental</b>	<b>Estimated</b>					
	<b>Liquid Z-factor Based Method</b>	<b>Standing's</b>	<b>Vasquez-Begg's</b>	<b>Glaso's</b>	<b>Al-Mahroun's</b>	<b>Sulaimon's</b>
<b>Bob (bbl/STB)</b>						
<b>1.184</b>	1.241	1.204	1.178	1.176	1.208	1.340
<b>1.186</b>	1.193	1.169	1.331	1.359	1.181	1.324
<b>1.193</b>	1.215	1.229	1.522	1.526	1.252	1.348
<b>1.195</b>	1.244	1.161	1.215	1.218	1.175	1.311
<b>1.216</b>	1.262	1.223	1.171	1.106	1.232	1.336
<b>1.221</b>	1.236	1.229	1.562	1.546	1.243	1.364
<b>1.231</b>	1.222	1.177	1.309	1.279	1.183	1.330
<b>1.247</b>	1.234	1.290	1.517	1.569	1.308	1.387
<b>1.253</b>	1.229	1.154	1.463	1.500	1.166	1.325
<b>1.253</b>	1.230	1.313	1.677	1.767	1.306	1.412
<b>1.256</b>	1.230	1.153	1.298	1.283	1.164	1.330
<b>1.264</b>	1.232	1.239	1.304	1.395	1.240	1.355
<b>1.265</b>	1.363	1.312	1.787	1.874	1.333	1.369
<b>1.265</b>	1.273	1.299	1.233	1.195	1.326	1.359
<b>1.268</b>	1.324	1.368	1.253	1.217	1.362	1.437
<b>1.276</b>	1.300	1.244	1.768	1.853	1.305	1.310
<b>1.284</b>	1.330	1.243	1.126	1.118	1.243	1.367
<b>1.289</b>	1.455	1.224	2.110	2.225	1.240	1.329
<b>1.294</b>	1.283	1.098	1.833	1.822	1.110	1.267
<b>1.304</b>	1.495	1.298	2.103	2.440	1.298	1.388
<b>1.310</b>	1.335	1.266	1.204	1.198	1.286	1.346
<b>1.310</b>	1.323	1.435	1.514	1.615	1.445	1.435
<b>1.319</b>	1.330	1.397	1.124	1.162	1.406	1.412
<b>1.322</b>	1.322	1.208	1.718	1.733	1.221	1.341
<b>1.324</b>	1.373	1.190	1.190	1.159	1.208	1.323
<b>1.327</b>	1.745	1.420	2.359	2.778	1.425	1.454
<b>1.331</b>	1.255	1.258	1.122	1.085	1.261	1.373
<b>1.342</b>	1.344	1.319	1.723	1.830	1.344	1.392
<b>1.343</b>	1.618	1.329	1.761	1.831	1.325	1.428
<b>1.348</b>	1.471	1.259	1.424	1.397	1.274	1.363
<b>1.352</b>	1.352	1.281	2.485	2.608	1.307	1.347
<b>1.352</b>	1.356	1.356	2.205	2.292	1.374	1.412
<b>1.354</b>	1.368	1.410	1.322	1.349	1.419	1.438
<b>1.355</b>	1.328	1.356	1.731	1.927	1.365	1.423
<b>1.358</b>	1.361	1.415	1.659	1.827	1.425	1.437
<b>1.362</b>	1.431	1.492	1.436	1.473	1.455	1.504
<b>1.366</b>	1.344	1.419	1.475	1.460	1.419	1.420
<b>1.369</b>	1.389	1.302	1.373	1.420	1.298	1.406

<b>TUC database</b>						
<b>Experimental</b>	<b>Estimated</b>					
	<b>Liquid Z-factor Based Method</b>	<b>Standing's</b>	<b>Vasquez-Begg's</b>	<b>Glaso's</b>	<b>Al-Mahroun's</b>	<b>Sulaimon's</b>
<b>Bob (bbl/STB)</b>						
<b>1.374</b>	1.491	1.398	2.451	2.601	1.394	1.436
<b>1.375</b>	1.437	1.254	1.695	1.850	1.265	1.366
<b>1.376</b>	1.555	1.352	1.438	1.506	1.376	1.373
<b>1.378</b>	1.698	1.306	1.274	1.297	1.318	1.378
<b>1.393</b>	1.655	1.352	2.288	2.383	1.360	1.397
<b>1.401</b>	1.361	1.259	1.527	1.508	1.269	1.362
<b>1.412</b>	1.370	1.514	1.710	1.756	1.500	1.480
<b>1.419</b>	1.362	1.497	1.523	1.660	1.439	1.491
<b>1.423</b>	1.375	1.460	1.421	1.407	1.459	1.462
<b>1.429</b>	1.445	1.388	1.347	1.360	1.388	1.434
<b>1.432</b>	1.434	1.463	1.319	1.322	1.457	1.438
<b>1.438</b>	1.471	1.483	1.211	1.205	1.458	1.473
<b>1.442</b>	1.446	1.495	1.429	1.463	1.464	1.498
<b>1.444</b>	1.611	1.409	1.461	1.486	1.424	1.406
<b>1.449</b>	1.374	1.630	1.503	1.461	1.585	1.544
<b>1.455</b>	1.381	1.544	1.277	1.341	1.497	1.510
<b>1.456</b>	1.549	1.496	1.771	1.794	1.497	1.447
<b>1.465</b>	1.451	1.433	1.619	1.673	1.416	1.440
<b>1.466</b>	1.385	1.561	1.451	1.500	1.500	1.537
<b>1.466</b>	1.436	1.548	1.786	1.879	1.529	1.494
<b>1.466</b>	1.443	1.537	1.530	1.562	1.524	1.491
<b>1.468</b>	1.427	1.405	1.595	1.667	1.397	1.434
<b>1.477</b>	1.967	1.609	2.868	3.096	1.577	1.533
<b>1.485</b>	1.455	1.602	1.533	1.646	1.566	1.524
<b>1.492</b>	1.510	1.526	1.790	1.948	1.492	1.514
<b>1.496</b>	1.740	1.513	2.426	2.517	1.489	1.465
<b>1.496</b>	1.797	1.577	1.099	1.093	1.546	1.520
<b>1.498</b>	1.485	1.508	1.241	1.196	1.468	1.490
<b>1.499</b>	1.797	1.554	1.478	1.547	1.528	1.510
<b>1.506</b>	1.481	1.517	1.029	1.030	1.499	1.462
<b>1.506</b>	1.401	1.440	1.149	1.132	1.412	1.463
<b>1.506</b>	1.139	1.519	1.791	1.913	1.476	1.505
<b>1.509</b>	1.670	1.506	1.117	1.076	1.476	1.470
<b>1.511</b>	1.461	1.409	1.481	1.462	1.398	1.437
<b>1.511</b>	1.566	1.528	1.446	1.462	1.506	1.508
<b>1.513</b>	1.769	1.573	2.103	2.349	1.543	1.519
<b>1.521</b>	1.503	1.501	1.320	1.261	1.494	1.448
<b>1.521</b>	1.467	1.675	1.940	2.064	1.628	1.568

TUC database						
Experimental	Estimated					
	Liquid Z-factor Based Method	Standing's	Vasquez-Begg's	Glaso's	Al-Mahroun's	Sulaimon's
Bob (bbl/STB)						
1.525	1.499	1.567	1.192	1.162	1.513	1.517
1.531	1.499	1.625	1.319	1.320	1.568	1.538
1.535	1.490	1.346	1.485	1.521	1.357	1.382
1.536	1.490	1.584	1.533	1.576	1.539	1.519
1.539	1.552	1.653	3.137	3.225	1.604	1.550
1.547	1.898	1.561	1.559	1.568	1.535	1.505
1.548	1.528	1.513	2.093	2.258	1.505	1.464
1.564	1.533	1.485	1.576	1.557	1.472	1.470
1.565	1.491	1.559	1.692	1.741	1.524	1.502
1.567	1.208	1.613	1.714	1.794	1.547	1.575
1.574	1.511	1.603	1.243	1.261	1.540	1.541
1.580	1.526	1.480	1.251	1.275	1.476	1.437
1.580	1.570	1.571	1.382	1.401	1.552	1.497
1.586	1.364	1.728	1.675	1.748	1.677	1.582
1.603	1.524	1.521	1.547	1.643	1.501	1.481
1.605	1.554	1.542	1.298	1.262	1.519	1.466
1.605	1.533	1.707	1.156	1.132	1.646	1.561
1.608	1.575	1.719	2.102	2.244	1.656	1.592
1.609	2.149	1.535	1.163	1.160	1.510	1.467
1.622	1.541	1.745	1.398	1.379	1.667	1.582
1.623	1.601	1.764	1.480	1.538	1.694	1.596
1.631	1.571	1.566	1.653	1.735	1.527	1.496
1.635	1.639	1.736	1.503	1.525	1.676	1.589
1.641	1.649	1.663	1.478	1.516	1.612	1.549
1.644	1.593	1.663	1.220	1.233	1.597	1.560
1.645	1.610	1.601	2.441	2.681	1.574	1.516
1.647	1.685	1.674	1.798	1.867	1.632	1.545
1.648	1.629	1.696	1.497	1.514	1.634	1.546
1.650	1.632	1.561	1.939	2.027	1.537	1.493
1.652	1.585	1.807	1.323	1.287	1.703	1.629
1.656	1.689	1.755	1.272	1.307	1.682	1.587
1.663	1.616	1.704	1.315	1.351	1.628	1.584
1.680	1.655	1.831	1.469	1.469	1.730	1.614
1.693	1.638	1.876	1.459	1.474	1.755	1.648
1.701	1.712	1.728	1.412	1.386	1.675	1.553
1.710	1.648	1.708	1.512	1.578	1.623	1.577
1.710	1.665	1.834	1.702	1.785	1.783	1.602
1.719	1.481	1.814	2.280	2.729	1.768	1.595

<b>TUC database</b>						
<b>Experimental</b>	<b>Estimated</b>					
	<b>Liquid Z-factor Based Method</b>	<b>Standing's</b>	<b>Vasquez-Begg's</b>	<b>Glaso's</b>	<b>Al-Mahroun's</b>	<b>Sulaimon's</b>
<b>Bob (bbl/STB)</b>						
<b>1.722</b>	1.684	1.685	2.238	2.330	1.618	1.557
<b>1.739</b>	2.310	1.841	1.501	1.640	1.766	1.606
<b>1.745</b>	1.729	1.761	1.027	1.032	1.668	1.588
<b>1.749</b>	1.734	1.749	1.021	1.022	1.647	1.566
<b>1.754</b>	1.748	1.801	2.020	2.154	1.723	1.601
<b>1.756</b>	2.082	1.831	1.758	1.883	1.750	1.608
<b>1.770</b>	1.830	1.968	1.814	1.922	1.828	1.696
<b>1.770</b>	1.791	1.908	1.300	1.282	1.803	1.655
<b>1.770</b>	1.717	1.771	1.607	1.682	1.707	1.581
<b>1.779</b>	1.763	1.907	1.456	1.485	1.817	1.640
<b>1.779</b>	1.721	1.894	2.098	2.314	1.806	1.642
<b>1.786</b>	1.769	1.847	1.750	1.818	1.762	1.619
<b>1.787</b>	1.758	1.791	1.210	1.183	1.713	1.559
<b>1.788</b>	1.817	1.872	2.119	2.497	1.741	1.686
<b>1.789</b>	1.838	2.008	3.024	3.238	1.849	1.747
<b>1.792</b>	1.692	1.859	1.592	1.664	1.731	1.681
<b>1.804</b>	1.776	1.782	1.296	1.273	1.688	1.584
<b>1.811</b>	1.840	1.928	1.667	1.738	1.806	1.665
<b>1.813</b>	1.773	1.850	1.676	1.849	1.741	1.644
<b>1.817</b>	1.778	1.773	1.673	1.868	1.689	1.600
<b>1.821</b>	1.817	1.931	1.454	1.483	1.836	1.648
<b>1.824</b>	1.822	1.908	1.495	1.604	1.768	1.702
<b>1.824</b>	1.822	1.871	1.730	1.834	1.784	1.624
<b>1.836</b>	1.796	1.844	1.614	1.687	1.747	1.639
<b>1.840</b>	1.775	1.951	1.644	1.740	1.801	1.668
<b>1.844</b>	1.850	1.926	1.728	1.825	1.806	1.653
<b>1.846</b>	1.969	1.932	1.722	1.829	1.813	1.655
<b>1.846</b>	1.836	1.890	1.515	1.499	1.787	1.645
<b>1.849</b>	1.895	1.821	1.628	1.646	1.723	1.611
<b>1.852</b>	1.814	1.836	1.351	1.350	1.723	1.637
<b>1.867</b>	1.929	1.924	1.379	1.372	1.803	1.660
<b>1.875</b>	1.899	2.259	2.888	3.289	2.077	1.827
<b>1.888</b>	1.821	1.914	1.555	1.607	1.799	1.648
<b>1.923</b>	1.912	1.851	1.080	1.067	1.741	1.602
<b>1.923</b>	1.874	2.011	1.651	1.731	1.860	1.719
<b>2.015</b>	1.904	1.999	1.291	1.295	1.851	1.697
<b>2.161</b>	1.948	2.424	1.848	1.937	2.158	1.870
<b>2.189</b>	1.891	2.450	1.411	1.460	2.208	1.891

<b>TUC database</b>						
<b>Experimental</b>	<b>Estimated</b>					
	<b>Liquid Z-factor Based Method</b>	<b>Standing's</b>	<b>Vasquez-Begg's</b>	<b>Glaso's</b>	<b>Al-Mahroun's</b>	<b>Sulaimon's</b>
<b>Bob (bbl/STB)</b>						
<b>2.219</b>	1.287	2.552	1.727	1.834	2.256	1.946
<b>2.241</b>	2.074	2.404	2.950	3.340	2.214	1.840
<b>2.248</b>	2.215	2.339	1.527	1.595	2.104	1.842
<b>2.267</b>	2.199	2.371	1.346	1.341	2.115	1.854
<b>2.269</b>	2.208	2.135	1.366	1.375	1.938	1.730
<b>2.296</b>	2.307	2.640	1.427	1.468	2.352	1.950
<b>2.315</b>	2.239	2.162	1.476	1.551	1.962	1.733
<b>2.349</b>	2.307	2.375	1.354	1.380	2.120	1.854
<b>2.360</b>	2.339	2.310	1.458	1.456	2.099	1.795
<b>2.370</b>	2.473	2.559	1.356	1.396	2.306	1.922
<b>2.400</b>	2.481	2.520	1.748	1.945	2.302	1.879
<b>2.428</b>	2.515	2.615	1.197	1.158	2.265	1.987
<b>2.597</b>	2.512	2.962	2.177	2.335	2.622	2.065
<b>2.624</b>	2.561	2.737	1.104	1.074	2.374	1.956
<b>2.628</b>	2.590	2.477	2.437	2.506	2.189	1.861
<b>2.634</b>	2.394	2.236	1.588	1.568	2.033	1.766
<b>2.694</b>	2.457	3.067	1.544	1.580	2.676	2.085
<b>2.779</b>	2.689	2.875	1.585	1.577	2.462	2.026
<b>2.931</b>	2.698	3.106	1.570	1.695	2.676	2.145
<b>2.947</b>	3.145	2.831	1.831	1.922	2.537	2.017
<b>3.005</b>	2.832	3.150	2.606	2.895	2.748	2.199
<b>3.006</b>	2.964	3.202	2.173	2.379	2.770	2.215
<b>3.184</b>	3.015	3.425	1.929	2.038	2.875	2.254
<b>3.432</b>	3.358	3.674	1.755	1.821	3.125	2.332
<b>3.578</b>	4.017	4.144	1.707	1.785	3.517	2.513
<b>3.599</b>	3.280	3.560	1.320	1.267	3.014	2.292
<b>3.944</b>	4.328	4.424	2.089	2.256	3.724	2.616
<b>4.083</b>	4.036	4.718	1.582	1.637	3.871	2.689

Table B.5 comparison of methods for $c_o$ prediction, 500 psi above $p_b$					
Experimental	Estimated				
	Vasquez-Begg's	Petrosky-Farshad's	Ahmed's	Mattar's	Using Densities
$c_o$ (1/psi)					
5.77E-06	8.60E-06	5.24E-06	2.61E-05	5.45E-06	5.63E-06
7.22E-06	1.10E-05	6.78E-06	2.57E-05	6.39E-06	6.69E-06
7.43E-06	1.15E-05	7.86E-06	2.44E-05	6.74E-06	7.13E-06
6.18E-06	7.14E-06	5.63E-06	2.42E-05	5.15E-06	5.34E-06
8.44E-06	2.65E-05	1.17E-05	2.43E-05	1.45E-05	1.69E-05
9.08E-06	1.41E-05	8.80E-06	3.05E-05	7.33E-06	2.84E-05
8.30E-06	1.13E-05	7.63E-06	2.34E-05	7.00E-06	7.46E-06
1.21E-05	1.10E-05	8.07E-06	2.33E-05	7.61E-06	8.17E-06
8.17E-06	9.63E-06	5.92E-06	2.74E-05	5.75E-06	5.98E-06
9.08E-06	1.19E-05	9.02E-06	2.09E-05	7.95E-06	8.67E-06
7.41E-06	8.33E-06	5.87E-06	2.22E-05	6.02E-06	6.37E-06
1.00E-05	1.12E-05	9.10E-06	2.12E-05	7.68E-06	8.35E-06
9.76E-06	1.41E-05	1.21E-05	1.97E-05	8.70E-06	9.70E-06
1.04E-05	2.02E-05	9.36E-06	3.05E-05	8.55E-06	1.82E-05
1.03E-05	1.24E-05	1.15E-05	1.62E-05	9.12E-06	1.04E-05
1.47E-05	1.31E-05	1.59E-05	6.20E-06	1.22E-05	1.51E-05
7.43E-06	-1.78E-05	8.55E-07	3.64E-05	4.73E-06	4.86E-06
8.10E-06	8.73E-06	7.03E-06	1.88E-05	7.06E-06	7.68E-06
1.07E-05	1.24E-05	9.67E-06	2.45E-05	7.55E-06	8.17E-06
1.30E-05	2.14E-05	1.33E-05	2.41E-05	1.28E-05	1.50E-05
9.88E-06	1.65E-05	1.37E-05	3.05E-05	6.66E-06	7.35E-06
8.08E-06	8.54E-06	6.72E-06	2.47E-05	6.38E-06	6.78E-06
8.64E-06	9.71E-06	7.88E-06	2.31E-05	6.86E-06	7.38E-06
1.74E-05	1.69E-05	1.55E-05	2.04E-05	1.10E-05	1.28E-05
1.52E-05	1.71E-05	1.64E-05	1.59E-05	1.25E-05	1.50E-05
1.17E-05	1.28E-05	1.29E-05	1.19E-05	1.08E-05	1.29E-05
2.93E-05	2.12E-05	2.65E-05	6.06E-06	1.89E-05	2.52E-05
1.53E-05	2.24E-05	1.75E-05	2.02E-05	1.51E-05	1.85E-05
1.63E-05	1.87E-05	1.94E-05	1.26E-05	1.50E-05	1.89E-05
2.91E-05	2.07E-05	2.65E-05	5.41E-06	1.86E-05	2.49E-05
1.61E-05	1.69E-05	1.50E-05	1.93E-05	1.17E-05	1.38E-05
1.21E-05	1.79E-05	1.49E-05	2.36E-05	1.08E-05	1.24E-05
1.11E-05	1.12E-05	9.83E-06	1.93E-05	8.01E-06	8.89E-06
1.02E-05	2.13E-05	1.90E-05	2.19E-05	1.24E-05	1.46E-05
1.64E-05	1.73E-05	1.68E-05	1.54E-05	1.28E-05	1.55E-05
1.16E-05	1.62E-05	1.43E-05	1.79E-05	1.09E-05	1.27E-05
7.68E-06	1.16E-05	9.38E-06	2.31E-05	7.99E-06	8.76E-06
2.02E-05	1.94E-05	2.06E-05	1.02E-05	1.62E-05	2.09E-05

Table B.5 comparison of methods for $c_o$ prediction, 500 psi above $p_b$					
Experimental	Estimated				
	Vasquez-Begg's	Petrosky-Farshad's	Ahmed's	Mattar's	Using Densities
$c_o$ (1/psi)					
2.13E-05	2.05E-05	2.12E-05	1.38E-05	1.75E-05	2.27E-05
1.65E-05	1.69E-05	1.81E-05	1.05E-05	1.42E-05	1.79E-05
1.07E-05	1.20E-05	1.08E-05	1.71E-05	9.02E-06	1.03E-05
2.07E-05	1.63E-05	2.00E-05	5.75E-06	1.48E-05	1.90E-05
9.16E-06	2.24E-05	5.46E-06	3.40E-05	7.02E-06	7.71E-06
1.53E-05	1.72E-05	1.95E-05	9.90E-06	1.50E-05	1.91E-05
6.51E-06	-3.13E-06	2.06E-06	3.62E-05	5.64E-06	5.95E-06
1.10E-05	1.54E-05	1.33E-05	1.83E-05	1.15E-05	1.35E-05
1.07E-05	1.90E-05	1.17E-05	2.73E-05	9.94E-06	1.11E-05
1.83E-05	1.70E-05	1.92E-05	9.21E-06	1.50E-05	1.91E-05
3.27E-05	2.52E-05	3.16E-05	4.67E-06	2.15E-05	2.96E-05
8.33E-06	1.79E-05	5.66E-06	3.14E-05	8.53E-06	1.40E-05
1.11E-05	1.62E-05	1.97E-05	7.79E-06	1.61E-05	2.08E-05
1.35E-05	1.38E-05	1.27E-05	1.81E-05	9.85E-06	1.13E-05
1.99E-05	1.72E-05	1.95E-05	8.54E-06	1.53E-05	1.97E-05
1.19E-05	1.43E-05	1.33E-05	1.67E-05	1.06E-05	1.24E-05
1.51E-05	1.56E-05	1.68E-05	1.17E-05	1.44E-05	1.81E-05
1.22E-05	1.56E-05	1.35E-05	1.79E-05	1.24E-05	1.48E-05
3.51E-05	2.67E-05	3.31E-05	4.68E-06	2.22E-05	3.08E-05
2.39E-05	1.94E-05	2.35E-05	5.31E-06	1.64E-05	2.16E-05
8.55E-06	1.61E-05	8.61E-06	2.92E-05	9.06E-06	9.91E-06
1.59E-05	1.72E-05	1.82E-05	1.14E-05	1.39E-05	1.74E-05
2.05E-05	2.00E-05	1.95E-05	1.61E-05	1.62E-05	2.05E-05
1.35E-05	1.54E-05	1.34E-05	1.81E-05	1.23E-05	1.47E-05
1.51E-05	1.57E-05	1.60E-05	1.37E-05	1.40E-05	1.73E-05
6.93E-06	2.08E-06	7.43E-07	3.64E-05	5.79E-06	6.15E-06
1.32E-05	1.52E-05	1.48E-05	1.31E-05	1.15E-05	1.38E-05
3.12E-05	3.42E-05	3.70E-05	9.01E-06	2.49E-05	3.54E-05
7.61E-06	1.03E-05	9.47E-06	1.83E-05	7.87E-06	8.78E-06
1.28E-05	1.43E-05	1.36E-05	1.65E-05	1.23E-05	1.48E-05
2.16E-05	2.15E-05	2.40E-05	9.77E-06	1.85E-05	2.45E-05
1.59E-05	1.63E-05	1.71E-05	1.19E-05	1.40E-05	1.75E-05
1.83E-05	1.98E-05	2.04E-05	1.34E-05	1.59E-05	2.02E-05
1.28E-05	1.56E-05	1.43E-05	1.62E-05	1.09E-05	1.29E-05
9.45E-06	1.11E-05	1.09E-05	2.07E-05	8.26E-06	9.19E-06
1.61E-05	1.68E-05	1.63E-05	1.53E-05	1.26E-05	1.53E-05
1.35E-05	1.47E-05	1.44E-05	1.35E-05	1.19E-05	1.44E-05
1.78E-05	1.77E-05	1.95E-05	1.10E-05	1.52E-05	1.94E-05

Table B.5 comparison of methods for $c_o$ prediction, 500 psi above $p_b$					
Experimental	Estimated				
	Vasquez-Begg's	Petrosky-Farshad's	Ahmed's	Mattar's	Using Densities
$c_o$ (1/psi)					
4.22E-05	2.52E-05	3.06E-05	6.01E-06	2.23E-05	3.10E-05
1.43E-05	1.54E-05	1.57E-05	1.29E-05	1.34E-05	1.65E-05
1.46E-05	1.76E-05	1.67E-05	1.46E-05	1.25E-05	1.51E-05
1.11E-05	2.05E-05	1.35E-05	2.73E-05	1.10E-05	1.26E-05
1.74E-05	1.88E-05	1.90E-05	1.54E-05	1.61E-05	2.04E-05
1.10E-05	1.17E-05	1.10E-05	2.07E-05	8.50E-06	9.50E-06
8.09E-06	1.37E-05	9.55E-06	2.74E-05	8.22E-06	8.98E-06
2.25E-05	2.21E-05	2.48E-05	1.02E-05	1.88E-05	2.50E-05
1.02E-05	1.19E-05	1.12E-05	2.09E-05	8.61E-06	9.64E-06
2.25E-05	2.15E-05	2.23E-05	1.10E-05	1.66E-05	2.15E-05
1.51E-05	1.82E-05	1.77E-05	1.58E-05	1.39E-05	1.72E-05
1.72E-05	1.87E-05	1.89E-05	1.53E-05	1.64E-05	2.08E-05
2.94E-05	2.73E-05	2.91E-05	8.60E-06	2.16E-05	2.97E-05
1.25E-05	1.69E-05	1.58E-05	1.61E-05	1.20E-05	1.44E-05
2.20E-05	2.72E-05	2.76E-05	1.41E-05	2.07E-05	2.80E-05
2.47E-05	2.25E-05	2.54E-05	9.66E-06	1.93E-05	2.59E-05
2.17E-05	2.08E-05	2.35E-05	1.00E-05	1.84E-05	2.44E-05
2.15E-05	2.29E-05	2.57E-05	1.02E-05	1.96E-05	2.64E-05
1.65E-05	1.75E-05	1.67E-05	1.55E-05	1.31E-05	1.60E-05
1.26E-05	1.61E-05	1.34E-05	2.42E-05	9.77E-06	1.11E-05
1.53E-05	1.55E-05	1.65E-05	1.27E-05	1.47E-05	1.84E-05
1.56E-05	1.57E-05	1.73E-05	1.15E-05	1.51E-05	1.91E-05
1.45E-05	2.00E-05	1.84E-05	1.87E-05	1.29E-05	1.56E-05
1.64E-05	1.93E-05	1.93E-05	1.58E-05	1.53E-05	1.93E-05
1.62E-05	1.58E-05	1.76E-05	1.00E-05	1.45E-05	1.83E-05
1.52E-05	1.78E-05	1.72E-05	1.49E-05	1.35E-05	1.67E-05
1.51E-05	1.81E-05	1.78E-05	1.59E-05	1.36E-05	1.68E-05
3.32E-05	3.38E-05	3.44E-05	4.37E-06	2.23E-05	3.12E-05
2.29E-05	2.02E-05	2.30E-05	1.01E-05	1.81E-05	2.39E-05
1.63E-05	1.90E-05	1.90E-05	1.37E-05	1.45E-05	1.83E-05
1.36E-05	4.09E-05	2.97E-05	2.04E-05	1.55E-05	1.95E-05
2.41E-05	2.30E-05	2.59E-05	9.45E-06	2.01E-05	2.72E-05
2.26E-05	2.24E-05	2.48E-05	1.14E-05	1.91E-05	2.55E-05
1.94E-05	2.00E-05	2.11E-05	1.36E-05	1.72E-05	2.23E-05
2.48E-05	2.64E-05	2.63E-05	6.58E-06	1.89E-05	2.56E-05
1.36E-05	2.20E-05	1.95E-05	1.96E-05	1.42E-05	1.74E-05
1.30E-05	1.65E-05	1.48E-05	1.75E-05	1.06E-05	1.25E-05
1.55E-05	2.33E-05	1.84E-05	2.29E-05	1.49E-05	1.82E-05

<b>Table B.5 comparison of methods for <math>c_o</math> prediction, 500 psi above <math>p_b</math></b>					
<b>Experimental</b>	<b>Estimated</b>				
	<b>Vasquez-Begg's</b>	<b>Petrosky-Farshad's</b>	<b>Ahmed's</b>	<b>Mattar's</b>	<b>Using Densities</b>
<b><math>c_o</math> (1/psi)</b>					
<b>1.49E-05</b>	1.49E-05	1.64E-05	1.14E-05	1.43E-05	1.80E-05
<b>1.66E-05</b>	2.38E-05	1.77E-05	2.45E-05	1.45E-05	1.75E-05
<b>1.92E-05</b>	2.13E-05	2.26E-05	1.33E-05	1.80E-05	2.36E-05
<b>1.68E-05</b>	2.43E-05	1.84E-05	2.44E-05	1.48E-05	1.79E-05
<b>3.27E-05</b>	2.49E-05	3.03E-05	6.28E-06	2.23E-05	3.10E-05
<b>1.27E-05</b>	1.56E-05	1.53E-05	1.41E-05	1.23E-05	1.49E-05
<b>1.76E-05</b>	1.68E-05	1.90E-05	1.14E-05	1.61E-05	2.06E-05
<b>1.70E-05</b>	1.93E-05	1.88E-05	1.39E-05	1.42E-05	1.78E-05
<b>1.71E-05</b>	1.78E-05	1.86E-05	1.02E-05	1.46E-05	1.85E-05
<b>1.51E-05</b>	2.37E-05	1.85E-05	2.35E-05	1.51E-05	1.85E-05
<b>1.47E-05</b>	2.45E-05	1.84E-05	2.38E-05	1.52E-05	1.87E-05
<b>1.20E-05</b>	2.80E-05	2.48E-05	1.38E-05	1.61E-05	2.08E-05
<b>1.52E-05</b>	3.06E-05	1.45E-05	2.89E-05	1.60E-05	1.94E-05
<b>2.01E-05</b>	2.28E-05	2.28E-05	1.22E-05	1.71E-05	2.23E-05
<b>1.59E-05</b>	2.81E-05	2.49E-05	1.37E-05	1.62E-05	2.09E-05
<b>1.46E-05</b>	2.36E-05	1.86E-05	2.31E-05	1.53E-05	1.88E-05
<b>1.47E-05</b>	1.57E-05	1.51E-05	1.51E-05	1.22E-05	1.48E-05
<b>1.78E-05</b>	2.06E-05	1.99E-05	1.40E-05	1.49E-05	1.88E-05
<b>1.38E-05</b>	2.12E-05	1.73E-05	2.35E-05	1.29E-05	1.54E-05
<b>2.02E-05</b>	2.67E-05	2.32E-05	1.55E-05	1.49E-05	1.89E-05
<b>1.91E-05</b>	1.97E-05	2.05E-05	1.50E-05	1.73E-05	2.24E-05
<b>1.68E-05</b>	2.23E-05	1.58E-05	2.37E-05	1.49E-05	1.82E-05
<b>1.49E-05</b>	2.17E-05	2.03E-05	1.78E-05	1.41E-05	1.74E-05
<b>2.42E-05</b>	2.55E-05	2.59E-05	1.21E-05	1.89E-05	2.52E-05
<b>3.79E-05</b>	2.86E-05	3.48E-05	8.86E-06	2.74E-05	3.97E-05
<b>1.18E-05</b>	1.58E-05	1.36E-05	2.59E-05	9.32E-06	1.04E-05
<b>2.16E-05</b>	2.01E-05	2.27E-05	1.14E-05	1.81E-05	2.39E-05
<b>2.61E-05</b>	2.76E-05	2.77E-05	8.09E-06	2.05E-05	2.80E-05
<b>1.69E-05</b>	1.89E-05	1.97E-05	1.51E-05	1.58E-05	2.00E-05
<b>4.23E-05</b>	4.85E-05	4.50E-05	3.23E-06	2.85E-05	4.21E-05
<b>1.82E-05</b>	2.09E-05	2.16E-05	1.37E-05	1.71E-05	2.22E-05
<b>2.00E-05</b>	1.94E-05	1.81E-05	1.83E-05	1.54E-05	1.93E-05
<b>2.44E-05</b>	2.38E-05	2.52E-05	1.17E-05	2.00E-05	2.69E-05
<b>1.84E-05</b>	1.77E-05	1.89E-05	1.34E-05	1.67E-05	2.15E-05
<b>1.92E-05</b>	1.79E-05	2.08E-05	1.01E-05	1.72E-05	2.25E-05
<b>1.37E-05</b>	1.56E-05	1.58E-05	1.31E-05	1.30E-05	1.61E-05
<b>3.06E-05</b>	2.42E-05	2.79E-05	8.62E-06	2.15E-05	2.96E-05
<b>2.15E-05</b>	2.38E-05	2.56E-05	1.29E-05	2.04E-05	2.76E-05

Table B.5 comparison of methods for $c_o$ prediction, 500 psi above $p_b$					
Experimental	Estimated				
	Vasquez-Begg's	Petrosky-Farshad's	Ahmed's	Mattar's	Using Densities
$c_o$ (1/psi)					
1.62E-05	1.65E-05	1.55E-05	1.83E-05	1.37E-05	1.68E-05
2.03E-05	1.99E-05	2.03E-05	9.98E-06	1.58E-05	2.05E-05
1.75E-05	3.31E-05	2.85E-05	1.52E-05	1.80E-05	2.37E-05
4.40E-05	4.03E-05	4.35E-05	5.07E-06	3.01E-05	4.48E-05
1.37E-05	1.62E-05	1.29E-05	2.09E-05	1.27E-05	1.51E-05
2.20E-05	3.69E-05	1.33E-05	2.97E-05	1.91E-05	2.42E-05
2.35E-05	2.00E-05	2.29E-05	1.09E-05	1.84E-05	2.44E-05
1.83E-05	1.93E-05	2.21E-05	1.13E-05	1.81E-05	2.39E-05
1.85E-05	1.96E-05	2.08E-05	1.42E-05	1.68E-05	2.16E-05
1.53E-05	2.13E-05	1.94E-05	1.94E-05	1.64E-05	2.08E-05
1.86E-05	1.79E-05	2.10E-05	1.12E-05	1.69E-05	2.20E-05
2.38E-05	2.06E-05	2.38E-05	1.03E-05	1.92E-05	2.57E-05
2.05E-05	2.25E-05	2.33E-05	1.17E-05	1.76E-05	2.32E-05
2.11E-05	2.23E-05	2.25E-05	1.55E-05	1.85E-05	2.44E-05
3.82E-05	3.59E-05	3.52E-05	6.82E-06	2.50E-05	3.58E-05
1.80E-05	2.66E-05	2.46E-05	1.87E-05	1.82E-05	2.37E-05
5.05E-05	3.13E-05	3.87E-05	8.64E-06	3.33E-05	5.04E-05
2.78E-05	2.36E-05	2.48E-05	1.05E-05	1.89E-05	2.54E-05
1.78E-05	1.85E-05	1.82E-05	1.44E-05	1.50E-05	1.89E-05
2.06E-05	2.43E-05	2.44E-05	1.63E-05	1.92E-05	2.55E-05
1.52E-05	1.70E-05	1.71E-05	1.57E-05	1.41E-05	1.76E-05
2.01E-05	2.20E-05	2.06E-05	1.96E-05	1.65E-05	2.09E-05
2.97E-05	2.98E-05	3.22E-05	8.40E-06	2.46E-05	3.50E-05
2.26E-05	3.02E-05	3.07E-05	1.29E-05	2.32E-05	3.25E-05
5.15E-05	4.30E-05	4.48E-05	5.16E-06	3.13E-05	4.72E-05
2.12E-05	2.00E-05	2.32E-05	1.10E-05	1.91E-05	2.55E-05
2.15E-05	2.46E-05	2.45E-05	1.26E-05	1.85E-05	2.46E-05
1.12E-05	2.02E-05	1.00E-05	3.31E-05	7.08E-06	3.34E-05
2.50E-05	2.03E-05	2.39E-05	1.02E-05	1.94E-05	2.60E-05
2.20E-05	2.50E-05	2.47E-05	1.28E-05	1.87E-05	2.49E-05
1.70E-05	2.32E-05	1.83E-05	2.29E-05	1.66E-05	2.08E-05
2.58E-05	2.12E-05	2.36E-05	1.26E-05	1.94E-05	2.60E-05
2.49E-05	2.38E-05	2.54E-05	1.10E-05	1.91E-05	2.57E-05
1.94E-05	2.48E-05	2.31E-05	1.77E-05	1.67E-05	2.14E-05
2.04E-05	2.43E-05	2.34E-05	1.26E-05	1.78E-05	2.36E-05
3.96E-05	3.41E-05	3.93E-05	9.26E-06	3.07E-05	4.60E-05
1.37E-05	3.67E-05	3.18E-05	1.80E-05	2.21E-05	3.05E-05
4.63E-05	5.28E-05	4.69E-05	8.88E-06	3.21E-05	4.99E-05

Table B.5 comparison of methods for $c_o$ prediction, 500 psi above $p_b$					
Experimental	Estimated				
	Vasquez-Begg's	Petrosky-Farshad's	Ahmed's	Mattar's	Using Densities
$c_o$ (1/psi)					
3.80E-05	3.35E-05	3.90E-05	8.57E-06	3.13E-05	4.71E-05
4.45E-05	3.16E-05	3.82E-05	8.20E-06	3.15E-05	4.73E-05
2.40E-05	3.26E-05	3.19E-05	1.48E-05	2.37E-05	3.34E-05
7.95E-05	6.46E-05	6.67E-05	5.92E-06	5.20E-05	9.02E-05
3.87E-05	2.79E-05	3.24E-05	1.09E-05	2.79E-05	4.07E-05
7.09E-05	5.84E-05	6.19E-05	6.05E-06	4.75E-05	7.99E-05
2.62E-05	2.41E-05	2.52E-05	1.56E-05	2.37E-05	3.30E-05
3.06E-05	1.97E-05	1.95E-05	1.72E-05	1.96E-05	2.60E-05
4.55E-05	5.42E-05	4.89E-05	1.02E-05	3.38E-05	5.35E-05
5.41E-05	4.38E-05	4.81E-05	6.91E-06	3.74E-05	5.92E-05
5.48E-05	3.95E-05	4.61E-05	7.33E-06	3.80E-05	6.00E-05

Table B.6 comparison of methods for $B_o$ prediction, 500 psi above $p_b$						
Experimental	Estimated					
	Liquid Z-factor Based Method	Standing's	Vasquez-Begg's	Glaso's	Al-Mahroun's	Sulaimon's
$B_o$ (bbl/STB)						
1.033	1.053	1.047	1.026	1.031	1.041	1.241
1.045	1.046	1.045	1.029	1.029	1.034	1.257
1.046	1.033	1.032	1.021	1.022	1.013	1.206
1.093	1.130	1.101	1.101	1.071	1.124	1.262
1.106	1.131	1.093	1.077	1.064	1.114	1.270
1.115	1.152	1.124	1.131	1.102	1.124	1.291
1.134	1.137	1.127	1.168	1.103	1.136	1.261
1.138	1.136	1.106	1.119	1.082	1.114	1.270
1.139	1.166	1.172	1.219	1.147	1.183	1.285
1.143	1.218	1.145	1.121	1.113	1.172	1.300
1.144	1.443	1.280	1.200	1.225	1.332	1.307
1.147	1.209	1.180	1.116	1.154	1.194	1.330
1.147	1.248	1.146	1.094	1.115	1.164	1.311
1.149	1.117	1.116	1.093	1.088	1.141	1.294

<b>Table B.6 comparison of methods for <math>B_o</math> prediction, 500 psi above <math>p_b</math></b>						
<b>Experimental</b>	<b>Estimated</b>					
	<b>Liquid Z-factor Based Method</b>	<b>Standing's</b>	<b>Vasquez-Begg's</b>	<b>Glaso's</b>	<b>Al-Mahroun's</b>	<b>Sulaimon's</b>
<b><math>B_o</math> (bbl/STB)</b>						
<b>1.151</b>	1.209	1.120	1.106	1.095	1.126	1.286
<b>1.154</b>	1.219	1.168	1.164	1.139	1.180	1.302
<b>1.158</b>	1.216	1.143	1.130	1.115	1.155	1.296
<b>1.159</b>	1.134	1.145	1.150	1.120	1.164	1.305
<b>1.164</b>	1.113	1.127	1.140	1.104	1.136	1.289
<b>1.165</b>	1.159	1.138	1.117	1.107	1.165	1.299
<b>1.171</b>	1.145	1.159	1.177	1.137	1.168	1.307
<b>1.180</b>	1.177	1.186	1.192	1.161	1.199	1.323
<b>1.181</b>	1.236	1.172	1.151	1.144	1.180	1.318
<b>1.187</b>	1.187	1.183	1.178	1.158	1.193	1.329
<b>1.188</b>	1.208	1.184	1.164	1.152	1.210	1.318
<b>1.210</b>	1.238	1.215	1.199	1.188	1.221	1.339
<b>1.213</b>	1.200	1.224	1.194	1.203	1.235	1.369
<b>1.226</b>	1.256	1.217	1.203	1.187	1.226	1.330
<b>1.240</b>	1.227	1.241	1.220	1.218	1.252	1.367
<b>1.246</b>	1.225	1.205	1.175	1.173	1.232	1.334
<b>1.248</b>	1.217	1.264	1.278	1.247	1.259	1.374
<b>1.248</b>	1.250	1.189	1.152	1.158	1.204	1.329
<b>1.257</b>	1.223	1.258	1.245	1.239	1.259	1.379
<b>1.258</b>	1.222	1.258	1.246	1.239	1.259	1.379
<b>1.259</b>	1.223	1.262	1.240	1.244	1.260	1.388
<b>1.261</b>	1.226	1.248	1.261	1.227	1.246	1.357
<b>1.266</b>	1.278	1.218	1.179	1.175	1.268	1.315
<b>1.275</b>	1.265	1.258	1.282	1.225	1.288	1.334
<b>1.280</b>	1.291	1.214	1.206	1.165	1.275	1.289
<b>1.281</b>	1.314	1.289	1.218	1.261	1.298	1.388
<b>1.298</b>	1.322	1.309	1.263	1.286	1.293	1.400
<b>1.299</b>	1.352	1.321	1.286	1.287	1.352	1.377
<b>1.304</b>	1.276	1.298	1.318	1.277	1.293	1.375
<b>1.311</b>	1.313	1.277	1.255	1.240	1.313	1.348
<b>1.312</b>	1.326	1.314	1.318	1.284	1.324	1.366
<b>1.316</b>	1.321	1.256	1.213	1.215	1.292	1.331
<b>1.318</b>	1.313	1.333	1.319	1.311	1.324	1.403
<b>1.320</b>	1.332	1.298	1.240	1.264	1.324	1.374
<b>1.331</b>	1.343	1.309	1.246	1.275	1.333	1.381
<b>1.334</b>	1.343	1.323	1.320	1.289	1.340	1.365
<b>1.338</b>	1.356	1.323	1.265	1.289	1.346	1.385
<b>1.342</b>	1.348	1.312	1.266	1.279	1.338	1.377

Table B.6 comparison of methods for $B_o$ prediction, 500 psi above $p_b$						
Experimental	Estimated					
	Liquid Z-factor Based Method	Standing's	Vasquez-Begg's	Glaso's	Al-Mahroun's	Sulaimon's
$B_o$ (bbl/STB)						
1.343	1.316	1.307	1.260	1.280	1.322	1.391
1.346	1.335	1.319	1.317	1.286	1.337	1.365
1.347	1.417	1.394	1.283	1.368	1.379	1.445
1.349	1.354	1.350	1.341	1.318	1.362	1.383
1.354	1.363	1.367	1.349	1.344	1.353	1.413
1.357	1.359	1.358	1.334	1.328	1.373	1.397
1.358	1.352	1.369	1.357	1.346	1.356	1.414
1.365	1.363	1.330	1.274	1.297	1.353	1.388
1.365	1.371	1.353	1.301	1.324	1.352	1.407
1.366	1.374	1.360	1.280	1.334	1.350	1.426
1.367	1.354	1.352	1.304	1.328	1.330	1.413
1.382	1.421	1.364	1.324	1.326	1.380	1.382
1.391	1.361	1.330	1.280	1.297	1.350	1.388
1.403	1.379	1.431	1.389	1.417	1.400	1.466
1.409	1.423	1.409	1.370	1.379	1.417	1.420
1.410	1.440	1.469	1.465	1.446	1.442	1.452
1.418	1.429	1.408	1.357	1.376	1.419	1.421
1.423	1.431	1.427	1.367	1.402	1.416	1.446
1.427	1.416	1.450	1.437	1.429	1.430	1.450
1.429	1.452	1.438	1.362	1.409	1.440	1.445
1.431	1.443	1.463	1.433	1.439	1.454	1.452
1.441	1.446	1.469	1.466	1.445	1.433	1.451
1.444	1.459	1.482	1.438	1.459	1.451	1.470
1.445	1.473	1.470	1.405	1.444	1.437	1.465
1.455	1.478	1.497	1.435	1.473	1.469	1.479
1.455	1.469	1.465	1.449	1.431	1.456	1.431
1.455	1.391	1.426	1.404	1.408	1.399	1.450
1.457	1.426	1.458	1.422	1.439	1.429	1.465
1.458	1.433	1.450	1.379	1.430	1.426	1.469
1.468	1.450	1.491	1.468	1.470	1.461	1.471
1.475	1.484	1.535	1.495	1.515	1.483	1.500
1.481	1.490	1.493	1.486	1.459	1.486	1.438
1.484	1.459	1.480	1.447	1.457	1.454	1.465
1.484	1.541	1.550	1.540	1.514	1.530	1.462
1.486	1.487	1.490	1.427	1.463	1.453	1.473
1.488	1.486	1.508	1.471	1.485	1.477	1.477
1.493	1.537	1.546	1.465	1.516	1.520	1.492
1.494	1.477	1.484	1.434	1.458	1.461	1.464

<b>Table B.6 comparison of methods for <math>B_o</math> prediction, 500 psi above <math>p_b</math></b>						
<b>Experimental</b>	<b>Estimated</b>					
	<b>Liquid Z-factor Based Method</b>	<b>Standing's</b>	<b>Vasquez-Begg's</b>	<b>Glaso's</b>	<b>Al-Mahroun's</b>	<b>Sulaimon's</b>
<b><math>B_o</math> (bbl/STB)</b>						
<b>1.495</b>	1.478	1.490	1.494	1.462	1.469	1.447
<b>1.495</b>	1.535	1.532	1.510	1.496	1.522	1.457
<b>1.498</b>	1.514	1.494	1.437	1.457	1.487	1.448
<b>1.499</b>	1.518	1.518	1.445	1.489	1.493	1.478
<b>1.503</b>	1.479	1.522	1.505	1.500	1.493	1.478
<b>1.507</b>	1.554	1.542	1.469	1.507	1.526	1.475
<b>1.510</b>	1.498	1.538	1.481	1.518	1.488	1.504
<b>1.511</b>	1.467	1.439	1.411	1.401	1.467	1.415
<b>1.514</b>	1.514	1.531	1.533	1.497	1.514	1.455
<b>1.520</b>	1.718	1.708	1.548	1.679	1.647	1.579
<b>1.522</b>	1.510	1.534	1.509	1.510	1.509	1.480
<b>1.528</b>	1.594	1.618	1.474	1.600	1.543	1.563
<b>1.535</b>	1.519	1.500	1.433	1.465	1.489	1.456
<b>1.535</b>	1.541	1.539	1.520	1.502	1.514	1.458
<b>1.549</b>	1.527	1.498	1.421	1.462	1.483	1.457
<b>1.552</b>	1.596	1.610	1.570	1.573	1.578	1.495
<b>1.552</b>	1.584	1.597	1.515	1.566	1.563	1.511
<b>1.561</b>	1.639	1.640	1.543	1.604	1.570	1.532
<b>1.566</b>	1.555	1.541	1.438	1.514	1.516	1.498
<b>1.568</b>	1.495	1.519	1.427	1.499	1.483	1.503
<b>1.574</b>	1.558	1.581	1.547	1.551	1.536	1.497
<b>1.586</b>	1.619	1.607	1.494	1.575	1.574	1.520
<b>1.590</b>	1.547	1.565	1.467	1.543	1.532	1.516
<b>1.591</b>	1.632	1.647	1.562	1.615	1.596	1.534
<b>1.592</b>	1.592	1.580	1.504	1.548	1.555	1.498
<b>1.595</b>	1.578	1.612	1.535	1.586	1.555	1.529
<b>1.607</b>	1.667	1.703	1.605	1.664	1.650	1.550
<b>1.610</b>	1.614	1.655	1.629	1.621	1.600	1.521
<b>1.615</b>	1.615	1.612	1.536	1.577	1.572	1.509
<b>1.621</b>	1.570	1.613	1.539	1.589	1.555	1.533
<b>1.625</b>	1.671	1.671	1.568	1.634	1.616	1.540
<b>1.627</b>	1.638	1.606	1.504	1.565	1.565	1.501
<b>1.628</b>	1.644	1.598	1.531	1.558	1.594	1.487
<b>1.629</b>	1.600	1.644	1.555	1.619	1.579	1.549
<b>1.632</b>	1.621	1.631	1.543	1.598	1.573	1.529
<b>1.633</b>	1.694	1.725	1.674	1.682	1.669	1.544
<b>1.638</b>	1.682	1.753	1.681	1.719	1.666	1.583
<b>1.643</b>	1.633	1.674	1.588	1.642	1.594	1.554

<b>Table B.6 comparison of methods for <math>B_o</math> prediction, 500 psi above <math>p_b</math></b>						
<b>Experimental</b>	<b>Estimated</b>					
	<b>Liquid Z-factor Based Method</b>	<b>Standing's</b>	<b>Vasquez-Begg's</b>	<b>Glaso's</b>	<b>Al-Mahroun's</b>	<b>Sulaimon's</b>
<b><math>B_o</math> (bbl/STB)</b>						
<b>1.649</b>	1.667	1.704	1.611	1.667	1.628	1.558
<b>1.667</b>	1.712	1.747	1.641	1.704	1.654	1.574
<b>1.680</b>	1.721	1.780	1.562	1.730	1.666	1.575
<b>1.683</b>	1.729	1.751	1.643	1.708	1.681	1.570
<b>1.691</b>	1.804	1.790	1.614	1.747	1.695	1.605
<b>1.692</b>	1.768	1.768	1.634	1.725	1.695	1.583
<b>1.700</b>	1.700	1.712	1.613	1.673	1.663	1.552
<b>1.703</b>	1.699	1.720	1.635	1.678	1.665	1.550
<b>1.725</b>	1.655	1.685	1.619	1.650	1.604	1.547
<b>1.726</b>	1.742	1.769	1.675	1.725	1.708	1.570
<b>1.733</b>	1.723	1.762	1.681	1.718	1.667	1.574
<b>1.734</b>	1.748	1.779	1.670	1.734	1.707	1.580
<b>1.746</b>	1.741	1.761	1.736	1.706	1.688	1.538
<b>1.752</b>	1.672	1.744	1.577	1.720	1.642	1.619
<b>1.754</b>	1.812	1.881	1.652	1.845	1.751	1.678
<b>1.759</b>	1.795	1.887	1.671	1.850	1.747	1.682
<b>1.760</b>	1.775	1.830	1.685	1.791	1.736	1.625
<b>1.761</b>	1.759	1.801	1.734	1.753	1.698	1.585
<b>1.765</b>	1.818	1.838	1.686	1.789	1.736	1.615
<b>1.768</b>	1.775	1.827	1.682	1.789	1.735	1.624
<b>1.769</b>	1.753	1.803	1.671	1.766	1.702	1.614
<b>1.770</b>	1.796	1.833	1.728	1.783	1.758	1.596
<b>1.771</b>	1.760	1.846	1.748	1.805	1.741	1.624
<b>1.782</b>	1.801	1.833	1.726	1.782	1.751	1.597
<b>1.794</b>	1.775	1.835	1.695	1.795	1.736	1.625
<b>1.797</b>	1.800	1.892	1.676	1.855	1.751	1.684
<b>1.799</b>	1.756	1.778	1.692	1.733	1.674	1.583
<b>1.801</b>	1.937	1.956	1.738	1.900	1.833	1.677
<b>1.805</b>	1.828	1.858	1.737	1.806	1.752	1.614
<b>1.805</b>	1.748	1.813	1.686	1.778	1.725	1.618
<b>1.814</b>	1.813	1.832	1.707	1.786	1.739	1.609
<b>1.819</b>	1.944	1.981	1.827	1.914	1.843	1.666
<b>1.824</b>	1.873	1.905	1.762	1.848	1.779	1.639
<b>1.826</b>	1.794	1.850	1.705	1.806	1.729	1.635
<b>1.826</b>	1.905	1.937	1.765	1.876	1.806	1.655
<b>1.827</b>	1.869	1.882	1.666	1.838	1.788	1.652
<b>1.831</b>	1.801	1.832	1.716	1.782	1.735	1.603
<b>1.845</b>	1.850	1.900	1.713	1.853	1.775	1.660

<b>Table B.6 comparison of methods for <math>B_o</math> prediction, 500 psi above <math>p_b</math></b>						
<b>Experimental</b>	<b>Estimated</b>					
	<b>Liquid Z-factor Based Method</b>	<b>Standing's</b>	<b>Vasquez-Begg's</b>	<b>Glaso's</b>	<b>Al-Mahroun's</b>	<b>Sulaimon's</b>
<b><math>B_o</math> (bbl/STB)</b>						
<b>1.855</b>	1.893	1.985	1.915	1.914	1.832	1.652
<b>1.866</b>	1.881	1.917	1.745	1.859	1.787	1.650
<b>1.875</b>	1.923	1.965	1.794	1.901	1.826	1.666
<b>1.896</b>	1.875	1.945	1.784	1.891	1.822	1.666
<b>1.899</b>	1.867	1.941	1.760	1.889	1.825	1.669
<b>1.976</b>	2.040	2.019	1.836	1.945	1.916	1.668
<b>2.135</b>	2.124	2.271	2.092	2.156	2.031	1.781
<b>2.161</b>	2.184	2.322	2.063	2.208	2.086	1.823
<b>2.187</b>	2.168	2.247	1.992	2.142	2.021	1.790
<b>2.208</b>	2.179	2.258	2.032	2.138	2.015	1.772
<b>2.214</b>	2.270	2.363	2.078	2.236	2.141	1.825
<b>2.234</b>	2.209	2.303	2.093	2.173	2.052	1.781
<b>2.235</b>	2.054	2.115	1.924	2.029	1.953	1.718
<b>2.268</b>	2.277	2.477	2.200	2.329	2.188	1.884
<b>2.272</b>	2.271	2.268	1.975	2.148	2.066	1.775
<b>2.311</b>	2.304	2.403	2.172	2.258	2.160	1.820
<b>2.314</b>	2.425	2.453	2.062	2.304	2.220	1.862
<b>2.317</b>	2.434	2.444	2.136	2.291	2.237	1.832
<b>2.363</b>	2.469	2.567	2.064	2.396	2.223	1.950
<b>2.382</b>	2.463	2.494	2.131	2.333	2.264	1.865
<b>2.569</b>	2.410	2.340	2.062	2.201	2.140	1.783
<b>2.573</b>	2.358	2.452	2.204	2.294	2.179	1.841
<b>2.581</b>	2.549	2.699	2.388	2.477	2.334	1.937
<b>2.647</b>	2.645	2.818	2.444	2.565	2.415	1.989
<b>2.727</b>	2.651	2.890	2.398	2.634	2.511	2.046
<b>2.852</b>	3.070	3.183	2.544	2.826	2.796	2.127
<b>2.881</b>	2.764	2.922	2.225	2.664	2.567	2.087
<b>2.924</b>	2.877	2.893	2.404	2.624	2.583	2.005
<b>2.937</b>	2.895	3.127	2.376	2.803	2.706	2.163
<b>3.132</b>	2.964	3.366	2.785	2.949	2.826	2.215
<b>3.344</b>	3.284	3.592	2.862	3.087	3.055	2.281
<b>3.454</b>	3.895	4.019	2.951	3.335	3.410	2.437
<b>3.521</b>	3.210	3.484	2.810	3.018	2.949	2.243
<b>3.790</b>	4.186	4.279	3.074	3.478	3.602	2.530
<b>3.998</b>	3.946	4.613	3.634	3.659	3.784	2.629

## REFERENCES

### • Chapter 1

- [1] [https://www.google.gr/search?q=petroleum+reservoir&espv=2&rlz=1C1TEUA\\_enGR484GR484&source=lnms&tbm=isch&sa=X&ved=0ahUKEwiSxcKru8\\_PAhXJchQKHWYHDIEQ\\_AUICCgB&biw=1366&bih=662#imgrc=4hU9Fe\\_puqtietM%3A](https://www.google.gr/search?q=petroleum+reservoir&espv=2&rlz=1C1TEUA_enGR484GR484&source=lnms&tbm=isch&sa=X&ved=0ahUKEwiSxcKru8_PAhXJchQKHWYHDIEQ_AUICCgB&biw=1366&bih=662#imgrc=4hU9Fe_puqtietM%3A)
- [2] Dake, L. P., "*Fundamentals of Reservoir Engineering*," Amsterdam: Elsevier Scientific Publishing Company, 1978. pg. 44.
- [3] Ahmed, T., "*Reservoir Engineering Handbook*," Elsevier Scientific Publishing Company, 2010. pg. 93.
- [4] Ahmed, T., "*Reservoir Engineering Handbook*," Elsevier Scientific Publishing Company, 2010. pg. 109.
- [5] Ahmed, T., "*Reservoir Engineering Handbook*," Elsevier Scientific Publishing Company, 2010. pg. 79.
- [6] Schilthuis, R.J., 1936. "*Active Oil and Reservoir Energy*," Trans., AIME, 118: 33-52.
- [7] Dake, L. P., "*Fundamentals of Reservoir Engineering*," Amsterdam: Elsevier Scientific Publishing Company, 1978. pg. 72.
- [8] Ahmed, T., "*Reservoir Engineering Handbook*," Elsevier Scientific Publishing Company, 2010. pg. 335.

### • Chapter 2

- [1] Lindsly, B. E.: "*A Study of 'Bottom Hole' Samples of East Texas Crude Oil*," R.I. 3212, USBM, (1934).
- [2] Lindsly, B. E., "*A Bureau of Mines Study of a 'Bottom Hole' Sample from the Crescent Pool, Okla.*," Pet. Eng., (Feb.-March, 1936), 7, (5) 34.
- [3] Sclater, K. c., and Stephenson, B. R.: "*Method of Obtaining Bottom Hole Data*," Oil and Gas Jour. (October 25, 1928).
- [4] Schilthuis, R. J.: "*Technique of Securing and Examining Subsurface Samples of Oil and Gas*," Drill. and Prod. Prac. for 1935, API (1936), 120.

- [5] Exline, P. G.: "*New Apparatus for Securing and Examining Subsurface Samples of Oil*," Drill. and Prod. Prac. for 1936, API, (1937), 126.
- [6] Agrawal P.: "*Measurement and Modeling of the Phase Behavior of Solvent Diluted Bitumens*," Master Thesis, Department of Chemical and Petroleum Engineering. Calgary, Alberta, March 2012, pg. 35.
- [7] McCain, W., "*The Properties of Petroleum Fluids*," Tulsa, OK: PennWell Publishing Company, 1990, pg 271.
- [8] McCain, W., "*The Properties of Petroleum Fluids*," Tulsa, OK: PennWell Publishing Company, 1990, pg 274.
- [9] Moses, P.L. "*Engineering Applications of Phase Behavior of Crude Oil and Condensate Systems*," J. Pet. Tech. (July 1986) 38, 715-723.
- [10] Dodson, L. P. et al, "*Application of Laboratory PVT Data to Reservoir Engineering Problems*," JPT, December 1953, pp. 287–298.
- [11] Al-Mahroun, M.A.: "*Adjustment of Differential Liberation Data to Separator Conditions*," SPE-84684-PA, June 2003.
- [12] McCain, W., "*The Properties of Petroleum Fluids*," Tulsa, OK: PennWell Publishing Company, 1990, pg 283.
- [13] Amyx. J. W., Bass, D.M. jr., and Whitting, R.L.: "*Petroleum Reservoir Engineering*," McGraw-Hill Book Co. Inc., New York City (1960), pg. 392-399.
- [14] Dake, L. P., "*Fundamentals of Reservoir Engineering*," Amsterdam: Elsevier Scientific Publishing Company, 1978. pg. 55-63.
- [15] Ahmed, T., "*Reservoir Engineering Handbook*," Elsevier Scientific Publishing Company, 2010. pg. 157-159.
- [16] Ahmed, T., "*Reservoir Engineering Handbook*," Elsevier Scientific Publishing Company, 2010. pg. 145.
- [17] Varotsis, and Gueze, P., "*On-Site Reservoir Fluid Properties Evaluation*," SPE paper 18317, first presented at the 1988 SPE Annual Technical Conference and Exhibition held in Houston, 2-5 Oct. 1988.
- [18] Katz, D. L., "*Prediction of Shrinkage of Crude Oils*," Drill and Prod. Pract., API, pp. 137-147, November, 1942.

- [19] Standing, M.B., "A Pressure Volume Temperature Correlation for Mixture of California Oils and Gases," Drill. & Prod. Prac., API, Dallas ,pp. 275-287 , May,1947.
- [20] Lasater, J.S., "Bubble Point Pressure Correlation," Trans., AIME,1958.
- [21] Glaso, O., "Generalized Pressure-Volume-Temperature Correlations," JPT, pp. 785-795, May, 1980.
- [22] Vasquez, M. and Beggs, H.D., "Correlation for Fluid Physical Property Predictions," JPT,pp. 968-970, June, 1980.
- [23] Al-Marhoun, M.A., "PVT Correlations for Middle East Crude Oils," JPT, pp. 650-666, (May, 1988).
- [24] Elmabrouk, S., Zekri,A. and Shirif, E., "Prediction of Bubble-point Pressure and Bubble-point Oil Formation Volume Factor in the Absence of PVT Analysis," paper SPE 137368, prepared for presentation at the SPE Latin American & Caribbean Petroleum Engineering Conference held in Lima, Peru, December 2010.
- [25] Sulaimon, A.A., Ramli, N., Adeyemi, B.J. and Saaid, I.M., "New Correlation for Oil Formation Volume Factor," paper SPE 172396, prepared for presentation at the SPE Nigeria Annual International Conference and Exhibition held in Lagos, Nigeria, August 2014.
- [26] Petrosky, G. E., and Farshad, F., "Pressure-Volume-Temperature Correlations for Gulf of Mexico Crude Oils," SPE Paper 26644, presented at the 68th Annual Technical Conference of the SPE in Houston, Texas, 3–6 October, 1993.
- [27] Ahmed. T., "Compositional Modeling of Tyler and Mission Canyon Formation Oils with Co<sub>2</sub> and Lean Gases," final report submitted to Montanans on a New Track Science (MONTS) (Montana National Science Foundation Gran Program), 1985- 1988.
- [28] Azubuike, I. I., Ikiensikimama, S. S., "Prediction of Oil Formation Volume Factor Using an Intelligent Tool: Artificial Neural Network," CSCanada, Vol. 5, No. 2, 2013, pp. 24-30 (2013).
- [29] Varotsis, N., Gaganis, V. and Guieze, P., "A Novel Non-Iterative Method for the Prediction of the PVT Behavior of Reservoir Fluids," paper SPE 56745, prepared for presentation at the 1999 SPE Annual Technical Conference and Exhibition held in Houston, Texas, 3–6 October 1999.

- [30] Osman, E. A., Abdel-Wahhab, O. A., & Al-Marhoun, M. A. (2001, March). "Prediction of Oil Properties Using Neural Networks," SPE Paper 68233, presented at the SPE Middle East Oil Show Conference, Bahrain.
- [31] Shokir, E. M., Goda, H. M., Sayyouh, M. H., & Fattah, K. A. (2004), "Modeling Approach for Predicting PVT Data," Engineering Journal of the University of Qatar, 17, 11-28.
- [32] Azubuiké, I. I., & Ikiensikimama, S. S. (2013), "Forecasting Oil Formation Volume Factor for API Gravity Ranges Using Artificial Neural Network," Advances in Petroleum Exploration Development, 5(1), 14-21.

### • Chapter 3

- [1] Standing, M. B., and Katz, D. L., "Density of Natural Gases," Trans. AIME, 1942, Vol. 146, pp. 140–149.
- [2] Sutton, R. P., "Compressibility Factors for High-Molecular-Weight Reservoir Gases," SPE Paper 14265, presented at the 60th Annual Technical Conference and Exhibition of the Society of Petroleum Engineers, Las Vegas, Sept. 22–25, 1985.
- [3] Sutton, R. P. 2007. "Fundamental PVT Calculations for Associated and Gas/Condensate Natural-Gas Systems," SPERE 10 (3): 270-284. SPE-97099-PA. DOI: 10.2118/97099-PA.
- [4] Hall, K. R. and Yarborough, L. 1973, "A New Equation of State for Z-factor Calculations," Oil & Gas J. (18 June 1973) 82-85, 90,92.
- [5] Hall, K. R. and Yarborough, L. 1974, "How to solve Equation of State for Z-factors," Oil & Gas J. (18 February 1974) 86-88.
- [6] Dranchuk, P.M., Purvis, R.A., and Robinson, D.B. 1974, "Computer Calculation of Natural Gas Compressibility Factors Using the Standing and Katz Correlations," London: Inst. Of Petroleum Technical Series, No IP74-008:1-3.
- [7] Dranchuk, P.M. and Abou-Kassem, J.H. 1975, "Calculation of Z Factors For Natural Gases Using Equations of State," J. Cdn. Pet. Tech. (July-September 1975) 34-36.
- [8] Brill, J.P. and Beggs, H.D.: "Two-Phase Flow in Pipes," paper presented at the U. Tulsa INTERCOMP Course, The Hague (1974).

- [9] Poettmann, F.H. and Carpenter, P.G. 1952, "*The Multiphase Flow of Gas, Oil, and Water Through Vertical Flow Strings with Application to the Design of Gas Lift Installations*," *Drill and Prod. Prac.*, API, 257-317.
- [10] Batzle, M. and Wang, Z. 1992, "*Seismic Properties of Pore Fluids*," *Geophysics* (November 1992) 1396-1408. DOI: 10.1190/1.1443207.
- [11] Londono, F.E., Archer, R.A., and Blasingame, T.A. 2002, "*Simplified Correlations for Hydrocarbon Gas Viscosity and Gas Density-Validation and Correlation of Behavior Using a Large-Scale Database*," paper SPE 75721 presented at the SPE Gas Technology Symposium, Calgary, 30 April-2 May. DOI: 10.2118/75721-MS.
- [12] Sutton, R.P. 2007, "*Fundamental PVT Calculations for Associated and Gas/Condensate Natural-Gas Systems*," *SPERE* 10 (3): 270-284. SPE-97099-PA. DOI: 10.2118/97099-PA.
- [13] Sutton, R.P. 2008, "*An Accurate Method for Determining Oil PVT Properties Using the Standing-Katz Gas Z-Factor Chart*," SPE 103155.
- [14] Takacs, G., "*Comparisons Made for Computer Z-Factor Calculations*," *Oil and Gas J.* (Dec. 20, 1976) 64-66.
- [15] Sutton, R.P., 1985, "*Compressibility Factors for High-Molecular-Weight Reservoir Gases*," paper SPE 14265 presented at the SPE Annual Technical Conference and Exhibition, Las Vegas, Nevada, 22-26 September. DOI: 10.2118/14265-MS.
- [16] Kumar, A., 1991, "*Correlations for the Prediction of PVT Behavior During Depletion of Dissolved Gas/Oil Reservoirs*," MS Thesis, Fairbanks, Alaska: The University of Alaska.
- [17] Sutton, R.P., 2006, "*Petroleum Engineering handbook, General Engineering*," Vol. 1, ed. J. Fanchi and L.W. Lake., Richardson, Texas: SPE, 257-331.
- [18] Matter, L., Brar, G. S., and Aziz, K., "*Compressibility of Natural Gases*," *Journal of Canadian Petroleum Technology*, Vol. 14, No. 4, pp. 77-80, Oct.-Dec. 1975.

- **Chapter 4**

- [1] Omar, M. I., and Todd, A. C., "*Development of New Modified Black Oil Correlations for Malaysian Crudes*," The paper was presented at the SPE Asia Pacific Oil & Gas Conference & Exhibition held in Singapore, 8 – 10 February 1993 SPE number: 025338.
- [2] Al-Mahroun, M. A., "*PVT Correlations for Middle East Crude Oils*", JPT (May 1988), pp 650-666.
- [3] Glaso, O., "*Generalized Pressure-Volume-Temperature Correlations*," JPT, pp. 785-795, May, 1980.
- [4] Technical University of Crete, Mineral Resources Engineering Department